DESY 11-045

Closed flux tubes and their string description in D=2+1 SU(N) gauge theories

Andreas Athenodorou[a], Barak Bringoltz[b] and Michael Teper[c]

[a]DESY, Platanenallee 6, 15738 Zeuthen, Germany

[b]IIAR, The Israeli Institute for Advanced Research, Rehovot, Israel

[c]Rudolf Peierls Centre for Theoretical Physics, University of Oxford, 1 Keble Road, Oxford OX1 3NP, UK

Abstract

We carry out lattice calculations of the spectrum of confining flux tubes that wind around a spatial torus of variable length l, in 2+1 dimensions. We compare the energies of the lowest ~ 30 states to the free string Nambu-Goto model and to recent results on the universal properties of effective string actions. Our most useful calculations are in SU(6) at a small lattice spacing, which we check is very close to the $N \to \infty$ continuum limit. We find that the energies, $E_n(l)$, are remarkably close to the predictions of the free string Nambu-Goto model, even well below the critical length at which the expansion of the Nambu-Goto energy in powers of $1/l^2$ diverges and the series needs to be resummed. Our analysis of the ground state supports the universality of the $O(1/l)$ and the $O(1/l^3)$ corrections to σl, and we find that the deviations from Nambu-Goto at small l prefer a leading correction that is $O(1/l^7)$, consistent with theoretical expectations. We find that the low-lying states that contain a single phonon excitation are also consistent with the leading $O(1/l^7)$ correction dominating down to the smallest values of l. By contrast our analysis of the other light excited states clearly shows that for these states the corrections at smaller l resum to a much smaller effective power. Finally, and in contrast to our recent calculations in $D = 3 + 1$, we find no evidence for the presence of any non-stringy states that could indicate the excitation of massive flux tube modes.

E-mail: andreas.athenodorou@desy.de, barak.bringoltz@gmail.com, m.teper1@physics.ox.ac.uk

Contents

1 Introduction

In this paper we calculate the energy spectrum of closed flux tubes in $D = 2+1$ SU(N) lattice gauge theories. These flux tubes are stabilised by being wound around a spatial torus and we calculate the energies of the lightest few eigenstates as a function of the flux tube length l, for various quantum numbers. This work greatly extends and supersedes that published in our earlier brief letter [1], and is part of a larger project which has included the calculation of the spectrum in $D = 3 + 1$ [2], as well as the spectrum and string tensions [3] of flux tubes with flux in some higher representations, e.g. k-strings. The most significant new calculations in this paper are at larger N, i.e. SU(6), and at a small lattice spacing, $a \simeq 0.086/\sqrt{\sigma}$, where σ is the string tension. The main purpose of these calculations is to learn about the effective string theory that describes closed flux tubes at $N = \infty$, and possibly at smaller N as well. The details of the analysis in our earlier $D = 2 + 1$ calculation [1] have been rendered out of

date by a great deal of recent analytic progress [4] towards determining the universal terms in the derivative expansion of this string action, which makes new predictions for the low-lying spectrum of long flux tubes, $l\sqrt{\sigma} \gg 1$. Our lattice calculations are largely complementary in that they concentrate on flux tubes that range from the very short to the moderately long, i.e. $l\sqrt{\sigma} \sim 1$ to ~ 6. So together with the analytic work they may tell us something about the effective string action over the whole range of l.

In the next Section we begin with some general remarks about closed flux tubes in $D = 2 + 1$, describe their quantum numbers, and how they differ from those in $D = 3 + 1$. We describe in some detail the spectrum of the free string theory (Nambu-Goto in flat space time) since the most striking result of our earlier lattice calculations is how close the actual spectrum is to this Nambu-Goto spectrum, even for very small values of l where the flux tube is hardly longer than it is wide and naively should 'look' nothing like an ideal thin string. We then give a brief summary of the current status of the analytic study of the effective string action, and point to some very recent lattice and analytic calculations relevant to our work. In Section 3 we describe some details of our lattice calculation of the spectrum, with the focus on the operators we use and how well we control our systematic errors. We briefly discuss the large-N limit and show how our calculations of the string tension provide rather precise evidence for the conventional large-N counting. In Section 4 we present and analyse our numerical results for the spectrum. We start with the absolute ground state and then move on to the excited states. We perform detailed fits to see how far we can confirm the established universality results, and what we can learn about the corrections to the universal terms at smaller l. We summarise and conclude in Section 5. Finally we list in an Appendix the energy eigenvalues from our new SU(6) calculation, so as to allow the interested reader to extend the present analysis as further theoretical progress is made.

We have kept the discussion in this paper relatively brief, since most of the relevant issues are discussed at greater length in our recent paper on the flux tube spectrum in $D = 3 + 1$ [2] and in a recent set of lectures by one of the authors [5], to which we refer the interested reader.

2 Flux tubes and strings

We begin with some general comments about closed flux tubes in 2+1 dimensions. We then describe in detail the spectrum in the free string theory, as given by the Nambu-Goto action in flat space-time, since this turns out to describe the numerically determined flux tube spectrum remarkably well. We then briefly summarise recent analytic progress on the form of the effective string action describing very long flux tubes. We also point to some lattice and analytic work that has appeared since our earlier papers, and discuss how the new results in this paper modify the conclusions of our earlier work. For a more complete but slightly less up-to-date discussion of many of these topics we refer the reader to [2, 5].

2.1 Closed flux tubes in D=2+1

We assume that we are in the confining phase of the gauge theory. In this phase a closed flux tube carrying fundamental flux cannot break, but it can contract. To stabilise such a flux tube at a given (minimal) length l, we make the x direction periodic with period l and we close the flux tube around this spatial torus. In our lattice calculations the other Euclidean directions will also be periodic tori, but these will be chosen large enough that they are effectively infinite. Such a winding flux tube will have a spectrum of states, which is a function of its length l, and it is this that we wish to calculate numerically. In this paper we will be able to calculate the energies of $O(30)$ of the lighter states of the spectrum.

One naively expects the flux tube to have some 'intrinsic' width which is $\sim 1/\sqrt{\sigma}$. For a very long flux tube, $l \gg 1/\sqrt{\sigma}$, the flux tube should appear string-like and the low-lying excitations should be the massless modes along the string that describe its transverse fluctuations. These are quantised, by the periodicity of the flux tube, to have momenta and energies $k\pi/l$, with k an integer. (This is just the Goldstone mode arising from the spontaneous breaking of the translation invariance transverse to the flux tube, with discrete rather than continuous momenta.) Thus the energies of the lightest excited states, $E_i(l)$, will converge to the absolute ground state energy, $E_0(l)$, at large l:

$$E_i(l) \stackrel{l\to\infty}{=} E_0(l) + O\left(\frac{\pi}{l}\right). \tag{1}$$

If, on the other hand, we excite a massive mode, e.g. one associated with the intrinsic width of the flux tube, then we would expect a finite gap above the ground state:

$$E_j(l) = E_0(l) + O(\sqrt{\sigma}). \tag{2}$$

To easily locate a massive mode excitation it needs to be amongst the lightest few states and so we need to be looking at smaller values of l where $\pi/l \sim O(\sqrt{\sigma})$, and the gaps between the lightest states are not small.

As we reduce l, we eventually encounter a phase transition to a phase where we no longer have a confining flux tube. This occurs at a critical length $l = 1/T_c$ where T_c is the deconfining temperature of the gauge theory. If we were to view x as our Euclidean time coordinate then this would be nothing but the usual finite temperature deconfining transition. Of course, we view x as a spatial coordinate, but a change of name cannot influence the presence of the phase transition, although it does affect how we interpret it. We will loosely refer to it as a finite-volume deconfining transition, although it is in fact only deconfining in the (x,t) plane: Wilson loops in the (y,t) plane continue to display an area law (just like the 'spatial' Wilson loops in the usual deconfined phase). Thus we can discuss the spectrum of our closed flux tubes only for $l > l_c = 1/T_c$. We recall [6] that $T_c \sim \sqrt{\sigma}$ for $D = 2+1$ SU(N) gauge theories, so this lower bound on l is $l_c\sqrt{\sigma} \sim 1$.

The eigenstates of such a closed flux tube can be labelled by a number of quantum numbers. Some of these we will not explore. For example, we could consider flux in representations other than the fundamental, e.g. k-strings [7, 3], but we will not do so here. Again, our flux tube could wind around the x-torus any number w of times: but we shall restrict ourselves to

$w = 1$. It could simultaneously wind around more than one spatial torus, but we do not analyse this case. Our flux tube could have an arbitrary transverse momentum $p_\perp$, but we expect that this would merely lead to $E^2(p_\perp) = E^2(0) + p_\perp^2$, so we will confine ourselves to states with $p_\perp = 0$. For $N > 2$ we have charge-conjugation, C, which reverses the direction of the flux. Since a flux tube cannot reverse the direction of the flux as it evolves in time, states with $C = \pm$ will be degenerate and this quantum number is not interesting for our purposes.

The quantum numbers we do explore are as follows.

• The longitudinal momentum p along the flux tube, i.e. in the x-direction. By periodicity this is quantised, $p = 2\pi q/l$ where q is an integer. We expect that the absolute ground state, with energy $E_0(l)$, is invariant under longitudinal translations, and so must have longitudinal momentum $p = 0$. To have $p \neq 0$ a flux tube must have a deformation so that it is not invariant under longitudinal translations. That is to say, it must be excited in some non-trivial way. Thus we do not simply have $E_0^2(p) = E_0^2(0) + p^2$, and the calculated value of $E(p)$ carries non-trivial dynamical information.

• The 2 dimensional parity operation P: $(x, y) \stackrel{P}{\to} (x, -y)$. We expect that the absolute ground state, with energy $E_0(l)$, is invariant under reflection in y, and so will have $P = +$ (with the $P = -$ linear combination being null). The lightest non-null $P = -$ state must involve a flux-tube with a non-trivial deformation, and so P is also an interesting quantum number.

• We can consider rotations in the (x, y) plane. Since we are on a spatial 2-torus we are at most interested in rotations that are an integer multiple of $\pi/2$. Moreover, since the orthogonal y-torus is effectively infinite, we are only interested in the rotation by π, i.e. R_π. Amongst other things this will reverse the direction of the flux, but this we can undo using charge conjugation. If we also apply P then all this corresponds to a reflection in x, i.e. $(x, y)\to(-x, y)$, followed by C. We shall call this our reflection parity, P_r. It clearly reverses the longitudinal momentum, and so is only useful for states with $p = 0$.

The main difference between closed flux tubes in $D = 2 + 1$ and $D = 3 + 1$ is that the latter also carry angular momentum. Another difference is that in $D = 2 + 1$ the deconfining transition is second order for SU(2) and SU(3), weakly first order for SU(4), and only becomes robustly first order for $N \geq 5$ [6], whereas in $D = 3 + 1$ it is already first order for SU(3) [8]. Since the behaviour of flux tubes of length l will be governed by the critical exponents of the second order transition as l approaches $l_c = 1/T_c$, and these are given by the universality class of a spin model in one lower dimension, we need to consider at least $N \geq 4$ or possibly $N \geq 5$ if we wish to investigate the large-N stringy behaviour of flux tubes down to values of l that are close to l_c. A further, but minor, difference is that the critical deconfining length scale is larger, $l_c\sqrt{\sigma} \sim 1.5$, in $D = 3 + 1$ [8] than it is in $D = 2 + 1$ [6], where $l_c\sqrt{\sigma} \sim 1$. So in $D = 2 + 1$ we can access significantly shorter flux tubes than in $D = 3 + 1$. We also recall that in $D = 2 + 1$ the coupling, g^2, has dimensions of mass. So the perturbative expansion parameter on the length scale l will be lg^2. Thus the theory is strongly coupled in the infrared and becomes rapidly free in the ultraviolet. This also has the consequence that the static potential is already confining, logarithmically, in perturbation theory. Indeed it also has a linear perturbative piece at $O(g^4)$, but the value [9] of this perturbative 'string tension' is not

very close to the observed lattice value [10]. This is no surprise given that yet higher orders in g^2 lead to yet higher powers in l, which is unphysical [11], and so this perturbative expression clearly cannot be used once $lg^2N > 1$.

At low N the spectrum will be complicated by mixing and decay. For example, a flux tube can emit and absorb a virtual glueball. In terms of the string world sheet swept out by the evolution of a flux tube, this means that we have to include surfaces of higher genus, with handles on all length scales. An effective string action for such world sheets is much more challenging [12] than one for world sheets of minimal topology, with fluctuations only on long wavelengths. The latter occurs for long flux tubes at large N, where the glueball emission vertex vanishes, flux tube states do not mix and there are no interactions between flux tubes. Thus we will attempt to calculate the closed flux tube spectrum at large N. In particular, the new calculations described in this paper are for SU(6) which for our purposes is 'close to' $N = \infty$.

2.2 Nambu-Goto spectrum

The simplest string theory is Nambu-Goto (in flat space-time) which is just a theory of free strings. While not consistent in 2+1 or 3+1 dimensions, its anomalies do not appear to affect the spectrum of long strings (see e.g. [13]). Moreover it is simple enough that the energy spectrum has been long known [14]. It is of particular interest to us because, as we have seen in our earlier work [1, 3], the flux tube spectrum is described remarkably well by its predictions, even when the flux tube length l is not much greater than the minimum, deconfining length l_c. Here we briefly summarise the aspects of the Nambu-Goto spectrum that will be useful for us in this paper.

The only degrees of freedom are the massless transverse fluctuations. Let $h(x,t)$ label the transverse displacement of the string at position x and at time t (i.e. we work in 'static gauge'). We write a Fourier decomposition of these transverse fluctuations and then quantise, thus promoting the Fourier coefficients to creation and annihilation operators. These represent 'phonons' running along the string in the +ve or -ve x-direction. We denote by $a_{\pm k}$ the creation operator for a phonon of momentum $p = \pm 2\pi k/l$ with k a positive integer. (Recall $h(x)$ has periodicity l.) The energy of the phonon is $\omega = |p| = 2\pi k/l$, since the mode is massless. The absolute ground state $|0\rangle$ has no phonons, but its energy acquires a correction from the zero mode contributions of all these oscillators.

The spectrum is then as follows. Call the positive momenta left-moving (L) and the negative ones right-moving (R). Let $n_{L(R)}(k)$ be the number of left(right) moving phonons of momentum $|p| = 2\pi k/l$. If we define the total energy of the left(right) moving phonons to be $2\pi N_{L(R)}/l$, then:

$$N_L = \sum_k n_L(k)k, \qquad N_R = \sum_k n_R(k)k. \tag{3}$$

If we define $p = 2\pi q/l$ to be the total longitudinal momentum of the string then, since it is the phonons that provide the momentum, we have

$$N_L - N_R = q. \tag{4}$$

We can now write down the expression for the energy levels of the Nambu-Goto string in $D = 2 + 1$ as

$$E^2_{N_L,N_R}(q,l) = (\sigma l)^2 + 8\pi\sigma\left(\frac{N_L + N_R}{2} - \frac{1}{24}\right) + \left(\frac{2\pi q}{l}\right)^2 \tag{5}$$

where the $1/24$ term arises from the oscillator zero-point energies. These energy levels have, in general, a degeneracy which depends on the number of ways the particular values of N_L and N_R can be formed from the n_L and n_R in eqn(3).

Under our parity $(x, y) \to (x, -y)$, so $h(x) \to -h(x)$ and $a_k \to -a_k$. Thus the parity of a state is simply given by the total number of phonons:

$$P = (-1)^{number\ of\ phonons}. \tag{6}$$

Under P_r, the symmetry that combines a reflection in x with charge conjugation, the individual phonon momenta are reversed, as is the overall momentum. Thus this quantum number is only useful in the $p = 0$ sector and here the lightest non-null pair of states with $P_r = \pm$ is $\{a_2a_{-1}a_{-1} \pm a_1a_1a_{-2}\}|0\rangle$ and is quite heavy. In practice this means that this quantum number is of minor utility in our calculations and we shall ignore it in the labelling of our states (but will return to it later).

In Table 1 we list a number of the lightest states of the Nambu-Goto model, labelling them by their momentum, $p = 2\pi q/l$, and parity, P. Note that in the $q = 0$ sector the very lightest states have reflection parity $P_r = +$, with the corresponding $P_r = -$ linear combinations being null. In the case of the heavier states, with $N_L = N_R \geq 2$, some can be paired into non-null linear combinations with $P_r = \pm$, and then it is these states that one should compare to the numerically determined spectrum. (This only has relevance when analysing corrections to Nambu-Goto that split the degeneracy of such an energy level.)

We note that if we take the square root of both sides of the energy in eqn(5), then the resulting expression can be expanded as a series in $1/\sigma l^2$. Assuming $p = 0$ for simplicity, one has

$$\begin{aligned} E_n(l) \quad &= \quad \sigma l\left(1 + \frac{8\pi}{\sigma l^2}\left(n - \frac{1}{24}\right)\right)^{\frac{1}{2}} \\ &\overset{l\sqrt{\sigma}\to\infty}{=} \quad \sigma l + \frac{4\pi}{l}\left(n - \frac{1}{24}\right) + O\left(\frac{1}{\sigma l^3}\right) \end{aligned} \tag{7}$$

where $n = (N_L + N_R)/2 = N_R = N_L$. Here the second term is the universal Lüscher correction [15]. We also see from eqn(5) that the ground state, $E_0(l)$, becomes tachyonic for $\sigma l^2 < \pi/3$ signalling a change of phase, which one might in the present context interpret as a deconfining Hagedorn transition. Of course, in the real world the large-N deconfining transition is first order and occurs for $l_c^2\sigma > \pi/3$ so such a tachyonic transition does not appear for any physically realisable value of the flux tube length, l. (But see [16].)

2.3 Effective string action

In this Section we shall begin with a sketch of the current status of analytic attempts to determine the effective string action for closed flux tubes. We shall focus on work directly

N_L, N_R	q	P	String State
$N_L = N_R = 0$	0	+	$\|0\rangle$
$N_L = 1, N_R = 0$	1	−	$a_1\|0\rangle$
$N_L = N_R = 1$	0	+	$a_1 a_{-1}\|0\rangle$
$N_L = 2, N_R = 0$	2	+	$a_1 a_1\|0\rangle$
		−	$a_2\|0\rangle$
$N_L = 2, N_R = 1$	1	+	$a_2 a_{-1}\|0\rangle$
		−	$a_1 a_1 a_{-1}\|0\rangle$
$N_L = 3, N_R = 0$	3	+	$a_2 a_1\|0\rangle$
		−	$a_3\|0\rangle$
		−	$a_1 a_1 a_1\|0\rangle$
$N_L = N_R = 2$	0	+	$a_2 a_{-2}\|0\rangle$
		+	$a_1 a_1 a_{-1} a_{-1}\|0\rangle$
		−	$a_2 a_{-1} a_{-1}\|0\rangle$
		−	$a_1 a_1 a_{-2}\|0\rangle$
$N_L = 3, N_R = 1$	2	+	$a_3 a_{-1}\|0\rangle$
		+	$a_1 a_1 a_1 a_{-1}\|0\rangle$
		−	$a_2 a_1 a_{-1}\|0\rangle$
$N_L = 4, N_R = 0$	4	+	$a_3 a_1\|0\rangle$
		+	$a_2 a_2\|0\rangle$
		+	$a_1 a_1 a_1 a_1\|0\rangle$
		−	$a_4\|0\rangle$
		−	$a_2 a_1 a_1\|0\rangle$
$N_L = 3, N_R = 2$	1	+	$a_3 a_{-2}\|0\rangle$
		+	$a_2 a_1 a_{-1} a_{-1}\|0\rangle$
		+	$a_1 a_1 a_1 a_{-2}\|0\rangle$
		−	$a_3 a_{-1} a_{-1}\|0\rangle$
		−	$a_2 a_1 a_{-2}\|0\rangle$
		−	$a_1 a_1 a_1 a_{-1} a_{-1}\|0\rangle$
$N_L = 4, N_R = 1$	3	+	$a_4 a_{-1}\|0\rangle$
		+	$a_2 a_1 a_1 a_{-1}\|0\rangle$
		−	$a_3 a_1 a_{-1}\|0\rangle$
		−	$a_2 a_2 a_{-1}\|0\rangle$
		−	$a_1 a_1 a_1 a_1 a_{-1}\|0\rangle$
$N_L = 5, N_R = 0$	5	+	$a_4 a_1\|0\rangle$
		+	$a_3 a_2\|0\rangle$
		+	$a_2 a_1 a_1 a_1\|0\rangle$
		−	$a_5\|0\rangle$
		−	$a_3 a_1 a_1\|0\rangle$
		−	$a_2 a_2 a_1\|0\rangle$
		−	$a_1 a_1 a_1 a_1 a_1\|0\rangle$
$N_L = 3, N_R = 3$	0	+	$a_3 a_{-3}\|0\rangle$
		+	$a_2 a_1 a_{-2} a_{-1}\|0\rangle$
		+	$a_1 a_1 a_1 a_{-1} a_{-1} a_{-1}\|0\rangle$
		+	$a_1 a_1 a_1 a_{-3}\|0\rangle$
		+	$a_3 a_{-1} a_{-1} a_{-1}\|0\rangle$
		−	$a_3 a_{-2} a_{-1}\|0\rangle$
		−	$a_2 a_1 a_{-3}\|0\rangle$
		−	$a_2 a_1 a_{-1} a_{-1} a_{-1}\|0\rangle$
		−	$a_1 a_1 a_1 a_{-2} a_{-1}\|0\rangle$
$N_L = 4, N_R = 2$	2	+	$a_4 a_{-2}\|0\rangle$
		+	$a_3 a_1 a_{-1} a_{-1}\|0\rangle$
		+	$a_2 a_2 a_{-1} a_{-1}\|0\rangle$
		+	$a_2 a_1 a_1 a_{-2}\|0\rangle$
		+	$a_1 a_1 a_1 a_1 a_{-1} a_{-1}\|0\rangle$
		−	$a_4 a_{-1} a_{-1}\|0\rangle$
		−	$a_3 a_1 a_{-2}\|0\rangle$
		−	$a_2 a_2 a_{-2}\|0\rangle$
		−	$a_2 a_1 a_1 a_{-1} a_{-1}\|0\rangle$
		−	$a_1 a_1 a_1 a_1 a_{-2}\|0\rangle$
$N_L = 5, N_R = 1$	4	+	$a_5 a_{-1}\|0\rangle$
		+	$a_3 a_1 a_1 a_{-1}\|0\rangle$
		+	$a_2 a_2 a_1 a_{-1}\|0\rangle$
		+	$a_1 a_1 a_1 a_1 a_1 a_{-1}\|0\rangle$
		−	$a_4 a_1 a_{-1}\|0\rangle$
		−	$a_3 a_2 a_{-1}\|0\rangle$
		−	$a_2 a_1 a_1 a_1 a_{-1}\|0\rangle$

Table 1: Table with the states of the lowest Nambu-Goto levels with $q = 0, 1, 2, \ldots, 5$ and $N_L + N_R \leq 6$.

related to the subject of this paper. We shall also point to relevant numerical work that has appeared over the last year or two. For earlier work we refer the reader to the literature quoted in these papers and in [2, 5]. Finally we briefly comment on our earlier paper [1] and specifically on those aspects that are superseded by the present analysis.

Consider a flux tube that is wrapped around the x-torus and propagates around the (Euclidean) time torus. It will sweep out a surface that is a simple 2-torus, at least if we are in the large-N limit where handles and higher genus surfaces are suppressed. If we have an effective string action for such surfaces, $S_{eff}[S]$, then we can calculate the path integral over all such surfaces, $Z_{torus}(l,\tau)$, where l and τ are the sizes of the x and t tori. This should equal the partition function of the closed flux tubes in this large-N gauge theory:

$$Z_{torus}(l,\tau) = \int_{T^2=l\times\tau} dS e^{-S_{eff}[S]} = \sum_{n,p} e^{-E_n(p,l)\tau} \tag{8}$$

where $E_n(p,l)$ is the energy of the n'th flux tube state of length l and of momentum p (which now also includes transverse momenta). Thus the effective string action predicts the spectrum of such closed flux tubes. On the other hand Lorentz invariance constrains the p-dependence of $E_n(p,l)$ and this in turn will constrain the possible form of S_{eff} [17, 18]. More generally, the conformal invariance of the effective string action [12] can also be used to constrain its form [19].

It was realised long ago that the leading $O(1/l)$ correction to the linear σl piece of $E_n(l)$ is in fact universal – the 'Lüscher correction' [15]. This corresponds to noting that if we write the effective string action in 'static gauge' and express it in a series of powers of the derivative of the transverse fluctuation field $h(x)$, then the leading Gaussian kinetic term for h gives this universal $O(1/l)$ contribution to $E_n(l)$. Much more recently it was found [17] that the next term in the derivative expansion of $S_{eff}[h]$ is universal, so that the next term in an expansion of $E_n(l)$, at $O(1/l^3)$, is also universal. This was also shown [19], at much the same time, and with a stronger result in $D = 3+1$, using the Polchinski-Strominger conformal gauge approach [12]. More recently there has been further progress [4] in both $D = 2+1$ and $D = 3+1$. (See also [20].) In particular, in $D = 2+1$ it is now known that the $O(1/l^5)$ term is also universal. The physical constraints that are used to derive this universality are satisfied by the Nambu-Goto model, so that we can write

$$\frac{E_n(l)}{\sqrt{\sigma}} \stackrel{l\to\infty}{=} l\sqrt{\sigma} + \frac{c_1^{NG}}{l\sqrt{\sigma}} + \frac{c_2^{NG}}{(l\sqrt{\sigma})^3} + \frac{c_3^{NG}}{(l\sqrt{\sigma})^5} + O\left(\frac{1}{l^7}\right) \tag{9}$$

where the coefficients c_i^{NG} are identical to those that arise in the expansion of E in powers of $1/l$ in the Nambu-Goto model, as in eqns(7).

An especially interesting result for us is the demonstration that all the operators that appear in the derivative expansion of the Nambu-Goto action appear with precisely the same coefficients in the general effective string action [4]. This provides a motivation for regarding $S_{eff}[h]$ as being given, in a non-trivial sense, by the full Nambu-Goto action plus a series of 'corrections': in particular at small l where the expansion of the Nambu-Goto energy diverges and needs to be resummed as in eqn(7). This result is particularly significant in view of the

numerical calculations [1, 2] that have shown that the spectrum of flux tubes of moderate l is close to the resummed Nambu-Goto prediction.

The above summarises the essential theoretical background for the analysis in this paper. There has of course been a great deal of theoretical and, particularly, numerical work on this and related problems, but most of that can be followed through the references in the papers we have quoted and we do not repeat them here. There are however a number of relevant papers that have appeared during the past year or so, which we would like to point the reader to. Most directly relevant is [21] where the static confining potential is calculated in the 3d Ising model and the term corresponding to the $O(1/l^5)$ term in our above discussion is found not to take the expected universal value. The authors discuss possible reasons for this, but it is obviously something that needs to be understood. Again in [22] the corresponding term in the finite temperature expansion of the string tension in a gauge dual of d3 random percolation is found not to take the universal Nambu-Goto value. (Note that this paper predates [4] and so does not comment on the expected universality of this term.) Our expectation that there should be massive modes is closely linked to the idea that the flux tube has an intrinsic width, and there have been papers calculating that at both zero and non-zero T in some confining field theories as well as ideas how to go about doing so [23]. There are interesting extensions to finite T [24], attempts to see to what scale the effective string action is valid [25], and a calculation of the excitations of the static potential in $D = 2 + 1$ [26]. There have also been some interesting calculations from the gauge-gravity side, on the flux tube intrinsic width [27] and on the Wilson line and Coulomb potential [28].

3 Background

3.1 Lattice and continuum

Our $D = 2+1$ Euclidean space-time is discretised to a periodic cubic $L_x \times L_y \times L_t$ lattice with lattice spacing a. The degrees of freedom are SU(N) matrices, $U_\mu(x, y, t)$ or more compactly U_l, assigned to the links l of the lattice. Our action is the standard (Wilson) plaquette action, so the partition function is

$$Z(\beta) = \int \prod_l dU_l \, e^{-\beta \sum_p \{1 - \frac{1}{N} \mathrm{ReTr} U_p\}} \tag{10}$$

where U_p is the ordered product of matrices around the boundary of the elementary square (plaquette) labelled by p. Taking the continuum limit of eqn(10), and comparing to the usual continuum path integral, one finds that

$$\beta \stackrel{a \to 0}{=} \frac{2N}{ag^2} \tag{11}$$

where g^2 is the coupling. In $D = 2 + 1$ g^2 has dimensions of mass, and so ag^2 is the dimensionless coupling on the length scale a. The continuum limit, $a \to 0$, is therefore approached by tuning $\beta = 2N/ag^2 \to \infty$.

If we calculate some physical masses (or energies) on the lattice, they will have lattice corrections and they will be in lattice units, i.e. we will obtain them as $am_i(a)$. To obtain the continuum limit one can take ratios of masses, calculate these over some substantial range of a, and extrapolate to $a = 0$, using the leading correction that is known to be $O(a^2)$ for our plaquette action:

$$\frac{am_i(a)}{am_j(a)} = \frac{m_i(a)}{m_j(a)} \stackrel{a\to 0}{=} \frac{m_i(0)}{m_j(0)} + c(a\mu)^2. \tag{12}$$

Here we can use $a\mu = am_i(a)$ or any other calculated mass – different choices correspond to different subleading $O(a^4)$ corrections in eqn(12), which we neglect. Obviously all this assumes that a is sufficiently small for the leading $O(a^2)$ correction to dominate. If this is not the case, i.e. if the fit using eqn(12) is found to be unacceptably poor, one can systematically drop the mass ratios coming from the largest values of a, i.e. the smallest values of β, until the fit becomes good. In practice one finds [29] that the approach to the continuum limit for typical dynamical quantities is very rapid.

An alternative approach is to calculate the continuum value of m_i/g^2, using eqn(11) and

$$\frac{\beta}{2N} am_i(a) \stackrel{a\to 0}{=} \frac{m_i(0)}{g^2} + \frac{c}{\beta}, \tag{13}$$

where again we have retained only the leading correction. The lattice correction is $O(1/\beta) \propto O(a)$ rather than $O(a^2)$ because different lattice coupling definitions will clearly differ at this order. In this way one can, for example, calculate the continuum string tension in units of g^2 [29, 10].

3.2 Large-N limit

One expects that at large N physical masses will be proportional to the 't Hooft coupling $\lambda \equiv g^2N$ with a leading correction that is $O(1/N^2)$ [30], i.e.

$$\frac{m_i}{g^2N} = \lim_{N\to\infty} \frac{m_i}{g^2N} + \frac{c}{N^2} \tag{14}$$

to leading order. So if we vary $\beta \propto N^2$ we will be keeping the lattice spacing a fixed in physical units, to leading order in N. These expectations are largely based on an analysis of all-orders perturbation theory, so it is interesting to ask how precisely they are confirmed by non-perturbative lattice calculations. This question has been addressed in the past [29, 31], but here we can go somewhat further using the very precise string tensions calculated for $N \in [2, 8]$ in [10]. We display in Fig. 1 the continuum values of $\sqrt{\sigma}/g^2N$ taken from the first row of Table 2 in [10]. (Using the values in the other rows would produce slightly larger errors but would lead to the same conclusions.) We also show in Fig. 1 the best fit of the conventional form, i.e. eqn(14) with $\sqrt{\sigma}$ replacing m_i:

$$\frac{\sqrt{\sigma}}{g^2N} = 0.19638(9) - \frac{0.1144(8)}{N^2}. \quad ; \quad \chi^2/ndf \sim 0.4 \tag{15}$$

Eqn(15) provides a very good fit to all our values of N, including SU(2). This is perhaps surprising given that higher order corrections in $1/N^2$ are surely present. To investigate this we can include an extra c'/N^4 term in eqn(15) and we then find $c' = 0.008(27)$, with little change in the first two terms. This indicates that in the $1/N^2$ expansion of $\sqrt{\sigma}/g^2N$ the coefficients decrease rapidly, so that the large-N limit is unexpectedly precocious.

If we now allow the power of the correction term in eqn(14) to vary we find

$$\frac{\sqrt{\sigma}}{g^2N} = c_0 + \frac{c_1}{N^\gamma} \qquad \longrightarrow \qquad \gamma = 1.97 \pm 0.10. \tag{16}$$

So if we assume that γ has to be an integer, we can unambiguously conclude that the leading correction is in fact $O(1/N^2)$, just as predicted by 't Hooft's diagrammatic analysis [30]. Let us now allow the leading power of N to vary, i.e. $g^2N \to g^2N^\alpha$, then we find

$$\frac{\sqrt{\sigma}}{g^2N^\alpha} = c_0 + \frac{c_1}{N^2} \qquad \longrightarrow \qquad \alpha = 1.002 \pm 0.004. \tag{17}$$

Thus if we assume a $O(1/N^2)$ correction, the lattice values of the string tension tell us that $g^2 \propto 1/N^{1.002(4)}$ i.e. the conventional expection of $g^2 \propto 1/N$ is confirmed very accurately. Finally, if we allow both powers to vary, then

$$\frac{\sqrt{\sigma}}{g^2N^\alpha} = c_0 + \frac{c_1}{N^\gamma} \quad \longrightarrow \quad \alpha = 1.008 \pm 0.015 \ , \ \gamma = 2.18 \pm 0.40. \tag{18}$$

The constraint on the power of the correction is now significantly looser, but the evidence for $g^2 \propto 1/N$ is still very convincing. Altogether, we can conclude that these lattice calculations provide strong support for the non-perturbative validity of the usual large-N counting.

3.3 Calculating the spectrum

To calculate the spectrum, we calculate the correlation functions of some suitable (see below) set of lattice operators $\{\phi_i\}$. Expanding the correlators in terms of the energy eigenstates, $H|n\rangle = E_n|n\rangle$ and expressing $t = an_t$ in lattice units, we have

$$C_{ij}(t) = \langle \phi_i^\dagger(t)\phi_j(0)\rangle = \langle \phi_i^\dagger e^{-Han_t}\phi_j\rangle = \sum_k c_{ik}c_{jk}^\star e^{-aE_kn_t} \tag{19}$$

where $c_{ik} = \langle vac|\phi_i^\dagger|k\rangle$. We can now perform a variational calculation of the spectrum as follows. Suppose that $\phi = \psi_0$ maximises $\langle\phi^\dagger(t')\phi(0)\rangle/\langle\phi^\dagger(0)\phi(0)\rangle$ over the vector space spanned by the $\{\phi_i\}$. (Obviously we can restrict the $\{\phi_i\}$ to a desired set of quantum numbers.) Here t' is some convenient small value of t, where all our $C_{ij}(t)$ are known quite precisely, and which we shall typically choose to be $t = a$. Then ψ_0 is our best estimate of the wave-functional of the ground state. Repeating this calculation over the basis of operators orthogonal to ψ_0 gives us ψ_1, our best estimate for the first excited state. And so on for the higher excited states. If our basis is large enough for ψ_i to be close to the true wave-functional, Ψ_i, then its

correlator should be dominated by the corresponding state, $\langle\psi_i^\dagger(t)\psi_i(0)\rangle \propto \exp(-E_i t)$, even for small values of t, where the signal to noise ratio is large and where we are able to extract an accurate value for the energy, aE_i.

Here the states that we are interested in are loops of flux closed around the x-torus. Thus our operators will also wind around the x-torus. The simplest such operator is the Polyakov loop

$$l_p(n_y, n_t) = \mathrm{Tr}\left\{\prod_{n_x=1}^{L_x} U_x(n_x, n_y, n_t)\right\} \tag{20}$$

where $l = aL_x$ and we have taken the product of the link matrices in the x-direction, around the x-torus. (We recall a standard argument that uses the fact that the gauge potentials are only periodic up to an element of the centre of the SU(N) group, to show that in the confining phase $\langle\phi_c\, l_p\rangle = 0$ for any contractible loop ϕ_c, thus showing that such a winding operator has zero projection onto glueball states.) The operator in eqn(20) is localised in n_y and so has transverse momentum $p_\perp \neq 0$. If we sum over n_y, to get $l_p(n_t) = \sum_{n_y} l_p(n_y, n_t)$, then we obtain an operator with $p_\perp = 0$, and from now on we assume this has been done. This operator is manifestly invariant under longitudinal translations, so $p = 0$. It is also invariant under parity P. So in order to have $p \neq 0$ or $P \neq +$ we must introduce a deformation into the operator defined in eqn(20). For this purpose we choose the deformations displayed in Table 2. Now, if we translate an operator by Δx in the x direction, multiply it by the phase factor $\exp\{i2\pi q\Delta x/l\}$ where q is an integer, and then add all such translations, we obtain an operator with longitudinal momentum $p = 2\pi q/l$. If we had done so with $p \neq 0$ to the simple Polyakov loop in eqn(20), we would have obtained a null operator. But for the other operators in Table 2 this will not, in general, be the case.

In practice, to obtain good overlaps onto any states at all, one needs to smear [32] and/or block [33] the 'link matrices' that appear in the operators in Table 2. Taking into account the various blocking levels, our typical basis has ~ 80 operators for each set of quantum numbers. (In our newer calculations we have not included the wavelike operators shown in box 2 of Table 2 since we found in our earlier calculations that they have $\sim 100\%$ overlap onto our simple blocked line operators in box 1 and therefore bring nothing new to the calculation.)

3.4 Control of systematic errors

The systematic errors in $D = 2+1$ are much the same as in $D = 3+1$ and the latter have been discussed in some detail in our recent companion paper [2]. In $D = 2+1$ our operator basis has a much better overlap onto the light flux tube states of interest, and so many of the systematic errors will be much smaller. We will not repeat here the full discussion in [2], some of which has been covered in our earlier $D = 2+1$ papers [1, 10], but will comment on three particular issues.

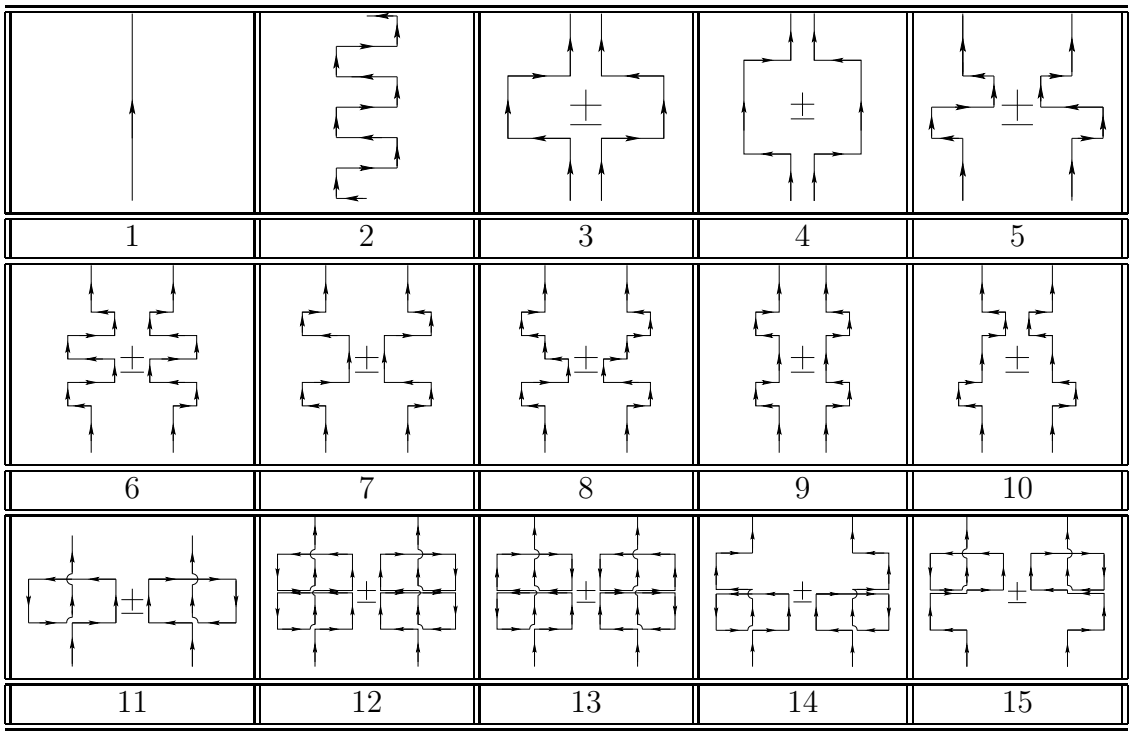

Table 2: The lattice paths used in the construction of Polyakov loops in this work. Our set of operators can be divided into three subsets: (a) the simple line operator (1) in several smearing/blocking levels; (b) the wave-like operator (2) whose number depends upon L_x, $L_\perp$, and the smearing/blocking level; (c) the pulse-like operators (3-15) in several different smearing/blocking levels. In addition the extent of the transverse deformations is varied. The $\pm$ combinations correspond to $P = \pm$. The operators in (1) and (2) are intrinsically $P = +$.

3.4.1 effective energies

We calculate energies by identifying the asymptotic exponential fall-off of correlation functions $\langle\psi_i^\dagger(t)\psi_i(0)\rangle$, as described above. Typically the statistical error is roughly constant in t, so the error/'signal' ratio grows exponentially with t. This means that we need to extract the energy at small t. So one requirement is that our best variational wavefunction ψ_i should have a high overlap onto the state $|i\rangle$, so that the corresponding exponential, $|c_i|^2 \exp\{-aE_i n_t\}$, already dominates the sum in

$$\langle\psi_i^\dagger(t)\psi_i(0)\rangle = \sum_k |c_{ik}|^2 e^{-aE_k n_t} \tag{21}$$

at small $t = an_t$. An additional requirement is that aE_i should be small enough that we can accurately identify such an exponential fall-off over a sufficient range of $t = an_t$ for us to be able to estimate aE_i, and indeed the overlap. That is to say, as the energy of interest becomes larger, both the statistical and systematic errors become larger.

To illustrate this systematic error we define an effective energy obtained by doing a local

exponential fit to neighbouring values of the correlation function:

$$e^{-aE_{i,eff}(n_t)} = \frac{\langle \psi_i^\dagger(n_t)\psi_i(0)\rangle}{\langle \psi_i^\dagger(n_t-1)\psi_i(0)\rangle} \tag{22}$$

It is apparent from eqn(21) that if $|i\rangle$ is the lightest state in some quantum number sector, then as n_t grows $E_{i,eff}(n_t)$ decreases and approaches E_i. So we can identify E_i when the values of $E_{i,eff}(n_t)$ form a plateau in n_t. If ψ_i is not a ground state it may contain some small component of a lower energy state, and then at larger n_t it will decrease to the corresponding lower plateau. This may create ambiguities which we note are absent for the lowest energy state of any given quantum numbers.

In Fig. 2 we display the values of $aE_{eff}(n_t)$ for a number of states from our SU(6) calculation at $\beta = 171$. The open circles are for the absolute $p = 0, P = +$ ground state, for flux tube lengths $l/a = 16, 24, 32, 64$. For all but the largest E, the statistical errors are invisible on this plot except at large n_t. The horizontal red lines are the extracted energies. We note how once the errors become large, at larger n_t, the points have a tendency to drift away from the plateau value. Nonetheless, even for $l = 64a$ where the plateau is shorter, it is clear that the calculation of $aE_0(l)$ is unambiguous and under good control. This is aided by the fact that the plateau begins at very small n_t: the overlaps are close to 100%.

The solid circles in Fig. 2 represent the 1st, 2nd and 3rd excited states of a flux tube with $p = 0, P = +$ and with a length $l/a = 32$. The lightest of these is still well determined, but the two higher excited states begin to demonstrate the joint problem of a less good overlap and larger energy making the identification of a plateau less clear-cut. In fact the normalised overlap of the second state is $|c_i|^2 \sim 0.9$. This problem becomes more pronounced for the lightest two states with $p = 0, P = -$ which are represented by the open diamonds. Here the identification of an energy plateau is still plausible, but we are clearly leaving the area of certainty. We note that the upper of the two states has an overlap $|c_i|^2 \sim 0.8$.

As we can see from the latter cases, if the overlap is smaller, there is a greater contribution from higher excited states at smaller n_t, so that the effective energy at those n_t appears larger. If the overlap is very small then the 'signal' will disappear into the statistical errors long before we reach large enough n_t to see an energy plateau, and we are then left with what appears to be an ill-defined but highly excited state. Roughly speaking, it is very hard to identify states with an overlap of less than $|c_i|^2 \sim 0.5$, and the energy calculation typically becomes difficult for $|c_i|^2 \leq 0.75$. As a good example of this, we expect any state that involves multi-trace operators to have a much smaller overlap onto our single trace operators than this, and to be completely invisible in our variational calculation. So a state consisting of the ground state flux tube accompanied by the lightest scalar glueball, although it is certainly present and although it is well within the range of the energies we study, at least at smaller l, does not appear in the spectrum we calculate. That is to say, for larger N all our states are composed of single closed flux tubes, that sweep out surfaces of the lowest genus.

In summary: the examples in Fig. 2 show that while our results in this SU(6) calculation are mostly under very good control, this control begins to slip for the states with highest energies, particularly when such a state is not the ground state of some quantum numbers.

The reader should bear this caveat in mind, although the detailed fits from which we attempt to draw quantitative conclusions will involve those states over which we believe we do have good control.

3.4.2 finite volume corrections

When we perform spectrum calculations of flux tubes of length l on $l \times l_\perp \times l_t$ lattices, it is important to make sure that corrections due to the finite transverse spatial size, $l_\perp$, and the finite temporal extent, l_t, are negligible. In our previous papers we have described tests of such corrections in some detail, and the volumes used in this paper have been chosen accordingly. However most of those tests were done with a small basis of operators, which allowed us to calculate the absolute ground state but did not allow an accurate determination of excited states. Since (some) excited states will have a larger total 'width' than the ground state, and hence might be more sensitive to the transverse boundaries (the temporal extent is not a problem here), we have performed a small selection of calculations with our full operator basis and with our usual statistics, so that we can test for finite volume effects at a level of accuracy appropriate to most of our calculations.

The test we do is in SU(3) at $\beta = 21$. Since many of the finite volume effects are suppressed with increasing N, by looking at $N = 3$ we are being deliberately conservative. Moreover as we reduce l towards l_c we expect the flux tube 'width' to diverge since, for $N \leq 3$, this is a critical point where the correlation length diverges. In our SU(6) calculation, the transition is robustly first order, and the finite volume corrections at small values of l should be much smaller than for SU(3).

We have performed calculations for two values of l, one moderately short, $l = 12a$, and one moderately long, $l = 20a$. In physical units these lengths correspond to $l\sqrt{\sigma} \simeq 2.0$, 3.5 respectively. We have not performed calculations for very small values of $l_\perp$ where the corrections will undoubtedly be large, but rather have compared results obtained with our 'standard' value of $l_\perp$ with those obtained with significantly larger $l_\perp$. We calculate the effective energy $E_{eff}(n_t)$ of a particular state using eqn(22) where the operator ψ_i is chosen by our variational calculation as the 'best' operator over our basis for this state. In practice our overlaps are good enough that the contribution of excited states to $aE_{eff}(n_t)$ is already very small for $t = a$, and often negligible for $t = 2a$. The calculations at such small values of t are very accurate and so even small finite volume corrections should be visible.

In Tables 3 and 4 we display the values of $E_{eff}(t = a)$ and $E_{eff}(t = 2a)$ for flux tubes of length $l = 12a$ and $l = 20a$ respectively. We do so for the lightest four states with $P = +$ and the lightest two with $P = -$. All this in SU(3) at $\beta = 21$ where $a\sqrt{\sigma} \simeq 0.174$. We show how the energies change when the transverse size is increased from $l_\perp = 18a$ to $22a$ to $28a$.

A preliminary aside is that in almost all cases the decrease in $E_{eff}(t)$ when we extract it from $t = 2a$ rather than $t = a$ is very small, at the $O(1\%)$ level. This confirms that our variationally selected operators are in fact very good wavefunctionals for these states.

Comparing the values of E_{eff} for different values of $l_\perp$, we see from Tables 3 and 4 that the change as we go from the smaller to the largest values of the transverse lattice size, is often invisible within errors (which are typically at the level of a fraction of a percent) and

$aE_{eff}(t, l = 12a)\ ,\ p = 0$					
P	state	t	$l_\perp = 28a$	$l_\perp = 22a$	$l_\perp = 18a$
+	1	a	0.3177(8)	0.3168(6)	0.3162(8)
		$2a$	0.3169(11)	0.3161(9)	0.3151(9)
+	2	a	0.9319(10)	0.9263(9)	0.9191(12)
		$2a$	0.9142(26)	0.9073(21)	0.9064(30)
+	3	a	1.2333(17)	1.2234(13)	1.2347(16)
		$2a$	1.1374(42)	1.1520(35)	1.1702(46)
+	4	a	1.3404(20)	1.3356(15)	1.3174(17)
		$2a$	1.3059(82)	1.2961(58)	1.2768(65)
-	1	a	1.3537(17)	1.3632(16)	1.3698(19)
		$2a$	1.2978(68)	1.3254(60)	1.3111(54)
-	2	a	1.4603(19)	1.4638(18)	1.4671(19)
		$2a$	1.3776(76)	1.3934(62)	1.3990(77)

Table 3: Effective energies extracted at $t = a$ and $t = 2a$ for the low-lying $p = 0$ and $P = \pm$ spectrum. For a short flux tube of length $l = 12a$, i.e. $l\sqrt{\sigma} \sim 2$, on lattices of transverse size $l_\perp$ (and temporal extent $l_t = 24a$).

where there might be some variation, it is almost always $< 1\%$. This check therefore provides us with important and convincing evidence that the finite volume corrections to our results in this paper are not significant.

3.4.3 approaching the critical point in SU(2)

When the 'deconfining' finite volume transition at $l = l_c$ is robustly first order, as it is for $N \geq 5$, it makes sense to compare the spectrum of closed flux tubes to the predictions of an effective string theory all the way down to $l = l_c$. However when the transition is second order one expects the behaviour of the spectrum as $l \to l_c$ to be governed by the critical exponents of the critical point. (Which might also influence a weakly first-order transition such as in SU(4).) For an SU(N) gauge theory in $D = 2 + 1$ these will be in the universality class of a Z_N spin model in two dimensions. That is to say, the behaviour of $E(l)$ will be governed by these critical exponents as $l \to l_c$ and we do not expect to obtain useful information about the generic effective string theory for SU(N) gauge theories by studying this limit in such a case.

That the ground state energy does indeed decrease as

$$E_0(l) \overset{l \to l_c^+}{\propto} (l - l_c)^\gamma \quad , \qquad \gamma = \begin{cases} 1 & SU(2) \\ \frac{5}{6} & SU(3) \end{cases} \tag{23}$$

was shown numerically a long time ago; see for example Fig 1 in [34] for the case of SU(2) and Fig 3 for an example in SU(3) [35]. It is interesting to see over what range of l the transition

$aE_{eff}(t, l = 20a)\ ,\ p = 0$				
P	state	t	$l_\perp = 22a$	$l_\perp = 28a$
+	1	a	0.5813(8)	0.5808(8)
		$2a$	0.5770(15)	0.5798(14)
+	2	a	1.0539(11)	1.0557(15)
		$2a$	1.0415(40)	1.0517(36)
+	3	a	1.3618(20)	1.3704(18)
		$2a$	1.3264(75)	1.3532(65)
+	4	a	1.3744(19)	1.3801(19)
		$2a$	1.3571(63)	1.3601(76)
-	1	a	1.4071(20)	1.4050(23)
		$2a$	1.3793(81)	1.3700(69)
-	2	a	1.4267(19)	1.4274(20)
		$2a$	1.3771(76)	1.3898(71)

Table 4: As in Table 3 but for a longer flux tube, $l = 20a$, i.e. $l\sqrt{\sigma} \sim 3.5$.

‘

from eqn(23) to something like the Nambu-Goto behaviour

$$E_0(l) \simeq E_0^{NG}(l) = \sigma l \left(1 - \frac{\pi}{3}\frac{1}{\sigma l^2}\right)^{\frac{1}{2}} \tag{24}$$

actually takes place. We analyse this for SU(2) where the location of the phase transition at $l_c\sqrt{\sigma} \simeq 0.9$ is significantly smaller than the value of l at which eqn(24) would imply that the state becomes tachyonic. The calculation [36] is with $l = 4a$ and this is varied by varying β (and hence a) in small increments. At each value of β the string tension is calculated in a separate calculation. As $aE_0(l)$ decreases, the other lattice dimensions are increased (ultimately up to $4 \times 72 \times 144$) so as to avoid finite volume corrections. The resulting values of $E_0/\sqrt{\sigma}$ are plotted against $1/l\sqrt{\sigma}$ in Fig 5. We also plot there the Nambu-Goto prediction in eqn(24) and the linear behaviour in eqn(23) that is predicted by universality. We see from Fig 5 that the transition between the critical and Nambu-Goto behaviours is very smooth and occurs at $l\sqrt{\sigma} \sim 1.2$, which is quite far from the critical point at $l_c\sqrt{\sigma} \sim 0.9$. It is interesting to note that if we expand the Nambu-Goto square root in eqn(24) and keep only the terms up to $O(1/l^5)$, which are the terms that have been shown to be universal for any effective string action [4], then we get the curve shown in Fig 5, which is quite close to the numerical values over the whole range of l. Finally we note that calculations like these have also been made for SU(3) [37] and for a percolation model [38].

4 Results

There are two main features of this paper that are new as compared to our earlier work [1]. (1) We have performed SU(6) calculations at $\beta = 171$, which corresponds to a small lattice spacing, comparable to that of our older SU(3) calculation at $\beta = 40$. In contrast to the latter, we cover a much wider range of flux tube lengths, $1.2 \leq l\sqrt{\sigma} \leq 5.5$. In addition, we cover a wider range of momenta. Altogether this is by far our 'best' calculation. And the fact that it is at larger N makes it of particular relevance, since the phase transition at $l = l_c$ is robustly first order, so that a simple effective string action might be applicable all the way down to l_c. (And indeed even somewhat below l_c if the metastability of the confined phase is strong enough [16].) Moreover mixings, decays, and higher genus contributions should be strongly suppressed.
(2) Our comparison with what one expects from an effective string action will take into account the important recent progress [4] described in Section 2.3.

We have also made some calculations in SU(4) and SU(5) at values of a that are intermediate between our large and small lattice spacings in SU(3) and SU(6). (These calculations were primarily performed to obtain higher representation $k = 2$ flux tube spectra [3].) We will occasionally comment upon these, but they will play a role that is very much secondary to our SU(6) analysis. Finally, we have some very high statistics calculations of the absolute ground state in SU(2) and SU(4) performed with a small basis of operators (and so not designed for extracting excited states).

In Table 5 we provide the values of some basic physical quantities, for each of the calculations in which we calculate the closed flux tube spectrum. In each case the string tension comes from fitting the ground state energy to the Nambu-Goto expression with a $O(1/l^7)$ correction, as expected from the most recent analytic analyses. (In actual fact the correction is so small that its particular form is not important to the extracted value of $a^2\sigma$.) The mass gap comes from [29, 31] and the critical length from calculations of the $D = 2+1$ deconfining temperature in [6]. In Table 6 we do the same for the SU(2) and SU(4) calculations that are dedicated to calculating the ground state.

Our earlier work [1], comparing the then available SU(3) and SU(6) spectra, provided good evidence that any a and N dependence was small. We will therefore initially assume this in our discussion of the ground state. That same work demonstrated that the simple Nambu-Goto free string spectrum is a remarkably good first approximation to the numerically determined spectrum, and we shall therefore focus upon that as our initial point of comparison.

We begin with an analysis of the absolute ground state. We then check for lattice corrections to the continuum limit, and for $O(1/N^2)$ corrections to the $N = \infty$ limit. We then move on to an overview of our results for the low-lying spectrum and follow that with a more detailed comparison with current theoretical expectations.

4.1 Absolute ground state

The energy $E_0(l)$ of the absolute ground state is our most easily and accurately calculated energy. However, because the string corrections to the linear piece, σl, come from the zero-

	β	$l/a \in$	$a\sqrt{\sigma}$	l_c/a	am_G
SU(3)	21.0	[8,32]	0.17392(11)	5.89(2)	0.760(7)
SU(3)	40.0	[16,48]	0.08712(10)	11.65(4)	0.381(3)
SU(4)	50.0	[12,24]	0.13084(21)	8.09(3)	0.563(2)
SU(5)	80.0	[12,32]	0.12976(11)	8.31(2)	0.548(3)
SU(6)	90.0	[8,24]	0.17184(12)	6.37(3)	0.738(4)
SU(6)	171.0	[14,64]	0.08582(4)	12.47(5)	0.367(2)

Table 5: Parameters of our flux tube spectrum calculations: the SU(N) group, the value of the inverse bare coupling, $\beta = 2N/ag^2$, and the range of flux tube lengths, l. Also listed are some of the corresponding physical properties: the string tension, σ, the deconfining length, l_c, and the mass gap, m_G, all in lattice units.

‘

	β	$l/a \in$	$a\sqrt{\sigma}$	l_c/a	am_G
SU(2)	5.6	[4,16]	0.27316(4)	3.43(3)	1.285(5)
SU(4)	32.0	[6,32]	0.21523(5)	4.98(1)	0.911(4)

Table 6: As in Table 5 but for the two high statistics calculations dedicated to the ground state of the flux tube.

‘

point energies of the string excitation modes, they are very small and it is not clear how well they can be pinned down. We can see this if we write down what has been established for $E_0(l)$ from the universal properties of the effective string action, [4]

$$\begin{aligned} E_0(l) = E_0^{NG}(l) + O\left(\frac{1}{l^7}\right) &= \sigma l\left(1 - \frac{\pi}{3}\frac{1}{\sigma l^2}\right)^{\frac{1}{2}} + O\left(\frac{1}{l^7}\right) \\ &= \sigma l - \frac{\pi}{6}\frac{1}{l} - \frac{\pi^2}{72}\frac{1}{\sigma l^3} - \frac{\pi^3}{432}\frac{1}{\sigma^2 l^5} + O\left(\frac{1}{l^7}\right). \end{aligned} \tag{25}$$

The second line shows explicitly all the known universal terms. These are identical to the Nambu-Goto energy in the first line, when that is expanded in powers of $1/\sigma l^2$ to that order. Since the higher order terms in the expansion are of $O(1/l^7)$ the equality between the two lines in eqn(25) is formally automatic. However we also know [4] that the operators that arise from the expansion of the Nambu-Goto action are universal to all orders, and in that sense the resummed Nambu-Goto term in the top line may be regarded as universal. Of course this expression becomes tachyonic for $l\sqrt{\sigma} \leq \sqrt{\pi/3}$, but such values of l are unphysical when N is large enough for the deconfining transition to be first order since $l_c\sqrt{\sigma} > \sqrt{\pi/3}$ in those cases. (And when the transition is second order, $E_0(l)$ is determined by the critical behaviour in this range of l, as we have seen in Fig 5.)

We shall begin with our high statistics SU(2) calculation. In Fig 6 we plot the ground

state energy, normalised to σl. (The variation in the value of σ as extracted from different fits to $E_0(l)$ is negligible in this context.) The deviation of $E_0(l)/\sigma l$ from unity exposes the $O(1/\sigma l^2)$ corrections to the leading linear term. We show the best fit with the Nambu-goto expression, and also the best fit using just the leading $O(1/l)$ Lüscher correction in eqn(25). We see that while the former is very close to the numerical values, except at the very smallest value of l, the latter fit, while accounting for much of the deviation from the dominant linear σl piece, visibly misses all except the largest l values. This tells us that our calculations of E_0 are indeed accurate enough to be very sensitive to corrections that are of higher order than the Lüscher term.

To analyse this in more detail, we subtract from $E_0(l)$ the Nambu-Goto expression $E_0^{NG}(l)$ and plot the difference, against $l\sqrt{\sigma}$, in Fig. 7. On this highly expanded scale we can now see a visible difference at the smallest values of l, starting at around $l\sqrt{\sigma} \sim 2$. Even there this is very small, $\leq 0.2\%$, until the very smallest value of l. Here the change of sign of the deviation is a clear signal that we are now in the basin of attraction of the critical point lying just below unity (see Fig. 5). It is interesting to see what happens if we subtract from $E_0(l)$ a model that includes only the universal terms up to $O(1/l)$, $O(1/l^3)$, and $O(1/l^5)$ respectively. This is shown in Fig. 7. If we (rather arbitrarily) decide to focus on the values with $l\sqrt{\sigma} \geq 1.5$ as perhaps being outside the influence of the $l = l_c$ critical point, then we clearly see that the fits that exclude the known universal term at $O(1/l^5)$ have larger deviations from the calculated values and so are disfavoured. However our numerical values cannot really tell us if the full Nambu-Goto expression is better or worse than if we just include all the known universal terms, i.e. up to and including $O(1/l^5)$. It is interesting to note from Fig. 7 that including a non-universal $O(1/l^7)$ correction to E_0^{NG} does not really help except in suggesting that all the values below $l\sqrt{\sigma} = 2$ are probably influenced by the deconfining critical point and hence not reflecting the behaviour of $E_0(l)$ at large N.

Since the higher powers of $1/l$ only become significant at smaller l, it is clear from the above SU(2) analysis that it is important not to be under the influence of a nearby critical point at small l. For this reason we now turn to SU(4) where the transition is (weakly) first order. We show in Fig. 8 the analogue of Fig. 7. We now see a monotonic increase of the deviation from Nambu-Goto as l becomes very small. As we can see in Fig. 8 this deviation can in fact be accounted for by a leading non-universal $O(1/l^7)$ correction. (How constraining this fit is, given that the deviations relevant to it are only from the two or three lowest values of l, is something we shall address more quantitatively below.) We also see from Fig. 8, that all this is also true if we take as our model all the known universal terms, up to and including $O(1/l^5)$. Here the deviation at the smallest value of l is significantly larger than for Nambu-Goto, although, as we can see, it can also be accommodated by a (larger) non-universal $O(1/l^7)$ correction. In this sense, our results slightly favour Nambu-Goto as being the better model of the two.

Irrespective of these details, the most striking feature of these comparisons is how well the known universal part of the effective string action describes very short flux tubes. As we see from Fig. 8 even at $l\sqrt{\sigma} \simeq 2$ any mis-match with $E_0(l)$ is at most at the $\sim 0.1\%$ level. To emphasise the significance of this we show in Fig. 8 the difference between $E_0(l)$ and the linear σl piece, with σ being determined at the largest l value. At $l\sqrt{\sigma} \simeq 2$ this difference would

be ~ 0.1, on this plot. So the fact that Nambu-Goto or just the universal pieces account for this difference, tells us that the zero-point energies from the excitations of an ideal thin string account for at least $\sim 99\%$ of the string excitation energy at this l. The fact that this should be so for a flux tube that, at $l\sqrt{\sigma} \simeq 2$, is not much longer than its expected $\sim 1/\sqrt{\sigma}$ intrinsic width, is quite counterintuitive. Why should what is essentially a short fat periodic blob behave so accurately like a thin string? Where are the contributions of the zero-modes of the massive modes of a flux tube? Clearly our calculations are telling us that the actual dynamics is somehow very much simpler than our naive intuition.

We can be more systematic about this flux tube/string agreement as follows. Consider Fig. 8. For $l\sqrt{\sigma} \simeq 3.5$, we see that the $O(1/l)$ Lüscher correction very nearly equals the difference $E_0(l) - \sigma l$, and the higher order contributions in $1/l$ contribute a negligible amount here. So this confirms the universal $O(1/l)$ correction to a corresponding high level of accuracy. Moving on to $l\sqrt{\sigma} \simeq 2.5$ and $l\sqrt{\sigma} \simeq 2.1$ we see that here the next universal $O(1/l^3)$ term accurately accounts for the gap between the linear plus Lüscher term contributions and the calculated energy, $E_0(l)$, while the higher order terms still contribute a total amount that is negligible. Thus we confirm the universal $O(1/l^3)$ correction to a corresponding level of accuracy. Going to smaller l we find that simultaneously with the $O(1/l^5)$ becoming important, unknown higher order contributions also become important, so we cannot claim to have evidence for the $O(1/l^5)$ contribution with any precision.

It is clear that to do better we need more values of $E_0(l)$ at the small values of l where the deviations from Nambu-Goto become visible. To achieve a much higher resolution in l at small l, one clearly needs a much smaller value of a. We make a small step towards this with our SU(6) calculation at $\beta = 171$. Of course, every time we increase N, our accuracy decreases significantly, since the cost of a basic matrix multiply increases $\propto N^3$. And decreasing a while keeping the volume fixed in physical units means that the cost grows $\propto 1/a^3$. Moreover this SU(6) calculation is designed to calculate excited states and so has a correspondingly large basis of operators, which is computationally expensive. So, despite some compensating factors, our SU(6) calculations are, statistically, far less accurate than the $N = 2, 4$ calculations at the small values of l relevant here; e.g. by a factor $O(10)$ at $l\sqrt{\sigma} \sim 2$. At large l, on the other hand, the benefits of the larger overlaps due to the larger operator basis make the SU(6) calculations much more accurate, and so they are the best place to confirm the asymptotic linearity of the ground state flux tube energy. We show the corresponding SU(6) plot in Fig. 9. Here the first order deconfining transition is robustly first order and the fact that the shape at small l is very similar to that in SU(4) reassures us that the weakness of the first order transition in the latter case plays no significant role. Apart from that the conclusions are much as for SU(4) except that the much larger statistical errors lessen the accuracy with which one confirms the universal terms, although the smaller systematic errors (in particular considerably smaller $O(a^2)$ lattice corrections) mean that one is much more confident about the relevance of the fits to the continuum limit. In particular we observe that the fitted coefficient of the non-Nambu-Goto $1/(l\sqrt{\sigma})^7$ contribution to $E_0(l)$ is ~ 0.09 which is comparable to the coefficient, ~ 0.05, of the corresponding term in the series expansion of Nambu-Goto, and so may be regarded as taking a 'natural' value.

We have seen that one can describe the deviations from the Nambu-Goto expression,

$E_0^{NG}(l)$, with a $O(1/l^7)$ correction. This is a natural choice since all lower powers are known to be universal. It is interesting to ask how well this $1/l^7$ power is determined by our calculations since it might be that this term will also turn out to be universal so that the first non-universal term actually starts at a higher power. If it is universal then it is plausible that it equals the corresponding term of Nambu-Goto, because of the universality of the scaling-0 operators in terms of which the Nambu-Goto action can be expanded [4]. (Although the $D = 3 + 1$ case shows us that a universal term can differ from Nambu-Goto [4].) Accordingly we fit our above SU(4) and SU(6) calculations to the form

$$E_0(l) = E_0^{NG}(l) + \frac{c}{l^\gamma} \tag{26}$$

and display the χ^2 per degree of freedom in Fig.10. To expose the importance of this correction, we include in the displayed value of χ^2 just the lowest 3 values of l, since only these are affected significantly by this correction term, and we take the number of relevant fit parameters to be 2, i.e. c and γ in eqn(26). (The value of σ is determined by the larger values of l.) Although we know on theoretical grounds that $\gamma \geq 7$ we show the χ^2 values for fits with $\gamma < 7$ as well. We observe that $\gamma = 11$ is excluded, $\gamma = 9$ is disfavoured (although not impossible), while $\gamma = 7$ is quite strongly favoured. The value $\gamma = 5$ would be equally plausible, and this is consistent with our above analysis where we saw that we could not claim significant numerical evidence for the universal $O(1/l^5)$ term. However $\gamma = 3$ is strongly excluded, as one would expect from the fact that we had good numerical evidence for the universal $O(1/l^3)$ term. So if we exclude $\gamma = 5$ on theoretical grounds, we see that the numerical evidence points to the leading non-Nambu-Goto like contribution being either $O(1/l^7)$ or, less probably, $O(1/l^9)$.

As we remarked earlier, the contributions of the string excitation modes to $E_0(l)$ are very small, because only the zero-point energies contribute, and this has an obvious practical disadvantage. But it also brings an important advantage: it is plausible to expect that the expansion of $E_0(l)$ in powers of $1/\sigma l^2$ is convergent throughout the range $l > l_c$ (or nearly all of it) just like $E_0^{NG}(l)$. This means that we can analyse the corrections order by order at smaller l, just as we have done above. Indeed it is plausible that an SU(4) calculation with a reduced by a factor of two and with the same statistical accuracy as the calculation presented here, would be able to confirm the universal $O(1/l^5)$ term quite accurately, and would simultaneously be able to determine unambiguously the power of the leading non-Nambu-Goto-like term.

4.2 Continuum limit

In [1] we compared our SU(3) flux tube spectra at the two lattice spacings listed in Table 5. We looked at the lightest few $p = 0$ states and found no significant differences between the two values of a, providing evidence that the $O(a^2)$ lattice corrections were negligible in these calculations. However in that paper our SU(3) calculations at the smaller value of a did not go to very small values of l and, in addition, we did not compare calculations with $p = 2\pi q/l \neq 0$.

Our new SU(6) calculation allows us to make a much more complete comparison. As we see from Table 5 the lattice spacings of our two SU(6) calculations differ by about a factor

of two. So the $O(a^2)$ lattice corrections at $\beta = 171$ should be about $\sim 1/3$ of any observed difference between $\beta = 90$ and $\beta = 171$.

In Fig 11 we compare the ground states in the two calculations. In each case we fit the Nambu-Goto expression $E_0^{NG}(l)$ to obtain the corresponding value of the string tension $a^2\sigma$. (This is primarily determined by the values at large l.) We see that at both values of β, one has $E_0(l) = E_0^{NG}(l)$ within errors (which are similar for both calculations) down to $l\sqrt{\sigma} \simeq 1.7$, i.e. down to these very short flux tubes there are no visible lattice corrections to the continuum Nambu-Goto expression. At the smallest common value of l, $l\sqrt{\sigma} \simeq 1.37$, we do appear to see a difference, although it is only at the 2 standard deviation level of significance. While it is amusing that a naive continuum extrapolation would bring the $a \to 0$ value at this l closer to the Nambu-Goto prediction, the errors are too large for this to be a significant observation. All this suggests that if there are any significant $O(a^2)$ corrections to our values of $E_0(l)$, they are confined to $l\sqrt{\sigma} \leq 1.4$. We note that any such uncertainty would only affect our determination in Section 4.1 of the non-universal correction to Nambu-Goto, and not the evidence for the lower-order universal terms.

We now compare some of the excited states in the two calculations. In Fig. 12 we plot the energies of the lightest three $P = +$ states and the lightest two with $P = -$, and compare these to the Nambu-Goto predictions, which for the excited states are completely parameter-free. As we can see, and have observed in our earlier calculations [1], these states coalesce to the first two excited energy levels of the Nambu-Goto model with the expected degeneracies and quantum numbers, as we increase l. (See eqn(5) and Table 1.) We see that to a good approximation the first excited state shows no a-dependence until we are down to $l\sqrt{\sigma} \simeq 1.37$. This is just like the ground state, except that here the deviations of $E_n(l)$ from $E_n^{NG}(l)$ already become visible at $l\sqrt{\sigma} \sim 3$. That is to say, here we can claim that our analysis of the corrections to Nambu-Goto will be largely unaffected by lattice corrections. For the four states belonging to the second energy level, it is again true that the discrepancy between the two calculations only becomes large once l is decreased to $l\sqrt{\sigma} \simeq 1.37$. All this suggests that we do not need to be concerned about $O(a^2)$ corrections in our analysis of the excited states, as long as we avoid placing too much weight on the energies for $l\sqrt{\sigma} < 1.4$.

We turn now to the states with non-zero momentum $p = 2\pi q/l$ along the flux tube axis. The momentum is carried by the 'phonons' running along the flux tube, and this leads to the energy-momentum dispersion relation in eqns(3,4,5) for the Nambu-Goto model in the continuum limit. We observe that as we decrease l at a fixed q, p^2 grows and can become the dominant component of the energy. Thus any $O(a^2)$ corrections to the dispersion relation could lead to a significant shift in the total energy. If such corrections affect the individual phonon contributions to p^2, then we would expect the effect to be largest for the states where the whole of the momentum is carried by a single phonon. These are states with $P = -$. (See eqn(6).) For $q = 1, 2$ this is the only state in the lowest $P = -$ energy level (see Table 1) and so it is easy to identify it. For higher q the degeneracy of the lowest $P = -$ energy level grows, but we shall assume that it is the lightest state that is relevant and plot that, since we shall see that the lattice spacing corrections to the dispersion relation typically act to decrease the energy.

So we plot in Fig 13 the energies of the lightest $P = -$ states with $q = 1$ and $q = 2$,

for SU(6) at $\beta = 90$ (together with the $q = 0$ $P = +$ ground state for comparison). The continuous curves are the continuum Nambu-Goto predictions: recall that there is no free parameter since $a^2\sigma$ is obtained from a fit to the $P = +$ ground state. We see that the agreement at larger l is excellent, but that as we reduce l there are increasing deviations, especially at $q = 2$. Here the lattice momentum at the smallest value of l, i.e. $l = 8a$, is $ap = \pi/2$. This is half the maximum momentum which is at $ap = \pi$, since on a lattice $ap = 0$ and $ap = 2\pi$ are the same. At $ap = \pi$ we expect $E(p^2)$ to have a maximum and to be far from its continuum value, so a significant lattice correction at $ap = \pi/2$ would be no surprise. We do not of course know the correct form of this correction, but what we can do is to see what happens if we replace p^2 by the form that enters the lattice dispersion relation for $E^2(p)$ for a free scalar field, i.e.

$$(ap)^2 \quad \to \quad 2 - 2\cos(ap), \tag{27}$$

if we use the most local lattice discretisation of the derivative. Making this replacement in eqn(5) we obtain the dashed curves in Fig 13. We observe that the calculated values are remarkably close to these 'lattice' Nambu-Goto predictions. Of course, to confirm that this is not just an accident, we need to look at a different a, and this we do in Fig 14 for our SU(6) calculation at $\beta = 171$. Since a is smaller by a factor of ~ 2 here, we would expect lattice spacing corrections in Fig 14 to be the same for q as they were for $q/2$ in Fig 13, at the same value of $l\sqrt{\sigma}$. This is indeed so and, as we see, the deviations from the continuum NG predictions are well accounted for by using eqn(27).

So we see that there are significant lattice corrections to $E(p)$ at large ap through its dispersion relation, at least for those states where all the momentum is carried by a single phonon. Presumably this will also be significant in states composed of several phonons, as long as some of these have large enough momenta. It would be useful to find a plausible way to estimate these effects for the general Nambu-Goto state on the lattice.

4.3 Large-N

Our earlier work provided evidence that the spectrum of flux tubes behaves like Nambu-Goto for values of l that are not very small, and since this is true for $N = 3$ and $N = 6$, one can safely assume that this is also true at $N = \infty$. Here we strengthen this observation using our new $N = 4, 5, 6$ calculations. And we address in some detail the remaining interesting question: can we assume that the deviations from Nambu-Goto that we observe at smaller l in SU(6), are similar to those that one would see at $N = \infty$?

We begin by comparing the deviations of the ground state energies from their best Nambu-Goto fits. We do so in Fig. 15 for the small-a SU(3) and SU(6) calculations in Table 5 and for the SU(4) and SU(5) calculations listed there. We observe in Fig. 15 no evidence for any N dependence, even on this expanded scale. Since all of these calculations are at small enough lattice spacings that we can expect any $O(a^2)$ corrections to be small, we can conclude that this N-independence also holds in the continuum limit.

In [1] we compared the first excited $q = 0, P = +$ state in our $\beta = 21$ SU(3) and $\beta = 90$ SU(6) calculations, and found no significant differences. Since we have just seen that $O(a^2)$

corrections are small at these a (except where high momenta are involved), this provides some evidence that the $O(1/N^2)$ corrections are already small for $N = 3$. In Fig. 16 we repeat the comparison, but now include the next two excited states in this channel, as well as the lightest two $q = 0, P = -$ states. As we can see, as we increase l these extra four states converge rapidly to the second excited Nambu-Goto energy level And for $l\sqrt{\sigma} > 3$ there appears to be no significant difference between the SU(3) and SU(6) values. However for $l\sqrt{\sigma} \lesssim 3$ the discrepancy between the two calculations rapidly grows, especially for the lighter of the two $P = +$ states. So here, at smaller l, the $O(1/N^2)$ corrections appear to be large, at least for SU(3).

To see if they are also significant for SU(6), we compare the spectrum of our new SU(6) calculation at $\beta = 171$ with the SU(4) and SU(5) calculations listed in Table 5 as well as with SU(3) at $\beta = 40$. These are all at smaller a than the calculations in Fig. 16. We begin with the three lightest $q = 0, P = +$ excited states, which we show in Fig. 17. We see that the first excited state indeed shows no significant N dependence. For the higher excited states it appears that the only large and significant N dependence comes from SU(3), as long as we remain with $l\sqrt{\sigma} \gtrsim 2$. In Fig. 18 we see that the same appears to be the case for the lightest two $q = 0, P = -$ states.

It may be that the anomalously large deviations seen at small l for the SU(3) excited states have to do with the fact that the small-l deconfining transition is second order for SU(3). Irrespective of that, the evidence is that any $O(1/N^2)$ corrections will be very small for SU(6), certainly as long as we remain at $l\sqrt{\sigma} \gtrsim 2$, and probably significantly below that. So in the case of SU(6) this leaves a substantial range of l where the observed deviations from Nambu-Goto are both significant and representative of the $N = \infty$ theory.

4.4 Excited states : an overview

If we consider an excited state of a long string in the Nambu-Goto model with $p = 0$, its energy can be expanded in powers of $1/\sigma l^2$ as in eqn(7). We also know [4] that the terms up to and including $O(1/l^5)$ are universal and equal to the corresponding terms in the Nambu-Goto expansion with any non-universal terms starting at $O(1/l^7)$ or later. As we see from eqn(7), this expansion only converges for

$$l\sqrt{\sigma} > l_c^{NG}(n)\sqrt{\sigma} = \left\{8\pi\left(n - \frac{1}{24}\right)\right\}^{\frac{1}{2}} \simeq \begin{cases} 4.91 & n = 1 \\ 7.02 & n = 2 \\ 8.62 & n = 3 \\ \dots \end{cases} \tag{28}$$

where $n = 1, 2, 3$ correspond to the first, second and third excited energy levels in the $p = 0$ sector. Nonetheless, as we see from Fig 19 where we plot our lattice values of $E(l)$ for the lightest $p = 0$ eigenstates in SU(6) at $\beta = 171$, these values do in fact remain very close to the full Nambu-Goto prediction for values of l that are well below the point at which the power expansion ceases to converge – and where we need to use the full, resummed (square root) formula in eqn(7). So it is no surprise that if we plot the sum of the known universal terms,

as in Fig 19, we find that they are unable to account for this precocious onset of free string behaviour.

We see the same phenomenon with the $p \neq 0$ eigenstates whose energies we calculate. To better expose any (dis)agreement between Nambu-Goto and our calculated values for these states, we construct the 'excitation energy (squared)' [3],

$$\Delta E^2(q,l) = E^2(q;l) - E_0^2(l) - \left(\frac{2\pi q}{l}\right)^2 \stackrel{NG}{=} 4\pi\sigma(N_L + N_R), \tag{29}$$

where $E_0(l)$ is the calculated energy of the (absolute) ground state (with $p = 0$), and where we show the Nambu-Goto prediction that follows from eqn(5). (We choose to subtract the calculated value of $E_0(l)$ rather than the Nambu-Goto prediction for it. In the present context the difference is insignificant.) Note that while eqn(29) assumes a continuum dispersion relation, we shall occasionally modify it as in eqn(27).

As our first example, consider the lightest $P = -$ state at each nonzero momentum $p = 2\pi q/l$, with $q = 1, 2, 3, 4, 5$. In the Nambu-Goto model we can expect these to be single phonon states $a_q|0\rangle$. (Certainly for $q = 1, 2$ and plausibly for $q > 2$.) In Fig 20 we plot the excitation energies from our SU(6) calculation at $\beta = 171$, using eqn(29) modified by the lattice dispersion relation in eqn(27). This is a replotting of Fig 14 designed to render more precise the comparison with Nambu-Goto. Where our errors are reasonably small, i.e. for $q = 1, 2, 3$, we observe very good agreement with Nambu-Goto for $l\sqrt{\sigma} > 1.5$. For $q = 4, 5$ there appears to be some systematic upward deviation from Nambu-Goto, but we note that the errors are much larger here, because these states have much larger energies, and for the same reason the systematic errors are also larger. In particular, as emphasised in Section 3.4 we cannot go to higher t in the correlation functions so as to check that there is no contamination from the presence of higher excited states, and this creates a systematic error that grows with q and which leads to an overestimate of $E(l)$. It is plausible that this explains the overshoot visible in Fig 20.

In Figs 21, 22 and 23 we show the excitation energies of the lightest few states with longitudinal momenta $p = 2\pi/l$, $4\pi/l$, $6\pi/l$ respectively. Again, where the errors are small, we observe excellent agreement with the Nambu-Goto prediction: roughly speaking, for $l\sqrt{\sigma} \geq 3$ for all our states, and for $l\sqrt{\sigma} \geq 2$ for the lighter ones with the smallest errors.

In summary, we have seen that all our calculated values of the flux tube energies are remarkably close to the Nambu-Goto prediction, down to values of l well below the point at which the series expansion in powers of $1/\sigma l^2$ has ceased to converge and all orders of Nambu-Goto are important to the resummed expression. We see this for the lightest $q = 0$ states in Fig. 19, for the $P = -$ ground states with $q = 1, 2, 3, 4, 5$ in Fig. 20, and for the lightest few states in each of the $q = 1, 2, 3$ sectors in Figs 21, 22 and 23. This provides much more evidence for our earlier claim [1] that a good first approximation to the effective string action must be the full resummed Nambu-Goto action, and that the corrections to that must be small even down to small values of l. This observation leads to the question we address in the next subsection: what do our results tell us about the specific nature of these corrections?

A final more general aside on all these results is that there appears to be no room for any states in addition to those that converge at larger l to the Nambu-Goto predictions. The

fact that the corrections to Nambu-Goto remain small even at small l, means that even here, where we are looking over a range of energies $E - E_0(l) \gg \sqrt{\sigma}$, there is no sign of the extra states one might expect to arise from the excitation of massive $\sim O(\sqrt{\sigma})$ modes.

4.5 Excited states: fits

The correction terms to Nambu-Goto are known [4] to begin with a power that is no less then seven, so we assume we can write

$$\begin{aligned} \frac{1}{\sqrt{\sigma}} E_n(l) &= \frac{1}{\sqrt{\sigma}} E_n^{NG}(l) + \frac{1}{\sqrt{\sigma}} \Delta E_n(l) \\ &\stackrel{l\to\infty}{=} \frac{1}{\sqrt{\sigma}} E_n^{NG}(l) + \frac{c}{(l\sqrt{\sigma})^7} \left\{ 1 + \frac{c_1}{l^2\sigma} + \frac{c_2}{(l^2\sigma)^2} + \cdots \right\} \end{aligned} \tag{30}$$

where the coefficients $c, c_1, ...$ are unknown. For large l we can also expand $E_n^{NG}(l)$ in powers of $1/l^2\sigma$ as in eqn(7). However as we decrease l this latter expansion diverges when $l = l_c^{NG}(n)$ in eqn(28). Nonetheless we have seen that even well below this value of l, at which all the terms in the expansion become important, the values of $E_n(l)$ remain very close to the resummed Nambu-Goto expression. It is possible that the correction $\Delta E_n(l)$, regarded as a series in $1/l$, also diverges at some finite $l = l_d(n)$ that is within or above the range of our calculations, i.e. $l_d \gtrsim l_c$. In that case, the fact that our calculated energies differ from Nambu-Goto by a finite amount for all $l \gtrsim l_c$ tells us that the series of correction terms in eqn(31) can be resummed for $l_c \lesssim l < l_d$ just like Nambu-Goto can be for $l < l_c^{NG}$. If on the other hand $l_d < l_c$ then we can expect the leading $(1/l^7)$ term to dominate $\Delta E_n(l)$ most of the way down to l_c. We attempt to capture these expectations with the heuristic parameterisation,

$$\frac{1}{\sqrt{\sigma}} \Delta E_n(l) = \frac{c}{(l\sqrt{\sigma})^7} \left(1 + \frac{c'}{l^2\sigma} \right)^{-\gamma} \simeq \begin{cases} \frac{c}{(l\sqrt{\sigma})^7} & l \gg l_d \\ \frac{cc'^{-\gamma}}{(l\sqrt{\sigma})^{7-2\gamma}} & l \ll l_d \end{cases} \tag{31}$$

where $l_d^2\sigma = c'$. The expression for $\Delta E_n(l)$ could certainly be more complicated, with more parameters. However, as we shall soon see, our calculated values of $E_n(l)$ are not good enough to justify an analysis with more parameters, and in any case eqn(31) embodies the essential feature of a resummed formula: the correct $\propto 1/l^7$ behaviour at large l, with the possibility of a quite different effective power behaviour at small l.

As an aside we remark that one exception to this is the absolute ground state, where the Nambu-Goto series expansion converges for all $l > l_c$, at least for $N \geq 4$ where the phase transition at $l = l_c$ is first order. So here it is particularly plausible (although not guaranteed) that the leading $O(1/l^7)$ correction to Nambu-Goto continues to dominate the total correction, $\Delta E_0(l)$, down to our smallest values of l i.e. that $l_d(n = 0) < l_c$. This is of course precisely what our analysis of the ground state in Section 4.1 suggested.

To analyse the correction to the Nambu-Goto prediction for the excited states, we need to look at those states where $E(l)$ is accurately determined at small l, and where there are simultaneously substantial deviations from Nambu-Goto. Looking at Fig. 19 and Fig. 21,

some obvious candidates are the first and second excited states in the $p = 0$, $P = +$ sector and the lightest state in the $p = 2\pi/l$, $P = +$ sector. We consider these in turn.

We begin with the first excited state in the $p = 0$, $P = +$ sector, plotting in Fig. 24 the deviation of its energy from the Nambu-Goto prediction. We include several fits. First, we show a 'fit' to c/l^7: this (or a higher power) is expected to be the leading correction term as $l \to \infty$. Its complete failure to describe the observed deviation (and a higher power would evidently perform even worse) emphasises that we must here be in a region of l where the correction to Nambu-Goto can no longer be expressed as a convergent series but must be resummed. We also show two fits that are variations on the form given in eqn(31):

$$\frac{1}{\sqrt{\sigma}}\Delta E_n(l) = \begin{cases} \frac{-1.0}{(l\sqrt{\sigma})^7}\left(\frac{1}{25.0} + \frac{1}{l^2\sigma}\right)^{-2.75} \\ \frac{-1.0}{(l\sqrt{\sigma})^7}\left(\frac{1}{31.1} + \frac{1}{l^2\sigma}\right)^{-2.61} \end{cases} \tag{32}$$

The first is the lower solid curve in Fig. 24, while the second is the one slightly higher. The latter has a slightly better overall χ^2 but the former fits the points in the middle somewhat better. In any case we see that:
(1) in both cases the radius of convergence of the correction term, $\sim 25 - 31$, is not far from that of the Nambu-Goto expression, i.e. ~ 24;
(2) the coefficient of the leading $1/(l\sqrt{\sigma})^7$ term at large l is in the range $0.7 - 0.8 \times 10^3$ which is of the same order as the coefficient of the $1/(l\sqrt{\sigma})^7$ term in the Nambu-Goto expansion, which is $\sim 1.3 \times 10^3$.
This tells us that the correction terms we are seeing have coefficients of the same order as those of the corresponding Nambu-Goto terms, as one would expect if they were to arise from 'natural' correction terms in the effective string action.

It is interesting to ask how well the calculations shown in Fig. 24 constrain the parameters of the fit in eqn(32). We perform separate fits that include (case A) and exclude (case B) the very smallest value of l, and find:

$$\begin{aligned} \gamma &= 2.61\binom{12}{17}, \quad c' = 31\binom{26}{9} \quad : \quad \text{fit A} \\ \gamma &= 2.88\binom{28}{33}, \quad c' = 20\binom{41}{7} \quad : \quad \text{fit B} \end{aligned} \tag{33}$$

This confirms that while the power γ is quite well constrained, the value of c' is much more weakly constrained. Indeed within two or three standard deviations, one can set $c' \to \infty$. That is to say, the values of $E(l)$ plotted in Fig. 24 provide little evidence for an asymptotic $\propto 1/l^7$ behaviour. We demonstrate this in Fig. 24 with the black dashed curve which is simply given by $-1.12/(l\sqrt{\sigma})^{2.51}$ and does not incorporate this asymptotic $1/l^7$ correction. This fit is visibly worse, but not very much worse. The reason is obvious: the onset of the $1/l^7$ dependence only occurs at larger l where the deviations from Nambu-Goto have become very small. Thus our use of a $1/l^7$ prefactor in eqn(31) must be primarily motivated by the theoretical analysis, with some significant support from our earlier analysis of the absolute ground state. Assuming such a prefactor, the location of the transition region, around $l^2\sigma \sim c'$, and the corresponding

coefficient of the asymptotic $1/l^7$ correction are, as we have noted already, not far from the corresponding Nambu-Goto values, and hence quite 'natural'.

It is interesting to see whether our other calculations support this analysis. In Fig. 25 we plot the same quantity as in Fig. 24, but this time for the SU(4) and SU(5) calculations at a coarser value of a and for SU(6) at the much coarser a corresponding to $\beta = 90$. (We exclude SU(3) from consideration because of its second order phase transition at $l = l_c$.) We plot just one curve from Fig. 24, the upper fit listed in eqn(34). We see that this curve is a good fit to the SU(6) values (except at the smallest value of l) and adequate for SU(5), and for the larger l values of SU(4). Bearing in mind possible $O(a^2)$ lattice corrections to this SU(6) calculation, and possible effects from the weak first order nature of the transition in SU(4), the level of agreement we see with this curve is reassuring. On the other hand, these calculations are visibly rougher than the new SU(6) calculations shown in Fig. 24, and it is clear that they would not add much to any quantitative analysis.

In Fig. 26 we show a corresponding plot for the second excited state, taken from our new SU(6) calculation. We also show the next higher excited state, which at large l converges to the same energy level, since the combined plot highlights a potential ambiguity: the two states might actually 'cross' at $l\sqrt{\sigma} \simeq 3$. It is obviously important, when we try to fit the energy of the state with a correction to Nambu-Goto, to be sure that it is the same state at all l. In principle this ambiguity can be resolved by a careful examination of the operators that contribute to the wavefunctionals of the two energy eigenstates, as a function of l. We do not attempt to do so here, but instead will assume that the lightest values of E do indeed belong to the same state at all l. Returning to Fig. 26, it is clear that these calculations are much less precise than those in Fig. 24, so we cannot expect to draw very detailed conclusions. Nonetheless it is clear that the corrections are larger and probably increase more slowly with decreasing l. We show some fits of the form in eqn(31). The fits with values of γ similar to those of the fits in Fig. 24, have much larger values of c': the transition region to the asymptotic $\propto 1/l^7$ behaviour occurs at $l\sqrt{\sigma} \sim \sqrt{c'} \sim 15 - 30$ rather than the $\sim 4 - 8$ in Fig. 24. (From the Nambu-Goto model one might expect a factor of only $\sim \sqrt{2}$.) In addition such fits do not seem to capture well the overall trend. In particular, the alternative curve which rises at very small l, because the power $\gamma = 4.16$ leads to the $(l^2\sigma)^\gamma$ factor overwhelming the $1/l^7$ factor at small l , looks 'better', and also has a modest c'. However the quality of these calculations is not good enough to justify anything more than such impressionistic remarks.

We now turn to the lightest state with non-zero momentum, $p = 2\pi/l$, and with $P = +$. In Fig.27 we plot the energy minus the value predicted by Nambu-Goto, using our SU(6), $\beta = 171$ calculation. We also plot a curve that is not a fit, but is exactly the same as the $\gamma = 2.75$ fit in eqn(32) which was displayed in Fig. 24. In Fig. 28 we show the energy of the same state from some of our other calculations, together with exactly the same curve. Again this calculation is not so precise that this comparison can be considered unambiguous, but what we do learn is that the correction to Nambu-Goto is certainly consistent with a resummed series with the correct large l behaviour and with natural coefficients.

In the $p = 2\pi/l$ sector, the above $P = +$ state is not the simplest, containing as it does two phonons $\sim a_2 a_{-1}|0\rangle$. The simplest state has $P = -$ and has just one phonon $\sim a_1|0\rangle$. In Fig. 29 we plot the energy of the latter minus the Nambu-Goto prediction. The values

of $E(l)$ are very accurate, and the reason we left it out till now is that it was already clear from Fig. 21 that the corrections were very small and only occur at very small l. At such small l even for the lowest non-zero momentum, i.e. $p = 2\pi/l$, we need to worry about lattice corrections to the dispersion relation, and so we plot values using both the lattice free-field and continuum dispersion relations, as shown. Although we can see in Fig. 29 that this does create a visible shift in the values of $E - E_{NG}$, this shift does not affect our conclusions. The first is that the deviations only begin at very small l, just as for the absolute ground state in Fig. 11. The second is that the deviation then grows rapidly with decreasing l consistent, just as in Fig. 11, with the leading asymptotic $\propto 1/l^7$ dependence. By contrast, as shown in Fig. 29, it is certainly not consistent with a much smoother resummed l dependence of the kind we saw working well in Fig. 24 and Fig.27. This naturally raises the question whether the same might not apply to other states containing a single phonon. We therefore repeat the exercise for the lightest $p = 4\pi/l$, $P = -$ state, which should be just $a_2|0\rangle$. The results, in Fig. 30, are both good and bad. The good is that we can confirm that, irrespective of the dispersion relation employed, here too the deviations are negligible except at very small l. The bad is that at the smallest l, where the deviations become significant, they depend so strongly on the dispersion relation used that it is hard to draw any useful conclusion about the functional form of the correction.

In summary, most of the excited states that are accurately calculated unambiguously demand a correction to Nambu-Goto that varies much more slowly with $1/l$ than the $\sim 1/l^7$ leading asymptotic behaviour that is expected theoretically and for which we have evidence from our analysis of the ground state. This gross discrepancy implies that in the range of l relevant to our fits, the correction to Nambu-Goto can no longer be expressed as a convergent series in $1/l$ but has to be resummed, just like the Nambu-Goto series itself. However, and unexpectedly, the $p \neq 0$ ground states with $P = -$, i.e. those with a single phonon, are consistent with just a leading $O(1/l^7)$ correction term just like the absolute ground state.

4.6 Reflection parity, P_r

Our choice of operators in Table 2, was not originally made with a view to labelling the states by their reflection parity, P_r. That is to say, for the majority of operators in the Table we have not included the corresponding x-reflected operators. Moreover, some of the operators are intrinsically $P_r = +$ after we sum over translations in x to produce $p = 0$. So our overlap onto $P_r = -$ states is likely to be smaller than onto the $P_r = +$ states. Since one of our goals is to search for states that manifest the excitation of massive modes and are additional to the stringy states that rapidly converge to Nambu-Goto, it is important that we have a good overlap onto sectors of all quantum numbers, including $P_r = -$, since otherwise we trivially risk not observing such extra states even if they are present.

Since the operators in Table 2 are mostly far from being orthogonal, it is quite possible that even if for most operators we do not have their exact x-reflections (where different), we may well have operators that are approximate x-reflections. This is of course hard to know just by staring at the operators. However if we calculate the lightest two $p = 0$ states with $P = -$, which in Nambu-Goto should be the $\sim \{a_2 a_{-1} a_{-1} \pm a_1 a_1 a_{-2}\}|0\rangle$ combinations

with $P_r = \pm$, we see from Fig. 19 that these two states do indeed converge rapidly to the appropriate Nambu-Goto energy level. So we certainly have enough overlap to identify the lightest $P_r = -$ Nambu-Goto-like state. We see this in more detail in our effective energy plot in Fig. 2, where we can estimate that in this particular case we have an overlap of $\sim 80\%$ onto the $P_r = -$ state. While this is not as good as the $> 90\%$ overlap onto the associated $P_r = +$ state, it reassures us that our overlap onto the $P_r = -$ sector is large enough that there is no special reason to worry about missing states in this particular sector.

We complete this section with an analysis of the l-dependence of the lightest of the two $p = 0$, $P = -$ states discussed above. The first question concerns their P_r quantum numbers. Due to the blocking choices, it turns out that for $l/a = 32, 48, 64$ we have enough pairs of operators that are exact P_r transforms of each other that we are able to cleanly identify the P_r quantum numbers. This tells us that the lightest of the the two states is the one with $P_r = +$. This is what one would naively expect: any splitting between the $P_r = \pm$ states leaves the one that is antisymmetric in x as the heavier one. Turning then to the lighter $P_r = +$ state, we plot its deviations from Nambu-Goto in Fig. 31. What we see is quite interesting. While the lowest l values are consistent with a steep fall-off, it is difficult not to ignore the values below Nambu-Goto around $l\sqrt{\sigma} \sim 3$ or those above, around $l\sqrt{\sigma} \sim 4.5$. In fact it is hard not to see here a clear hint of an oscillating behaviour around something like the top fit in eqn(32), which we have also plotted in Fig. 31. Although we have not remarked upon it earler in this paper, hints of oscillations can be equally found in Fig. 27, in the third excited state in Fig. 26 and elsewhere. And where we have more than one state converging on an energy level, with both oscillating, then states may also 'intertwine'. Our fitting functions are of course only heuristic and chosen for simplicity; it is entirely possible that the real variation can also incorporate something like a Bessel-function oscillation. A relatively minor improvement in the quality of the calculation would unambiguously clarify this issue of possible oscillations.

5 Summary and conclusions

We have calculated the low-lying energy spectrum of closed flux tubes with lengths ranging from the moderately long, $l\sqrt{\sigma} \simeq 5.5$, down to the very short, close to the 'deconfining' phase transition at $l = l_c \simeq 1.1/\sqrt{\sigma}$. By contrast analytic investigations of the effective string action [4], which make powerful predictions for the first few terms of the expansion of $E_n(l)$ in powers of $1/l^2\sigma$, focus on large values of l where such a series converges and where the energy gaps are small, i.e. $E_n(l) - E_0(l) \ll \sqrt{\sigma}$. Thus our calculations are mostly complementary to the analytic ones, although there is a substantial overlap for the absolute ground state and some overlap, at our largest values of l, for the very lightest excited states.

We checked that for our main SU(6) calculation the $O(a^2)$ lattice corrections are small, except possibly for the very smallest values of l and for large momenta where deviations from the continuum energy-momentum dispersion relation can be significant (as shown in Fig. 14). We also saw from comparisons such as those in Figs 15-18, that $N = 6$ is very close to $N = \infty$ (with any significant correction once again limited to the smallest l). Thus we can assume that the states whose energies we calculate using our basis of single-trace

operators contain only a single flux tube, so that the partition function is over surfaces of lowest genus that wrap around the torus. Such a partition function can be calculated using what we have recently learned about the universal terms of the effective string action [4], with corresponding predictions for the energy spectrum. Comparing this to our numerical spectrum is one of the main motivations of this work. However equally interesting is to see how much our more accurate calculations confirm and quantify our earlier observation [1] that the free string Nambu-Goto model provides a very good description of the low-lying energy spectrum, even at very small l, and to attempt to find some states that reflect the excitation of the additional massive modes of the flux tube.

Our most accurate calculation is that of the absolute ground state. In this case the stringy corrections to the dominant linear σl term are small because they come from the zero-point energies of the modes of the string. Thus it is plausible that the expansion of $E_0(l)$ in powers of $1/l^2$ converges all the way down to l_c, just like the Nambu-Goto energy, and that we can attempt to identify the leading correction. We were able to show, in Section 4.1, that both Nambu-Goto and the sum of known universal terms work very well down to small l. In the process we found that we could find good numerical evidence for the universality of the $O(1/l)$ and $O(1/l^3)$ terms (which are the same as Nambu-Goto) but were not able to test the known universality of the $O(1/l^5)$ term. Assuming the latter, we can then predict that the first term that differs from Nambu-Goto is most likely to be $O(1/l^7)$ or, less likely, $O(1/l^9)$, but not a higher power. (See Fig. 10 and also Figs 7-9.) This is consistent with the known universality results [4] that predict a power ≥ 7.

For the excited states the analysis is very different. As we see in Figs 19-23, the calculated energies are very close to Nambu-Goto well below the value of l at which the Nambu-Goto power series no longer converges. Here all orders are important, and we have to use the well-known resummation. It is thus no surprise that merely using the known universal terms of the effective string action cannot capture this striking agreement, as we see in Fig. 19. Moreover it is also no surprise that the deviations from Nambu-Goto at smaller l cannot be fitted with some leading $1/l^{\gamma \geq 7}$ correction, as we see from Fig. 24 and Fig. 25. Indeed one important conclusion of this study is that one requires a resummation of the correction terms, which we heuristically parameterised by $\frac{c}{(l\sqrt{\sigma})^7}\left(1+\frac{c'}{l^2\sigma}\right)^{-\gamma}$. A good example is provided in Fig. 24, suggesting a power $\gamma \sim 2.7$ and a radius of convergence similar to that of the corresponding Nambu-Goto expression. So the effective power of the correction for smaller l is $\sim 1/l^{7-2\gamma} \sim 1/l^{\sim 2}$ rather than $\sim 1/l^7$, and in fact we cannot claim any significant evidence for the latter power from this excited state's calculation. A similar conclusion follows from an analysis of the lightest $P = +$ state with momentum $p = 2\pi/l$ as shown in Fig. 27 and Fig. 28. By contrast the lightest $P = -$ state with $p = 2\pi/l$, shown in Fig. 29, behaves like the absolute ground state, displaying a correction that only becomes significant at very small l and varies rapidly in a manner consistent with $\sim 1/l^7$, but is definitely not consistent with the softer resummed behaviour discussed above. This state is special in that it contains a single phonon, $\sim a_1|0\rangle$, in the Nambu-Goto model. The lightest $P = -$ state with $p = 4\pi/l$ also has one phonon in Nambu-Goto, and displays a similar behaviour.

In summary, we have confirmed in some detail our earlier observation [1] that typical

low-lying energy eigenstates of a closed flux tube remain close to the free-string Nambu-Goto prediction well below the values of l where a series expansion of $E_n^{NG}(l)$ in $1/l^2\sigma$ diverges, and where all powers become important. Our analysis of the (absolute) ground state suggests that the leading correction to Nambu-Goto is most likely to be $O(1/l^7)$, consistent with recent analytic studies of the effective action [4]. By contrast, at modest values of l our lightest excited states show corrections to the Nambu-Goto predictions which clearly demand a resummation of the series of correction terms, so as to give a behaviour closer to $\sim 1/l^2$ than $\sim 1/l^7$. The exceptions appear to be the lightest states with a single 'phonon' which are very much like the absolute ground state: the corrections are small, only becoming visible at very small l, and are consistent with a $\sim 1/l^7$ behaviour. Interestingly, very recent analytic studies have shown that the 'scaling 0' operators that arise in the expansion of the square-root Nambu-Goto action are all universal [4]. If for some reason the series of correction terms displays the desired resummation properties, then one may be most of the way to a theoretical understanding of most of these remarkably simple numerical results. Of course, one needs to understand the special behaviour of the single phonon states and, most importantly, why there is no sign of excitations of massive modes, even at small l, (unlike the case of $D = 3 + 1$ [2]). The answer to the latter might explain how even at $l\sqrt{\sigma} \sim 2$, where the flux tube surely 'looks like' a fat periodic blob rather than a thin string, at least 99% of the difference $E_0(l) - \sigma l$ is given by the zero-point energies of the excitations of an ideal thin string.

Acknowledgements

During the course of this work, MT participated in the *Confining Flux Tubes and Strings* Workshop at the ECT*, Trento, where there were many talks relevant to the present work (available on the ECT web-site): MT is grateful to the participants for useful discussions and to the ECT for its support in part of this research under the European Community - Research Infrastructure Action under the FP7 'Capacities' Specific Programme, project 'Hadron-Physics2'. The computations were carried out on EPSRC and Oxford funded computers in Oxford Theoretical Physics.

A Compilation of energy spectra

In this Appendix we list the energies that we have calculated in our SU(6) calculation at $\beta = 171.0$. These are our best results for the flux tube spectrum, both in terms of closeness to the continuum limit, $a = 0$, and closeness to $N = \infty$, and indeed in terms of accuracy. We present the spectrum in enough detail so that interested readers are able to make their own analyses.

In Table 7 we list the lightest 5 states in the with longitudinal momentum $p = 2\pi q/l = 0$ and parity $P = +$. We also show the lattice sizes used (in lattice units). Table 8 lists the 3 lightest $P = -$ states with $p = 0$. Table 9 lists the lightest states with $p = 2\pi q/l = 2\pi/l$, in both $P = \pm$ sectors. Table 10 and Table 11 do the same for $p = 4\pi/l$ and $p = 6\pi/l$ respectively. And Table 12 lists the ground states with momenta $p = 8\pi/l$, $10\pi/l$, $12\pi/l$ and parities $P = \pm$.

l/a	$l_\perp \times l_t$	$aE(l; q = 0)$; $P = +$				
14	100×200	0.0519(4)	0.3620(99)			
16	100×200	0.0777(3)	0.3963(25)	0.4954(93)	0.5768(222)	
20	70×120	0.1176(5)	0.4219(19)	0.5809(41)	0.6300(63)	0.6787(155)
24	48×60	0.1528(9)	0.4369(30)	0.5986(55)	0.6284(86)	0.6964(119)
28	48×60	0.1842(8)	0.4550(36)	0.6038(72)	0.6393(76)	0.7375(123)
32	40×48	0.2177(10)	0.4736(36)	0.6033(83)	0.6328(63)	0.7292(171)
36	40×48	0.2490(12)	0.4903(27)	0.6303(77)	0.6428(97)	0.7406(89)
40	48×48	0.2817(14)	0.5065(27)	0.6464(93)	0.6649(60)	0.7789(76)
44	48×48	0.3113(14)	0.5281(19)	0.6535(56)	0.6777(71)	0.7959(92)
48	48×48	0.3425(13)	0.5481(23)	0.6806(53)	0.6985(60)	0.8035(110)
52	52×52	0.3723(10)	0.5652(19)	0.7011(45)	0.7225(57)	0.8097(115)
56	56×56	0.4056(9)	0.5886(19)	0.7178(68)	0.7371(78)	0.8441(106)
60	60×60	0.4340(11)	0.6134(12)	0.7328(50)	0.7533(42)	0.8484(106)
64	64×64	0.4637(17)	0.6343(45)	0.7630(39)	0.7626(59)	0.8694(108)

Table 7: The energies, $E(q, l)$, of the lightest five flux tube states with length l, parity $P = +$ and longitudinal momentum $p = 2\pi q/l = 0$. For SU(6) at $\beta = 171.0$.

l/a	$aE(l;q=0)\ ;\ P=-$		
16	0.5243(71)	0.6182(117)	0.6794(101)
20	0.5808(74)	0.6718(127)	0.7237(159)
24	0.6151(70)	0.6739(102)	0.7399(107)
28	0.6377(80)	0.6624(75)	0.7586(79)
32	0.6270(66)	0.6531(99)	0.7754(82)
36	0.6384(81)	0.6699(115)	0.7641(92)
40	0.6572(93)	0.6717(99)	0.7931(107)
44	0.6810(98)	0.6900(107)	0.7993(82)
48	0.6966(62)	0.7129(56)	0.8350(108)
52	0.7174(72)	0.7262(63)	0.8409(99)
56	0.7394(57)	0.7395(76)	0.8443(111)
60	0.7462(74)	0.7555(57)	0.8902(102)
64	0.7697(69)	0.7713(80)	0.8748(111)

Table 8: The energies, $E(q,l)$, of the lightest three flux tube states with length l, parity $P=-$ and longitudinal momentum $p=2\pi q/l=0$. For SU(6) at $\beta=171.0$.

$aE(l; q=1)$					
l/a	$P=-$			$P=+$	
14	0.5222(32)	0.7331(109)		0.6457(152)	
16	0.4927(41)	0.6553(63)	0.7666(169)	0.6207(128)	0.7979(203)
20	0.4524(11)	0.6255(31)	0.7704(118)	0.5853(123)	0.7385(205)
24	0.4297(19)	0.6005(41)	0.7415(71)	0.5805(148)	0.7240(133)
28	0.4206(20)	0.5898(56)	0.7413(74)	0.5916(116)	0.7205(124)
32	0.4226(14)	0.5980(54)	0.7244(60)	0.5987(65)	0.7155(113)
36	0.4288(16)	0.6091(38)	0.7279(71)	0.5947(70)	0.7247(125)
40	0.4393(22)	0.6185(44)	0.7504(78)	0.6049(58)	0.7362(83)
44	0.4595(26)	0.6295(52)	0.7499(81)	0.6216(43)	0.7452(85)
48	0.4769(24)	0.6362(48)	0.7651(76)	0.6414(23)	0.7503(97)
52	0.4997(20)	0.6581(58)	0.7883(99)	0.6600(24)	0.7637(70)
56	0.5163(19)	0.6790(64)	0.8098(84)	0.6745(25)	0.7868(77)
60	0.5423(22)	0.6974(51)	0.8298(98)	0.6915(29)	0.7950(87)
64	0.5645(21)	0.7107(67)	0.8445(102)	0.7108(24)	0.8314(93)

Table 9: The energies, $E(q, l)$, of the some of the lightest flux tube states with length l, parity $P = \pm$ and longitudinal momentum $p = 2\pi q/l = 2\pi/l$. For SU(6) at $\beta = 171.0$.

$aE(l; q=2)$							
l/a	$P=-$			$P=+$			
14	0.9636(55)			1.011(15)			
16	0.8758(115)	1.046(11)		0.913(13)			
20	0.7519(93)	0.902(10)	1.006(6)	0.759(9)	0.876(6)	0.916(11)	
24	0.6941(42)	0.834(9)	0.909(16)	0.691(9)	0.820(7)	0.845(9)	0.950(14)
28	0.6485(45)	0.800(16)	0.915(15)	0.654(10)	0.788(9)	0.796(11)	0.927(14)
32	0.6266(49)	0.792(18)	0.859(12)	0.612(9)	0.748(14)	0.747(9)	0.888(12)
36	0.6042(47)	0.741(8)	0.857(12)	0.612(6)	0.755(8)	0.744(6)	0.847(12)
40	0.5999(44)	0.754(7)	0.855(11)	0.610(5)	0.734(8)	0.742(9)	0.838(13)
44	0.6010(43)	0.745(8)	0.854(12)	0.606(5)	0.737(8)	0.743(7)	0.850(11)
48	0.6164(52)	0.746(8)	0.880(12)	0.612(5)	0.758(4)	0.768(7)	0.859(10)
52	0.6190(48)	0.756(9)	0.877(12)	0.622(4)	0.761(7)	0.774(9)	0.874(11)
56	0.6341(50)	0.775(7)	0.893(12)	0.633(5)	0.758(9)	0.772(8)	0.857(11)
60	0.6488(97)	0.778(9)	0.904(11)	0.656(8)	0.772(7)	0.785(8)	0.873(13)
64	0.6615(87)	0.792(7)	0.911(14)	0.656(6)	0.802(8)	0.826(8)	0.900(14)

Table 10: The energies, $E(q, l)$, of the some of the lightest flux tube states with length l, parity $P = \pm$ and longitudinal momentum $p = 2\pi q/l = 4\pi/l$. For SU(6) at $\beta = 171.0$.

$aE(l;q=3)$							
l/a	$P=-$			$P=+$			
14	1.340(7)	1.518(10)	1.587(14)	1.459(48)	1.481(42)		
16	1.190(16)	1.342(28)	1.448(11)	1.284(24)	1.382(29)		
20	1.051(12)	1.115(7)	1.228(10)	1.091(23)	1.184(25)		
24	0.945(12)	0.991(7)	1.110(10)	0.992(20)	1.056(23)		
28	0.886(10)	0.907(11)	1.003(23)	0.875(14)	0.960(19)		
32	0.823(11)	0.816(25)	0.931(42)	0.844(12)	0.903(35)		
36	0.796(9)	0.782(19)	0.885(35)	0.790(10)	0.886(13)		
40	0.770(8)	0.772(10)	0.890(34)	0.771(9)	0.885(15)	0.928(28)	
44	0.746(8)	0.745(14)	0.843(30)	0.737(17)	0.862(14)	0.867(29)	0.999(59)
48	0.745(8)	0.737(18)	0.880(27)	0.751(19)	0.876(29)	0.852(27)	0.986(20)
52	0.749(6)	0.749(14)	0.864(27)	0.754(10)	0.874(12)	0.872(20)	0.960(13)
56	0.734(15)	0.743(17)	0.875(31)	0.757(7)	0.868(13)	0.875(28)	0.957(18)
60	0.764(7)	0.784(8)	0.892(33)	0.772(7)	0.861(12)	0.887(28)	0.989(20)
64	0.774(8)	0.788(8)	0.898(23)	0.770(14)	0.871(19)	0.913(27)	0.999(19)

Table 11: The energies, $E(q,l)$, of the some of the lightest flux tube states with length l, parity $P=\pm$ and longitudinal momentum $p=2\pi q/l=6\pi/l$. For SU(6) at $\beta=171.0$.

$aE(l;q)$						
	$q=4$		$q=5$		$q=6$	
l/a	$P=-$	$P=+$	$P=-$	$P=+$	$P=-$	$P=+$
14	1.523(60)					
16	1.505(11)					
20	1.339(15)	1.389(51)	1.553(29)	1.684(40)		
24	1.202(12)	1.259(11)	1.389(23)	1.497(32)		
28	1.065(23)	1.139(9)	1.240(49)	1.377(21)		
32	1.019(7)	1.035(8)	1.156(41)	1.286(21)		
36	0.984(8)	0.953(16)	1.141(31)	1.184(40)	1.295(66)	1.339(73)
40	0.935(15)	0.908(15)	1.104(29)	1.140(37)	1.182(47)	1.174(61)
44	0.917(14)	0.926(14)	1.058(28)	1.066(29)	1.164(38)	1.234(48)
48	0.889(15)	0.892(14)	1.006(23)	1.050(25)	1.116(35)	1.176(47)
52	0.877(10)	0.855(29)	0.997(22)	1.007(16)	1.147(31)	1.096(34)
56	0.881(10)	0.865(13)	1.020(18)	0.989(18)	1.091(26)	1.063(24)
60	0.855(11)	0.845(26)	0.971(18)	0.981(16)	1.075(22)	1.072(21)
64	0.855(14)	0.879(10)	0.972(20)	0.985(20)	1.105(26)	1.052(21)

Table 12: The energies, $E(q,l)$, of the some of the lightest flux tube states with length l, parity $P=\pm$ and longitudinal momentum $p=2\pi q/l$ as indicated. For SU(6) at $\beta=171.0$.

References

[1] A. Athenodorou, B. Bringoltz and M. Teper, Phys. Lett. B656 (2007) 132 [arXiv:0709.0693].

[2] A. Athenodorou, B. Bringoltz and M. Teper, JHEP02(2011)030 [arXiv:1007.4720].

[3] A. Athenodorou, B. Bringoltz and M. Teper, JHEP0905 (2009) 019 [arXiv:0812.0334].
B. Bringoltz and M. Teper, Phys. Lett. B663 (2008) 429 [arXiv:0802.1490].

[4] O. Aharony and E. Karzbrun, JHEP 0906:012,2009 [arXiv:0903.1927].
O. Aharony amd M. Field, arXiv:1008.2636
O. Aharony and N. Klinghoffer, JHEP 1012:058,2010 [arXiv:1008.2648].
O. Aharony, Talk at *Confining Flux Tubes and Strings* (ECT, July 2010).

[5] M. Teper, Acta Physica Polonica B40 (2009) 3249 [arXiv:0912.3339].

[6] J. Liddle and M.Teper, arXiv:0803.2128; PoS LAT2005 (2005) 188 [hep-lat/0509082].
K. Holland, M. Pepe and U-J Wiese, JHEP 0802 (2008) 041 [arXiv:0712.1216].
K. Holland, JHEP 0601 (2006) 023 [hep-lat/0509041].

[7] B. Lucini and M. Teper, Phys. Rev. D64 (2001) 105019 [hep-lat/0107007]; Phys. Lett. B501 (2001) 128 [hep-lat/0012025].
L. Del Debbio, H. Panagopoulos, P. Rossi and E. Vicari, Phys. Rev. D65 (2002) 021501 [hep-th/0106185].

[8] B. Lucini, M. Teper and U. Wenger, Phys.Lett. B545 (2002) 197-206 [hep-lat/0206029]; JHEP0401:061,2004 [hep-lat/0307017]; JHEP0502:033,2005 [hep-lat/0502003].

[9] Y. Schroder, Ph. D. Thesis, DESY-THESIS-1999-021; 'The Static Potential In QCD(3) At One Loop' in: F. Csikor, Z. Fodor (eds.), Strong and Electroweak Matter 97, (World Scientific, 1998) 394.

[10] B. Bringoltz and M. Teper, Phys. Lett. B645 (2007) 383 [hep-th/0611286].

[11] E. Seiler, Phys. Rev. D18 (1978) 482.

[12] J. Polchinski and A. Strominger, Phys. Rev. Lett. 67 (1991) 1681.

[13] P. Olesen, Phys. Lett. 160B (1985) 144.

[14] J. Arvis, Phys. Lett. 127B (1983) 106.

[15] M. Lüscher, K. Symanzik and P. Weisz, Nucl. Phys. B173 (1980) 365.
M. Lüscher, Nucl. Phys. B180 (1981) 317.

[16] B. Bringoltz and M. Teper, Phys.Rev. D73 (2006) 014517 [hep-lat/0508021].

[17] M. Lüscher and P. Weisz, JHEP 0407 (2004) 014 (hep-th/0406205).

[18] H. Meyer, JHEP 0605 (2006) 066 (hep-th/0602281).

[19] J. Drummond, hep-th/0411017; hep-th/0608109.

[20] N. Hari Dass, P. Matlock and Y. Bharadwaj, arXiv:0910.5615.
N. Hari Dass and Y. Bharadwaj, arXiv:0910.5620.
N. Hari Dass, arXiv:0911.3236.

[21] M. Caselle and A. Zago, arXiv:1012.1254.
M. Billo, M. Caselle, V. Verduci and A. Zago, arXiv:1012.3935.

[22] P. Giudice, F. Gliozzi and S. Lottini, JHEP 0903 (2009) 104 [arXiv:0901.0748].

[23] F. Gliozzi, M.Pepe and U.-J. Wiese, JHEP 1101(2011)057 [arXiv:1010.1373]; arXiv:1006.2252; Phys. Rev. Lett. 104 (2010) 232001 [arXiv:1002.4888]
M. Caselle, JHEP 08(2010)063 [arXiv:1004.3875].
A. Allais and M. Caselle, JHEP 0901 (2009) 073 [arXiv:0812.0284].
M. Pepe, arXiv:1011.0056.
H. Meyer, Phys. Rev. D82 (2010) 106001 [arXiv:1008.1178].

[24] M. Caselle, A. Feo, M. Panero and R. Pellegrini, arXiv:1102.0723.
M. Caselle, L. Castagnini, A. Feo, F. Gliozzi and M. Panero, arXiv:1011.4883.

[25] A. Bakry,D. Leinweber and A. Wiliams, arXiv:1011.1380.

[26] B. Brandt, arXiv:1010.3625.

[27] V. Vyas, arXiv:1004.2679.

[28] U. Kol and J. Sonnenschein, arXiv:1012.5974.

[29] M. Teper, Phys.Rev. D59 (1999) 014512 [hep-lat/9804008].

[30] G. 't Hooft, Nucl. Phys. B72 (1974) 461; B75 461 (1974).
S. Coleman, 1979 Erice Lectures.
E. Witten, Nucl. Phys. B160 (1979) 57.
A. Manohar, 1997 Les Houches Lectures, hep-ph/9802419.

[31] B. Lucini and M. Teper, Phys.Rev. D66 (2002) 097502 [hep-lat/0206027].
B. Lucini, M. Teper and U. Wenger, JHEP 0406 (2004) 012 [hep-lat/0404008].

[32] APE Collaboration, Phys. Lett. B192 (1987) 163; B197 (1987) 400.

[33] M. Teper, Phys. Lett. B183 (1987) 345; B185 (1987) 121.

[34] M. Teper, Phys. Lett. B313 (1993) 417.

[35] M. Teper, unpublished.

[36] M. Teper: lectures at *Gauge Fields and Strings*, Isaac Newton Institute, September 17-27 2007. See: http://www.newton.ac.uk/programmes/SIS/seminars/092408301.pdf

[37] P. Bialas, L. Daniel, A. Morel, B. Petersson, Nucl. Phys. B836 (2010) 91 [arXiv:0912.0206].

[38] P. Giudice, F. Gliozzi, S. Lottini, JHEP 0903 (2009) 104 [arXiv:0901.0748].

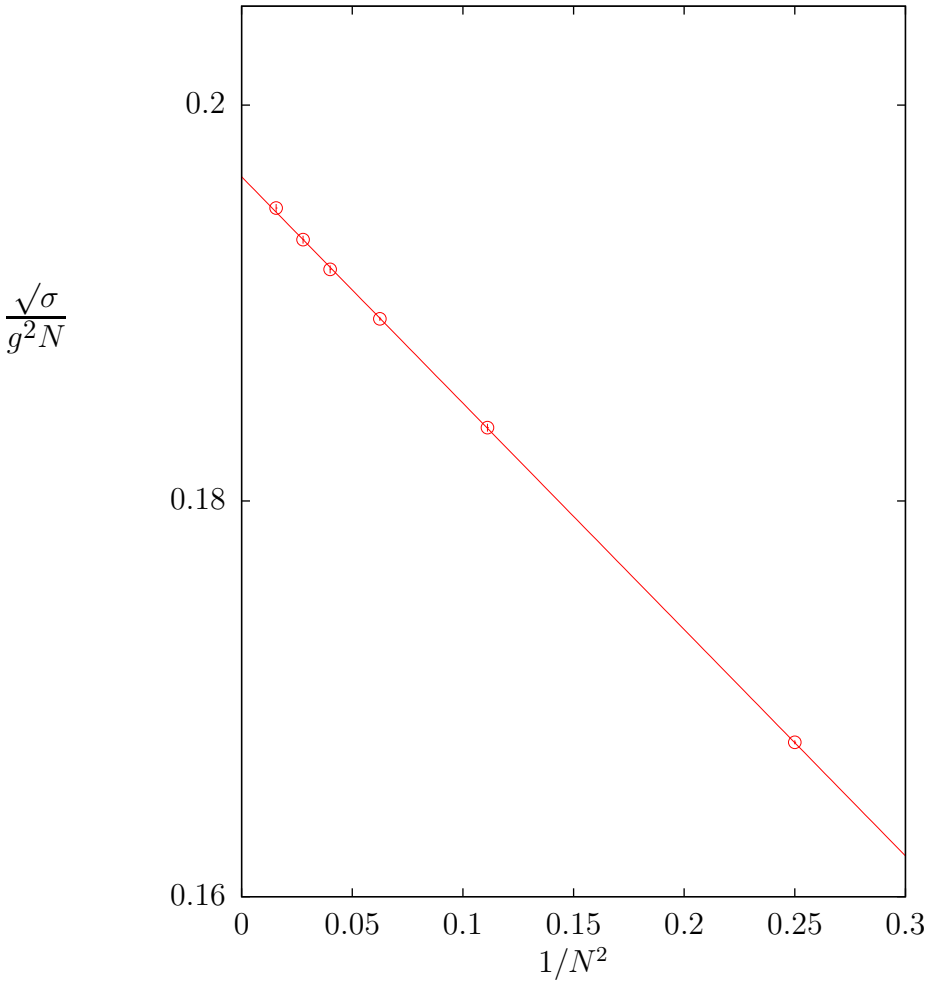

Figure 1: String tension in units of g^2N for various continuum SU(N) gauge theories. The curve is a best fit to $N \geq 2$ of the conventional functional form: $\frac{\sqrt{\sigma}}{g^2N} = 0.19638 - \frac{0.1144}{N^2}$.

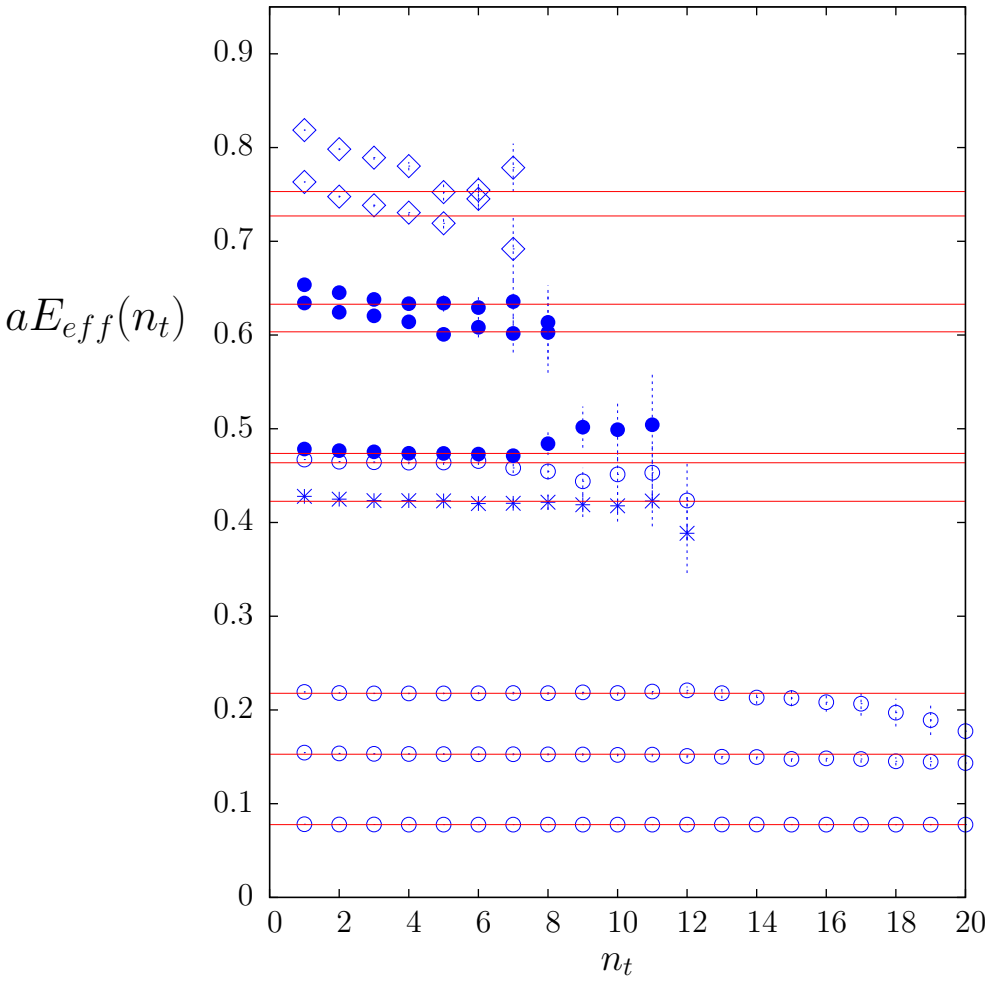

Figure 2: Effective energies extracted from the correlator $C(t = an_t)$ using eqn(22). For the absolute ground state of a flux tube of length $l/a = 16, 24, 32, 64$, $\circ$ in ascending order. Also for the $l = 32a$ flux tube: the first, second and third excitations with $p = 0$, $P = +$, $\bullet$; the ground state with $p = 2\pi/l$ and $P = -$, $\star$; the ground and first excited states with $p = 0$, $P = -$, $\diamond$, shifted upwards by $\Delta E = 0.1$ for clarity. All from SU(6) at $\beta = 171$.

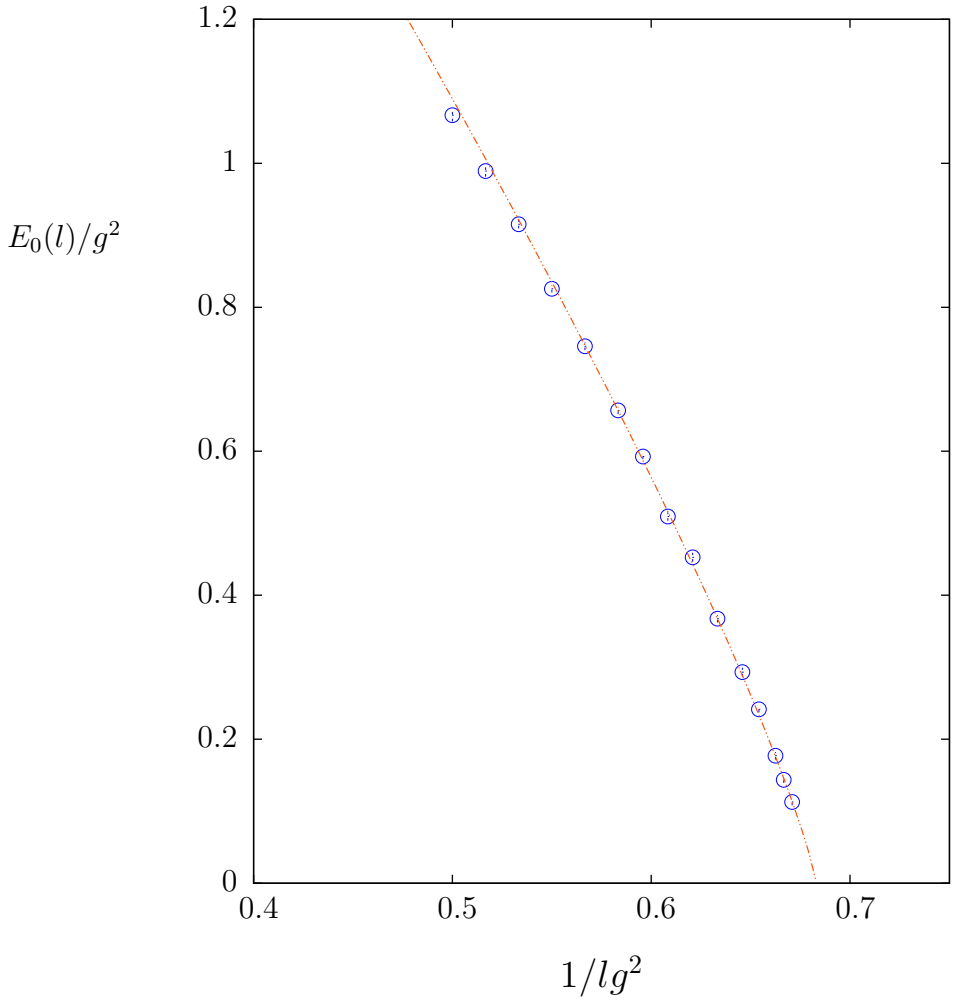

Figure 3:

Figure 4: Energy of the ground state versus $1/lg^2 \equiv T/g^2$ for SU(3) with $l = 2a$ and $a(\beta)$ being varied. The curve is $\propto (T_c - T)^{\frac{5}{6}}$, as expected from the universality class of the critical point.

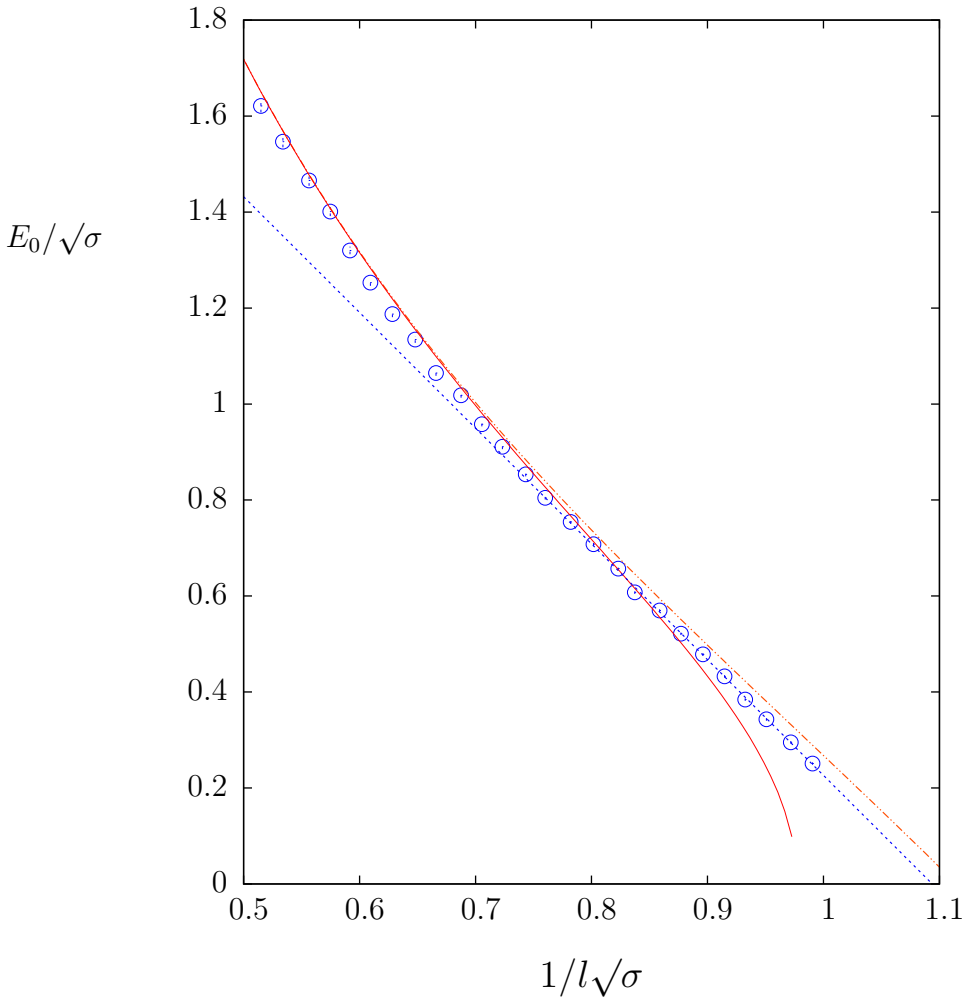

Figure 5: Energy of ground state versus $1/l\sqrt{\sigma} \equiv T/\sqrt{\sigma}$ for SU(2) with $l = 4a(\beta)$, and β being varied. Solid line is Nambu-Goto; dashed blue line is $\propto (T_c - T)$ as expected from the universality class of the critical point, and dashed red line is the universal prediction for E_0 up to $O(1/l^5)$.

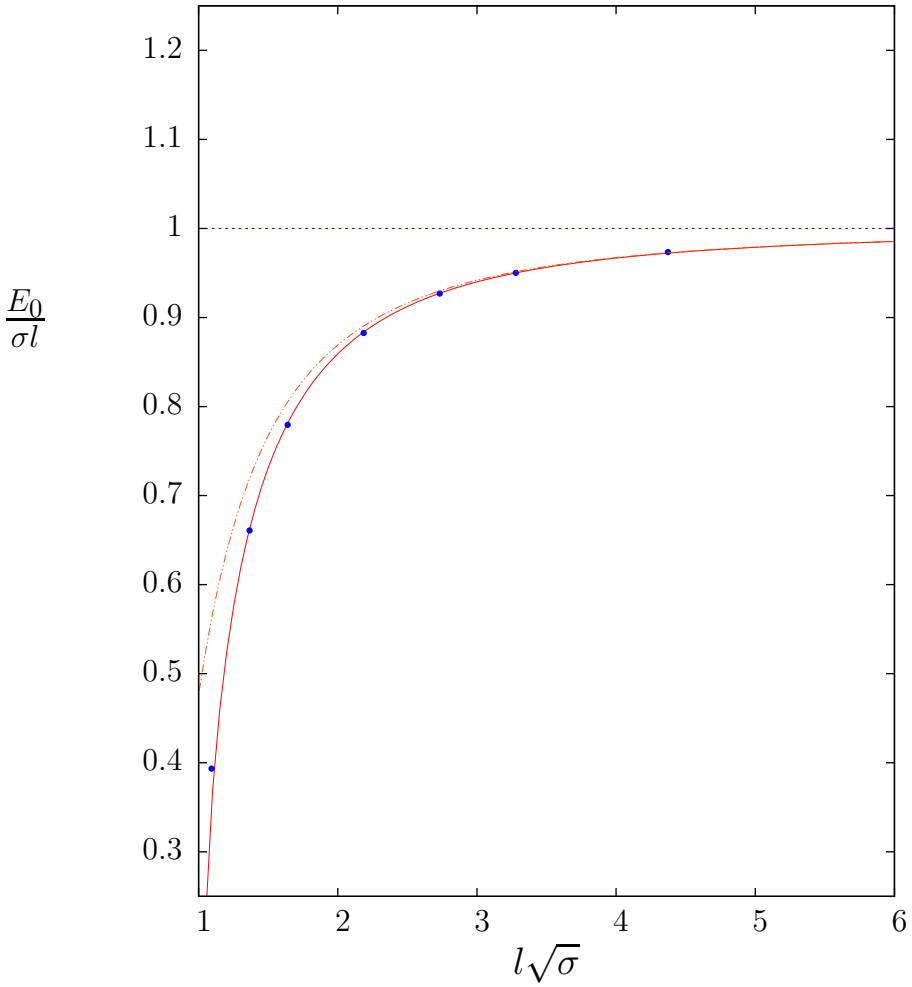

Figure 6: Energy of absolute ground state for SU(2) at $\beta = 5.6$. Compared to full Nambu-Goto (solid curve) and just the Lüscher correction (dashed curve).

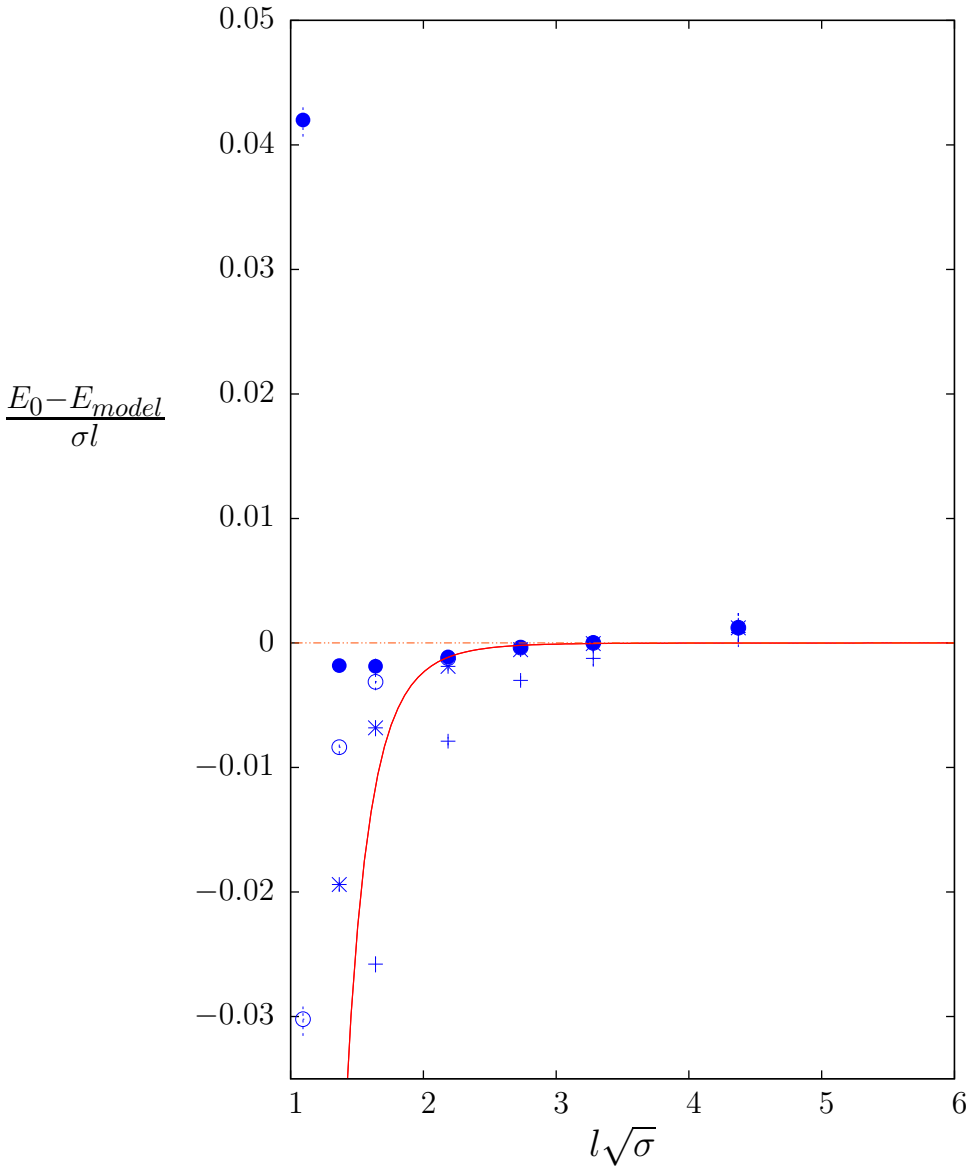

Figure 7: Energy of ground state minus the best fit of several models for E_0: full Nambu-Goto, •; the linear piece plus all the known universal terms, ∘; the latter without the $O(1/l^5)$ term, ⋆; linear plus Lüscher correction, +. Curve is Nambu-Goto with a fitted $O(1/l^7)$ correction. For SU(2) at $\beta = 5.6$.

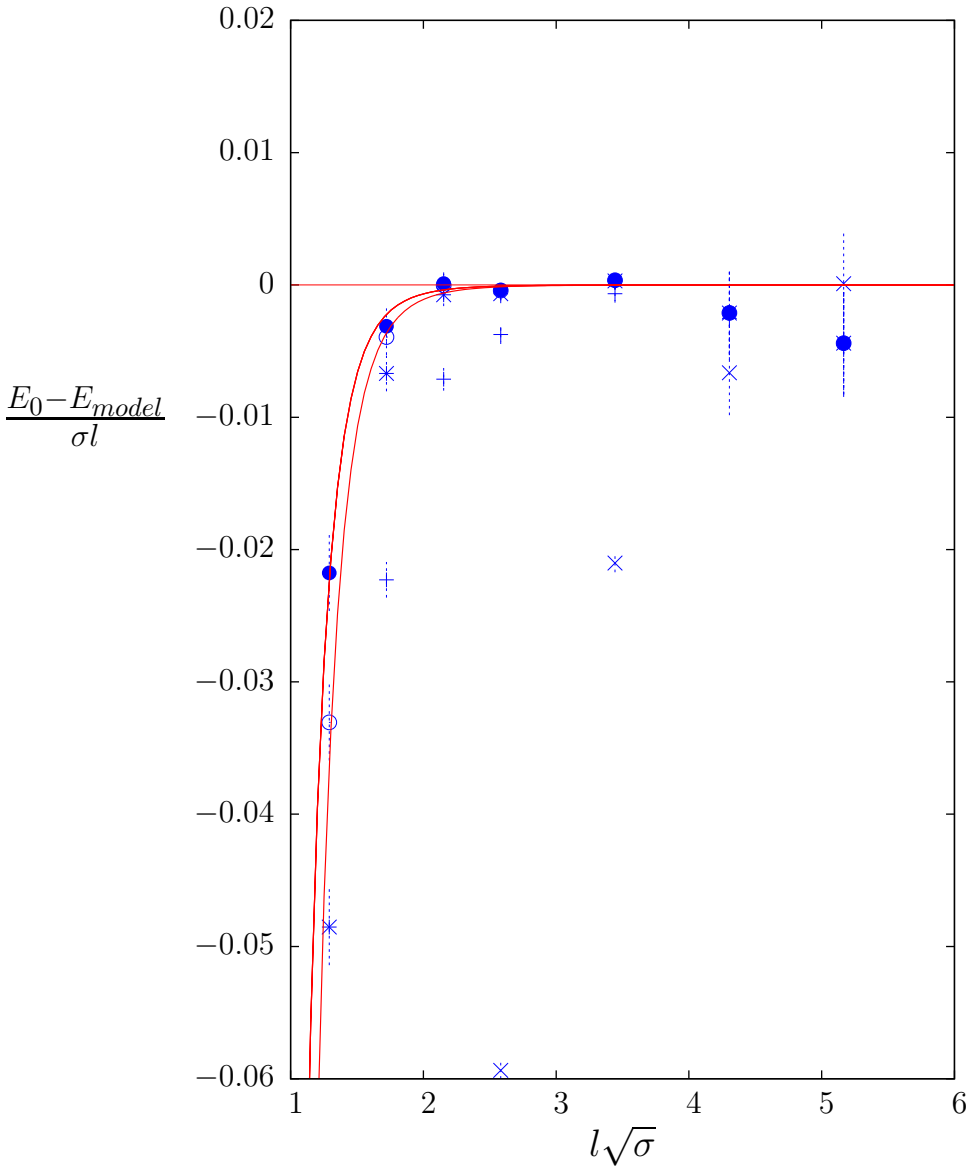

Figure 8: Energy of ground state minus the best fit of several models for E_0: full Nambu-Goto, $\bullet$; the linear piece plus all the known universal terms, $\circ$; the latter without the $O(1/l^5)$ term, $\star$; linear plus Lüscher correction, $+$; just the linear σl piece, $\times$. Curves are fits with an $O(1/l^7)$ correction to the first of these two. For SU(4) at $\beta = 32.0$.

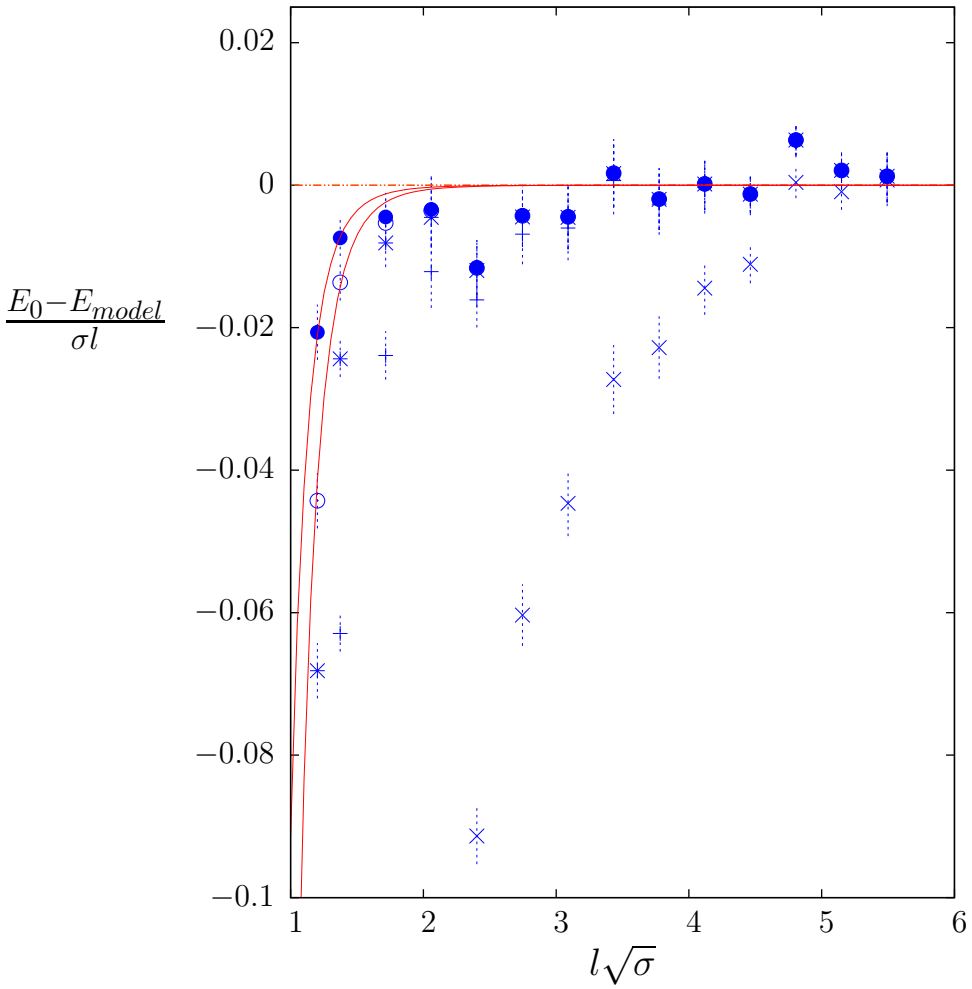

Figure 9: Energy of ground state minus the best fit of several models for E_0: full Nambu-Goto, $\bullet$; the linear piece plus all the known universal terms, $\circ$; the latter without the $O(1/l^5)$ term, $\star$; linear plus Lüscher correction, $+$; just the linear σl piece, $\times$. Curves are fits with an $O(1/l^7)$ correction to the first of these two. For SU(6) at $\beta = 171.0$.

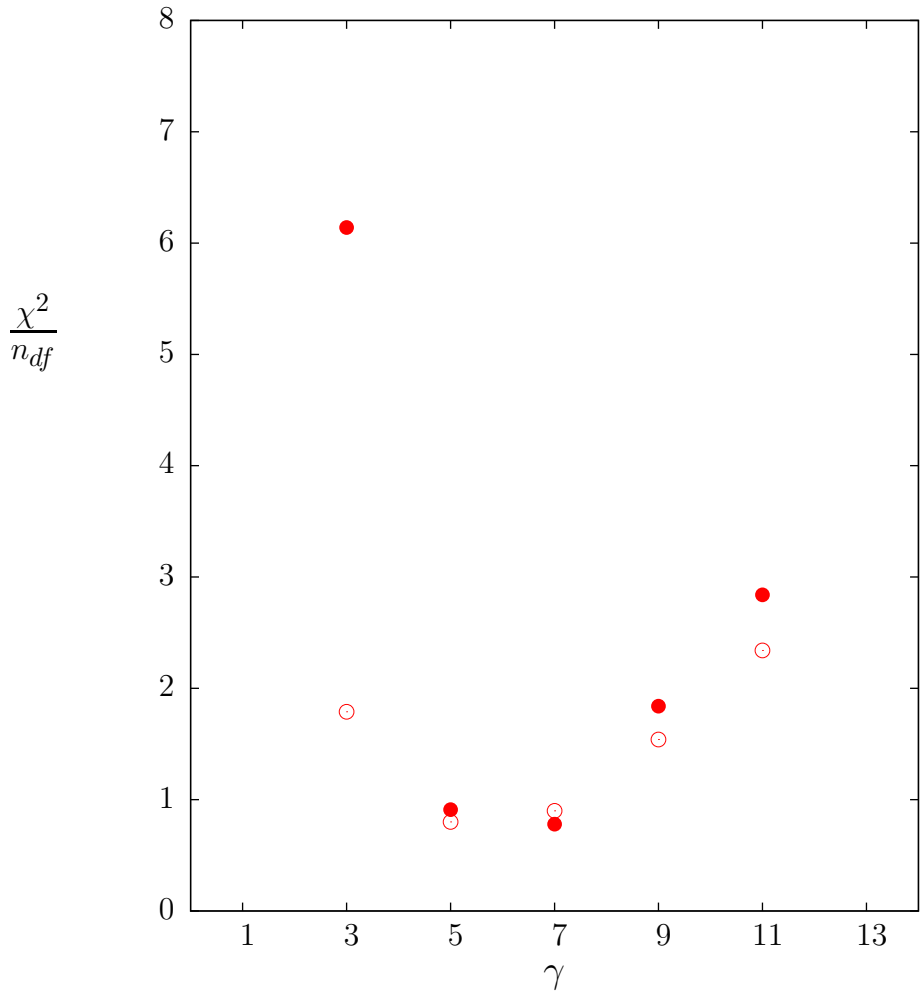

Figure 10: χ^2 per degree of freedom for the best fit of the power of the leading correction to $E_0(l)$ minus Nambu-Goto, using eqn(26). For SU(6) at $\beta = 171$, $\circ$, and for SU(4) at $\beta = 32$, $\bullet$.

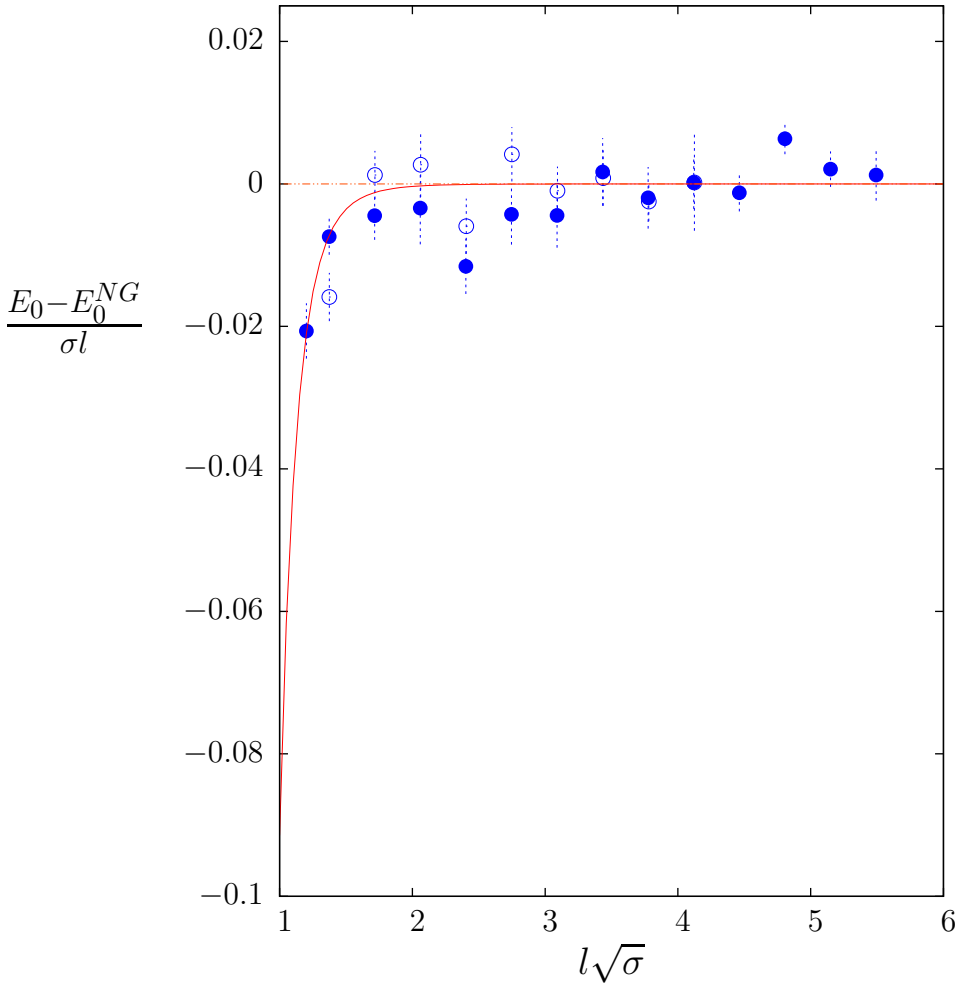

Figure 11: Energy of ground state minus the Nambu-Goto fit, for SU(6) at $\beta = 90$, $\circ$ and $\beta = 171$ $\bullet$. Curve is an $O(1/l^7)$ correction to the second of these.

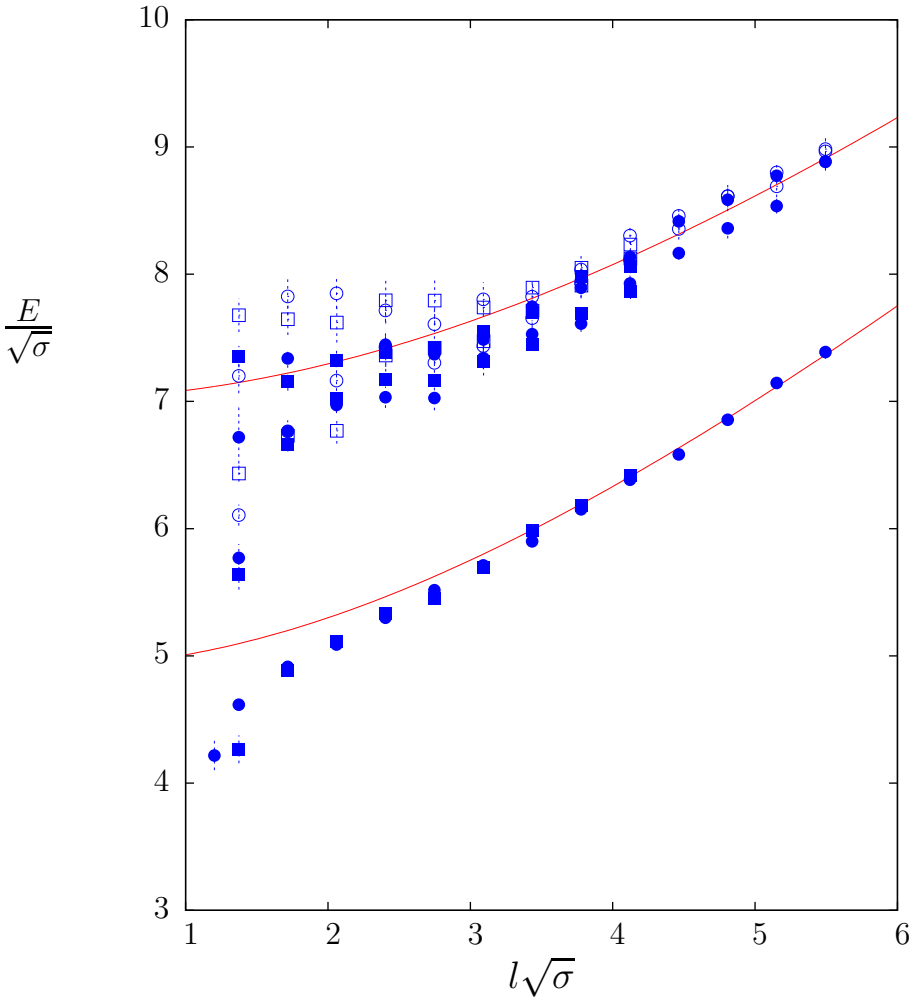

Figure 12: Lightest excited states with $p = 0$ in SU(6): $P = +$ at $\beta = 171$, $\bullet$, and $\beta = 90$, $\blacksquare$; $P = -$ at $\beta = 171$, $\circ$, and $\beta = 90$, $\square$.

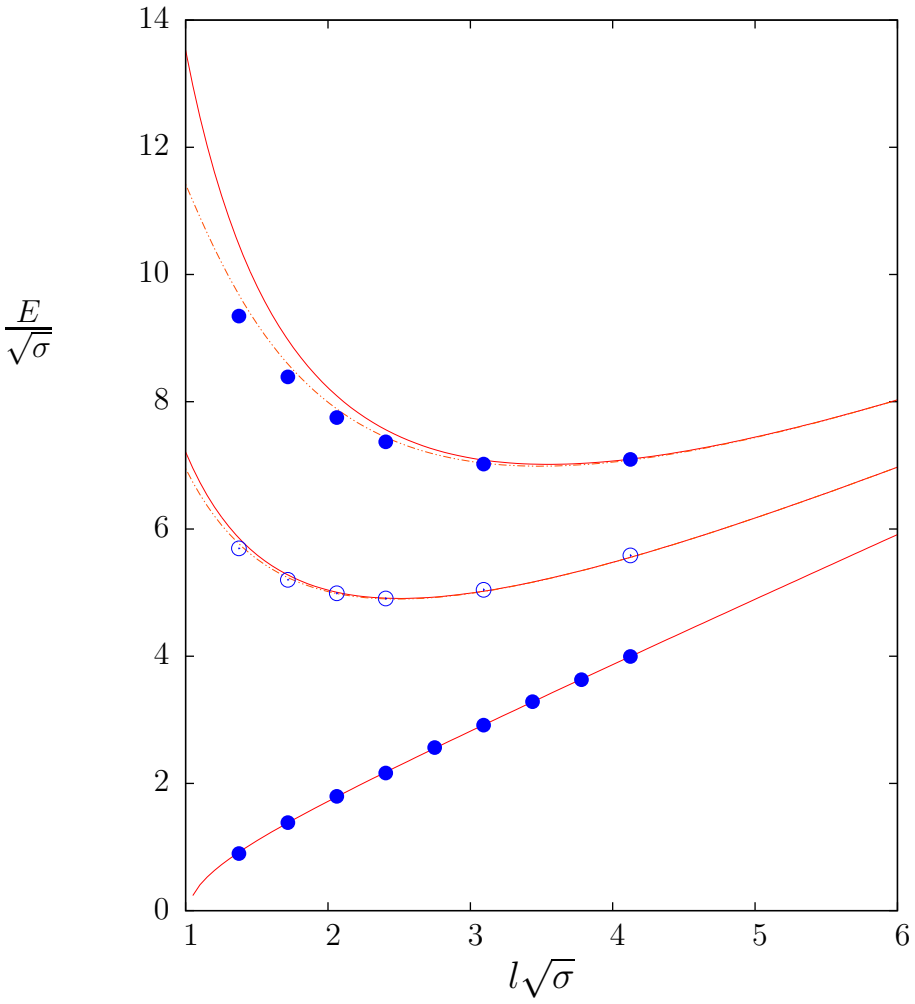

Figure 13: Energies of the ground states with momenta $q = 1, 2$ and with $P = -$. Also the $q = 0$, $P = +$ absolute ground state. For SU(6) at $\beta = 90$. Lines are Nambu-Goto predictions; solid use a continuum p^2 contribution, while dashed use the free-field lattice version, $2 - 2\cos(ap)$.

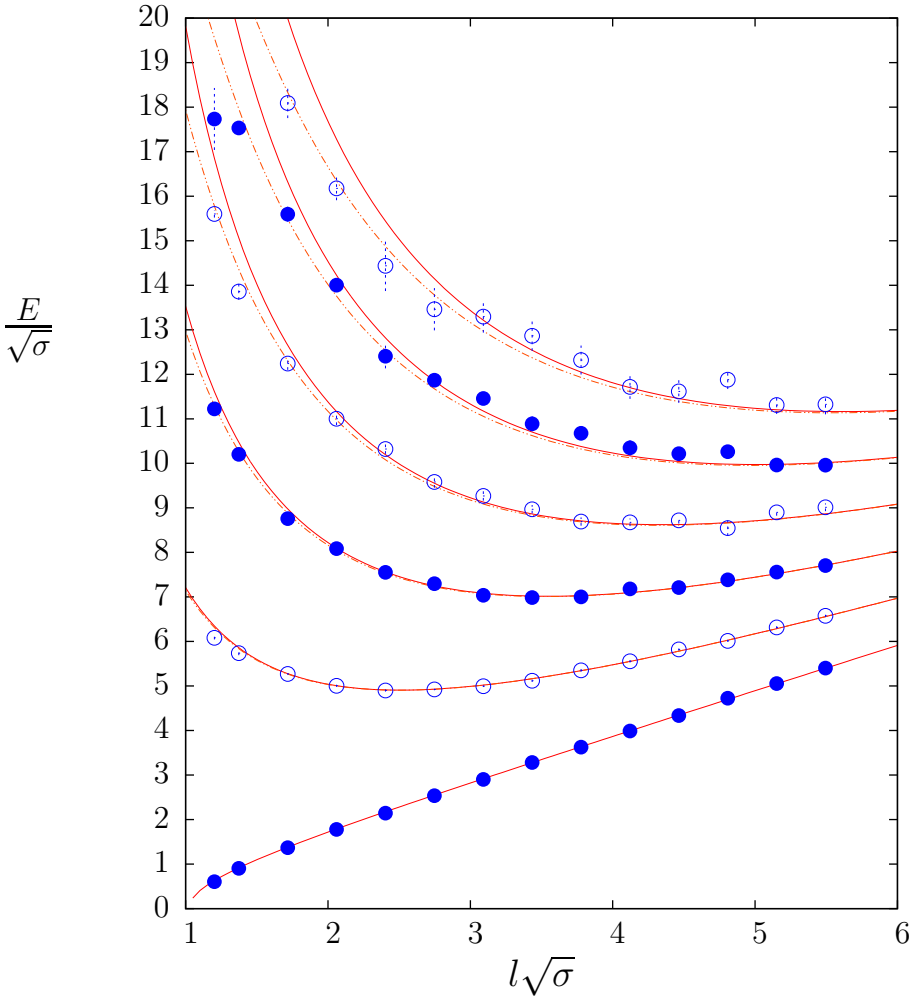

Figure 14: Energies of the ground states with $q = 1, 2, 3, 4, 5$ and $P = -$. Also the $q = 0$ absolute ground state, with $P = +$. For SU(6) at $\beta = 171$. Lines are Nambu-Goto predictions; solid use a continuum p^2 contribution, while dashed use the free-field lattice version, $2 - 2\cos(ap)$.

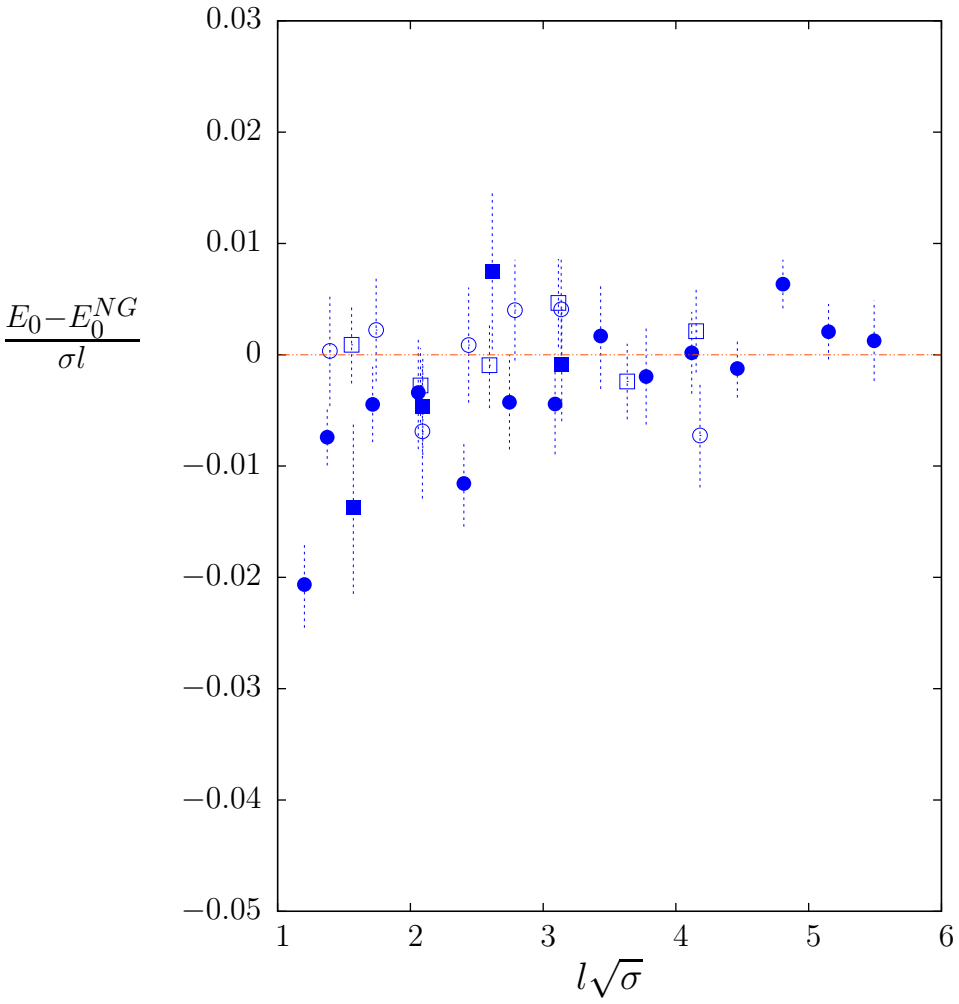

Figure 15: Energy of ground state minus its Nambu-Goto fit, for: SU(6) at $\beta = 171$, •; SU(5) at $\beta = 80$, □; SU(4) at $\beta = 50$, ■; SU(3) at $\beta = 40$, ∘.

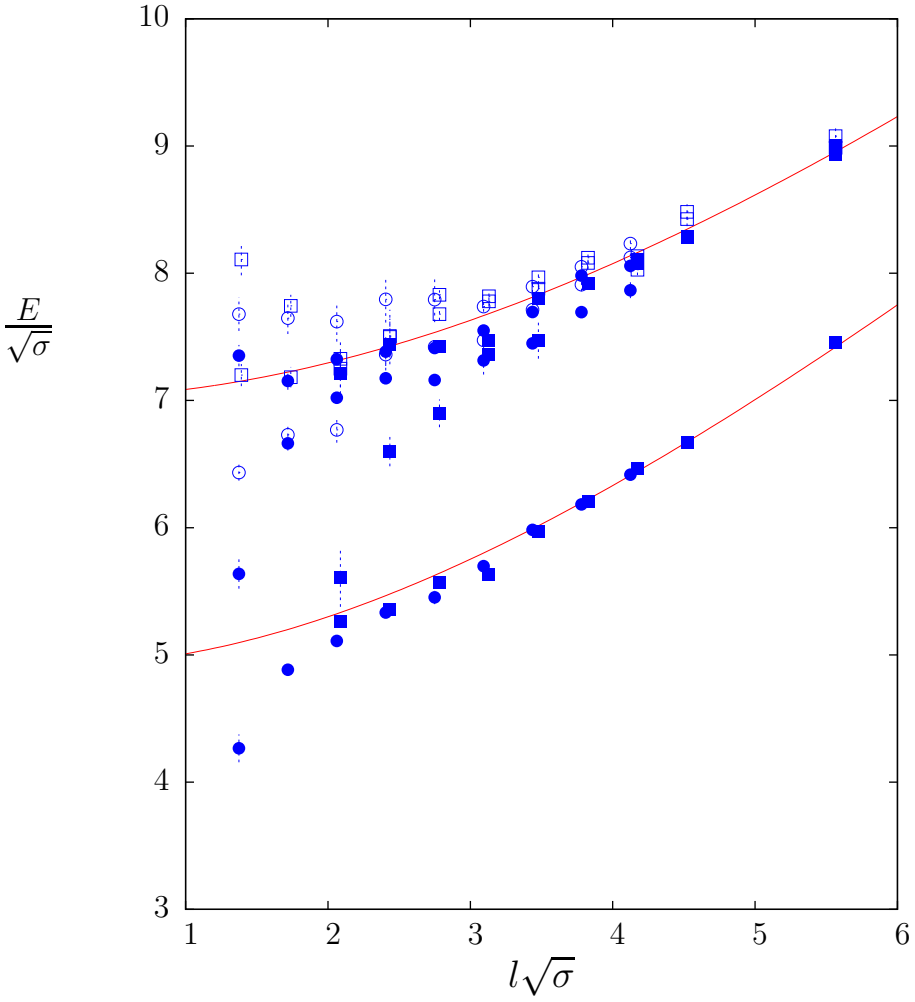

Figure 16: Comparing lightest $p = 0$ excited states in SU(3) at $\beta = 21$ with SU(6) at $\beta = 90$: $P = +$ in SU(6), $\bullet$, and in SU(3), $\blacksquare$; $P = -$ in SU(6), $\circ$, and in SU(3), $\square$.

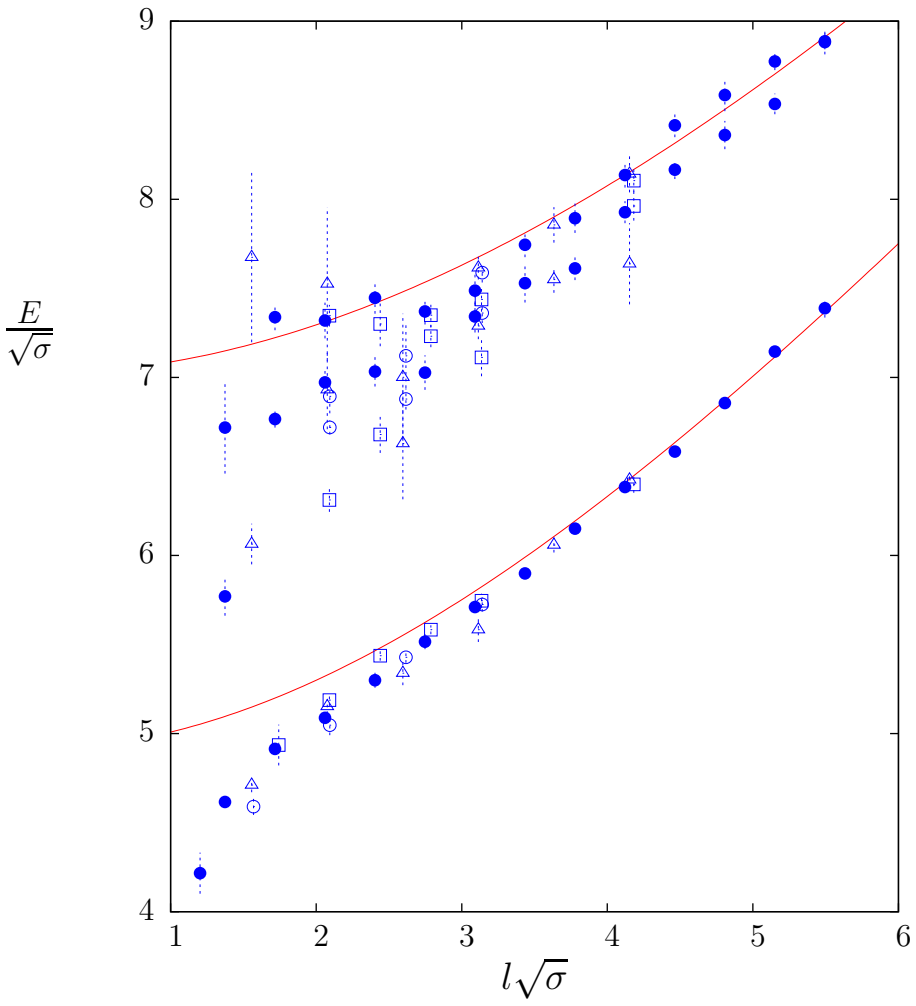

Figure 17: Comparing the three lightest $p = 0$ and $P = +$ excited states in SU(3) at $\beta = 40$, $\square$, SU(4) at $\beta = 50$, $\circ$, SU(5) at $\beta = 80$, $\triangle$, and SU(6) at $\beta = 171$, $\bullet$.

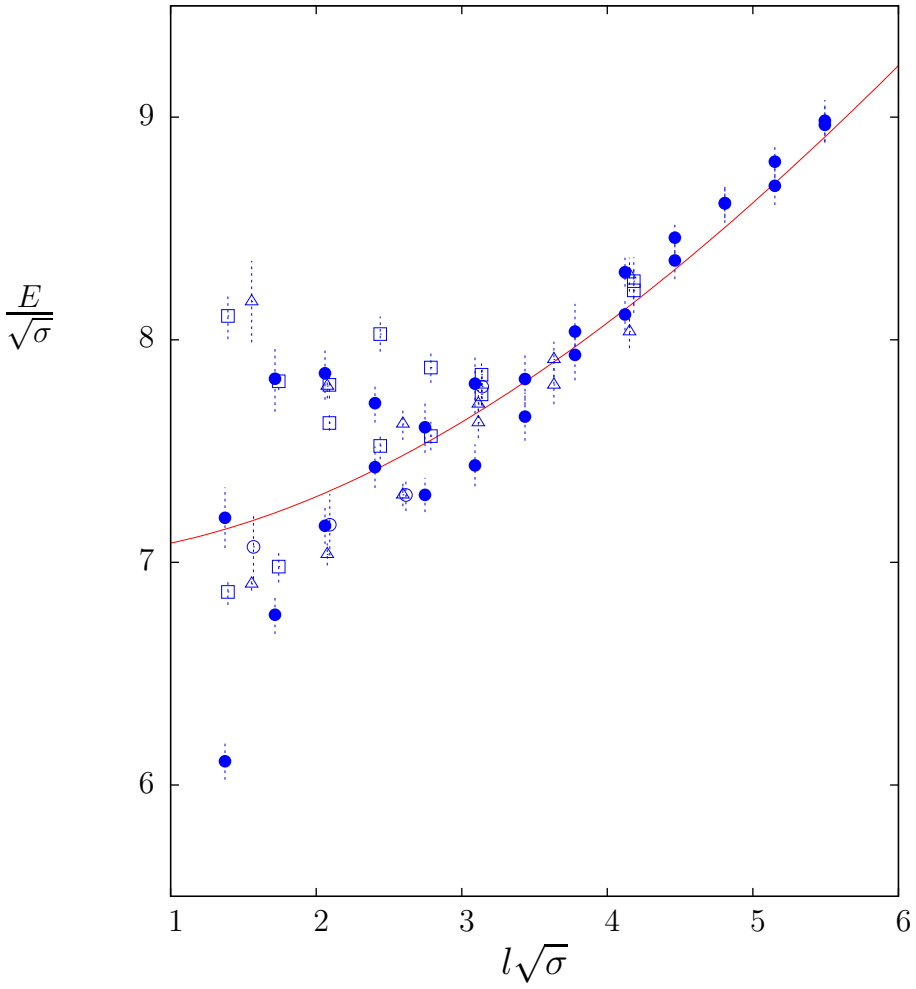

Figure 18: Comparing the two lightest $p = 0$, $P = -$ excited states in SU(3) at $\beta = 40$, $\square$, SU(4) at $\beta = 50$, $\circ$, SU(5) at $\beta = 80$, $\triangle$, and SU(6) at $\beta = 171$, $\bullet$.

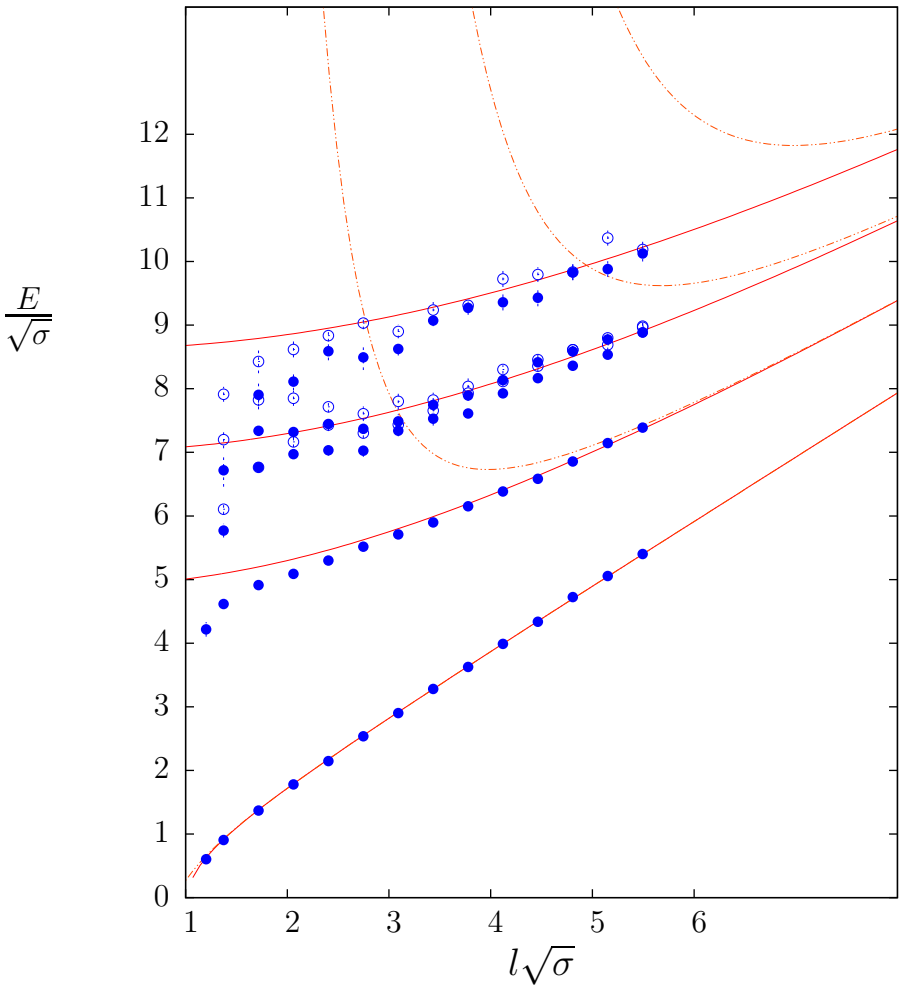

Figure 19: The lightest four $p = 0$ excited states in SU(6) at $\beta = 171$ with $P = +$, $\bullet$, and the lightest three with $P = -$, $\circ$. Solid curves are the Nambu-Goto predictions, while the dashed curves are the contributions of the known universal terms. Also shown is the absolute ground state (lowest curve).

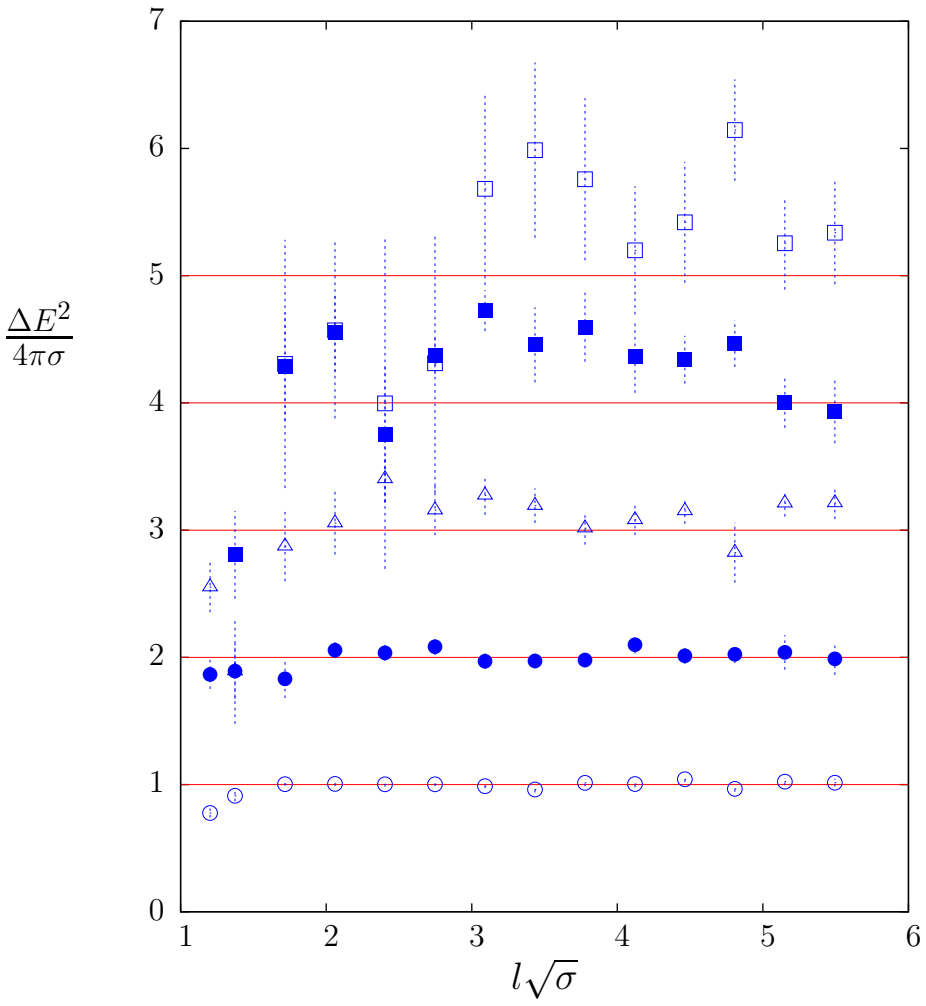

Figure 20: Excitation energies of the lightest $P = -$ states with non-zero momenta $q = 1, 2, 3, 4, 5$, using eqn(29), and with $2 - 2\cos(ap)$ in place of $(ap)^2$. For SU(6) at $\beta = 171$. Nambu-Goto predictions shown.

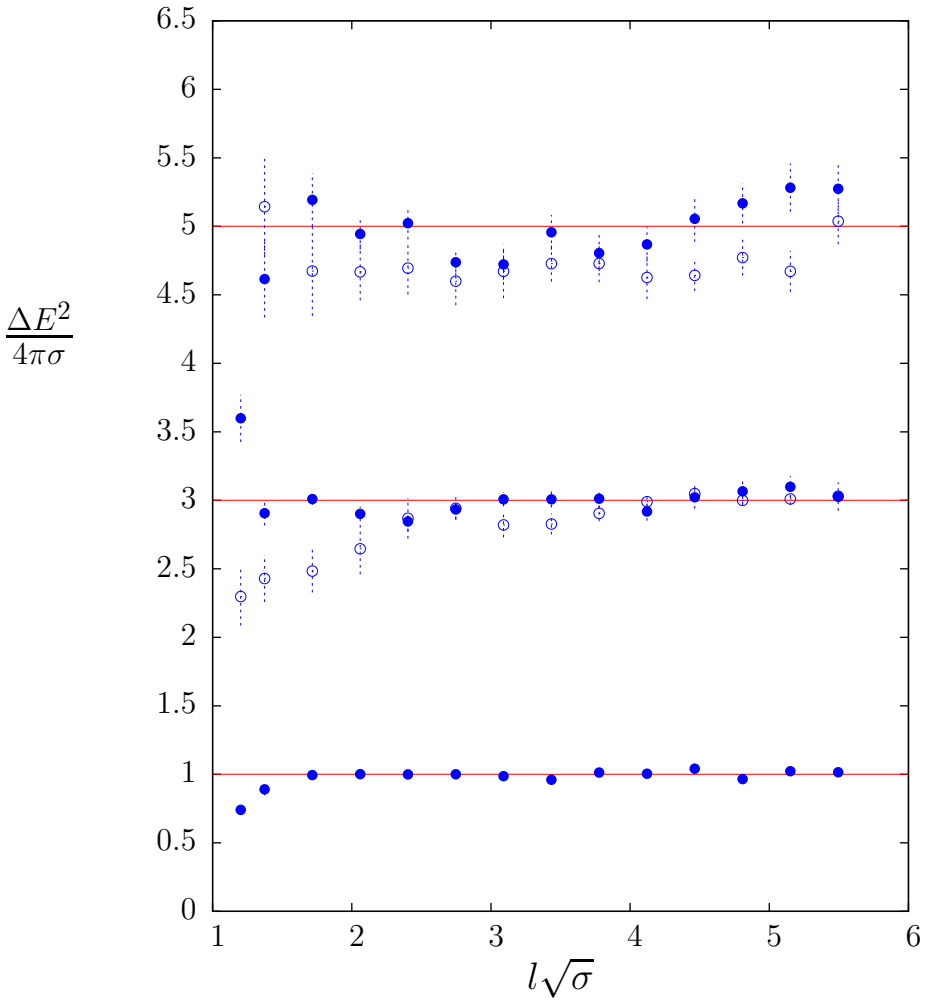

Figure 21: Excitation energies of the lightest few states with momentum $q = 1$ and with $P = -$ ($\bullet$) or $P = +$ ($\circ$). For SU(6) at $\beta = 171$. Nambu-Goto predictions shown.

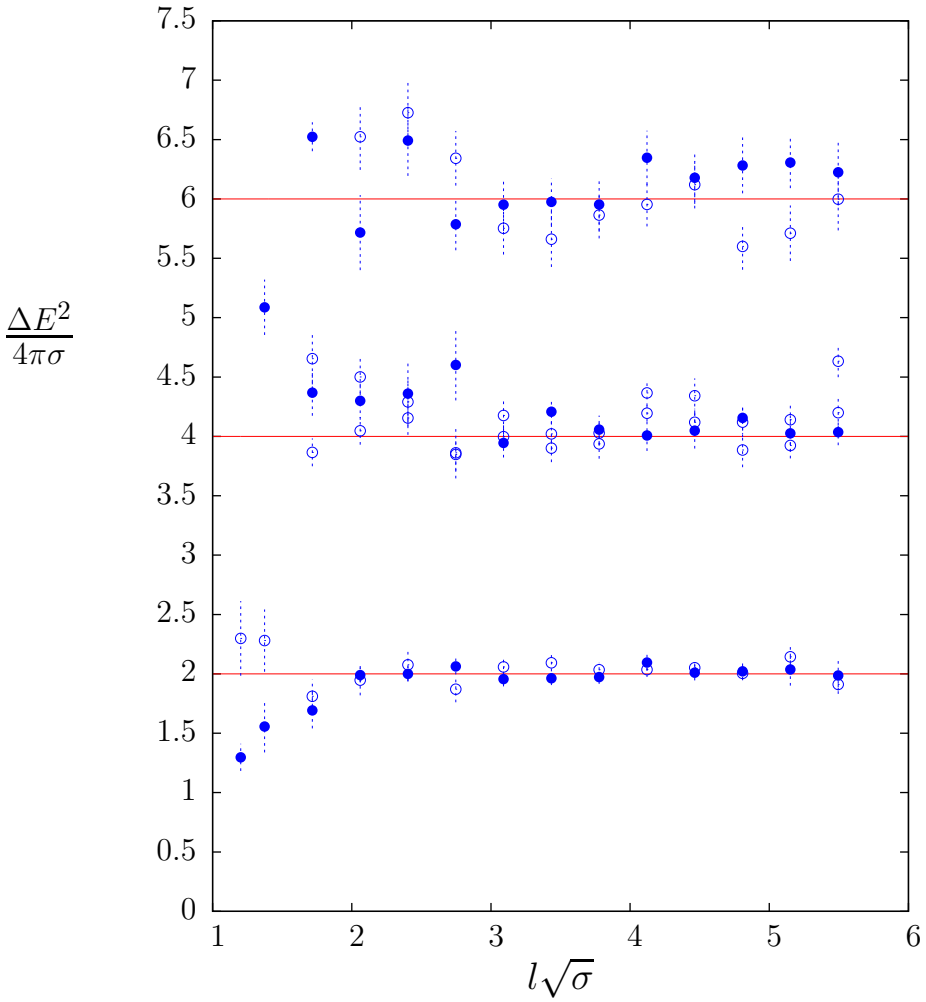

Figure 22: Excitation energies of the lightest few states with momentum $q = 2$ and with $P = -$ ($\bullet$) or $P = +$ ($\circ$). For SU(6) at $\beta = 171$. Nambu-Goto predictions shown.

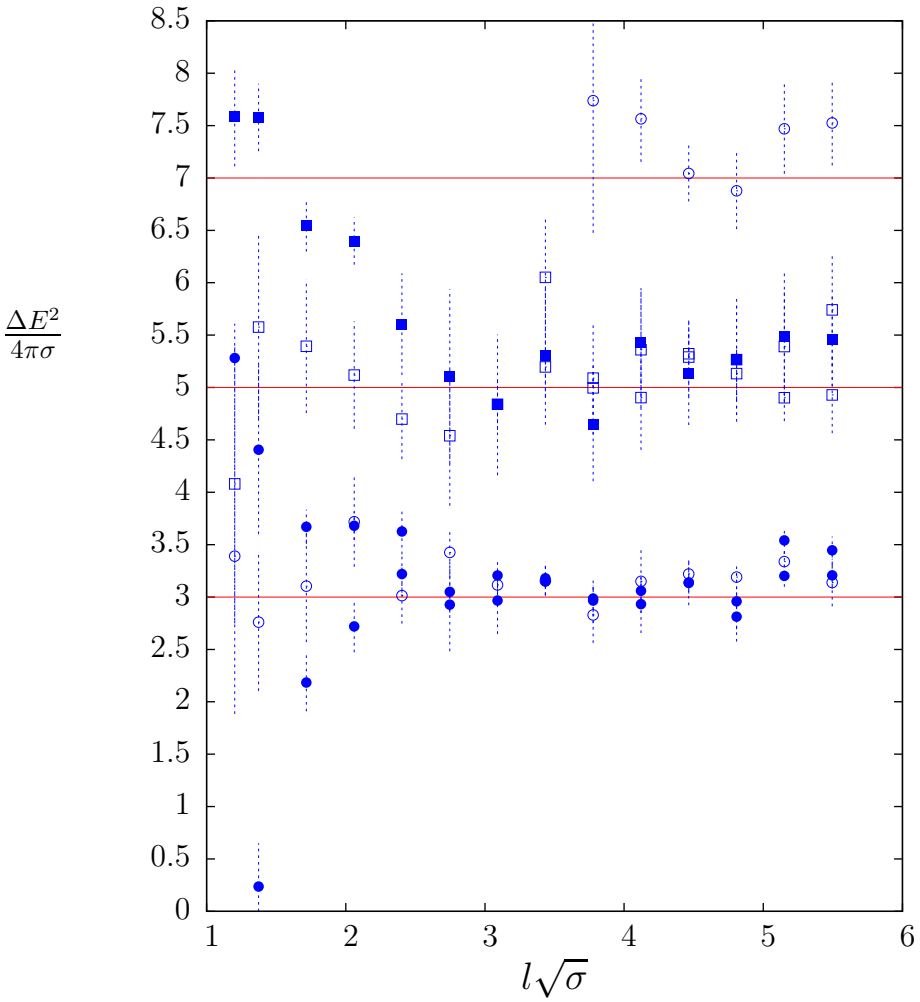

Figure 23: Excitation energies of the lightest few states with momentum $q = 3$ and with $P = -$ ($\bullet$) or $P = +$ ($\circ$). For SU(6) at $\beta = 171$. Nambu-Goto predictions shown.

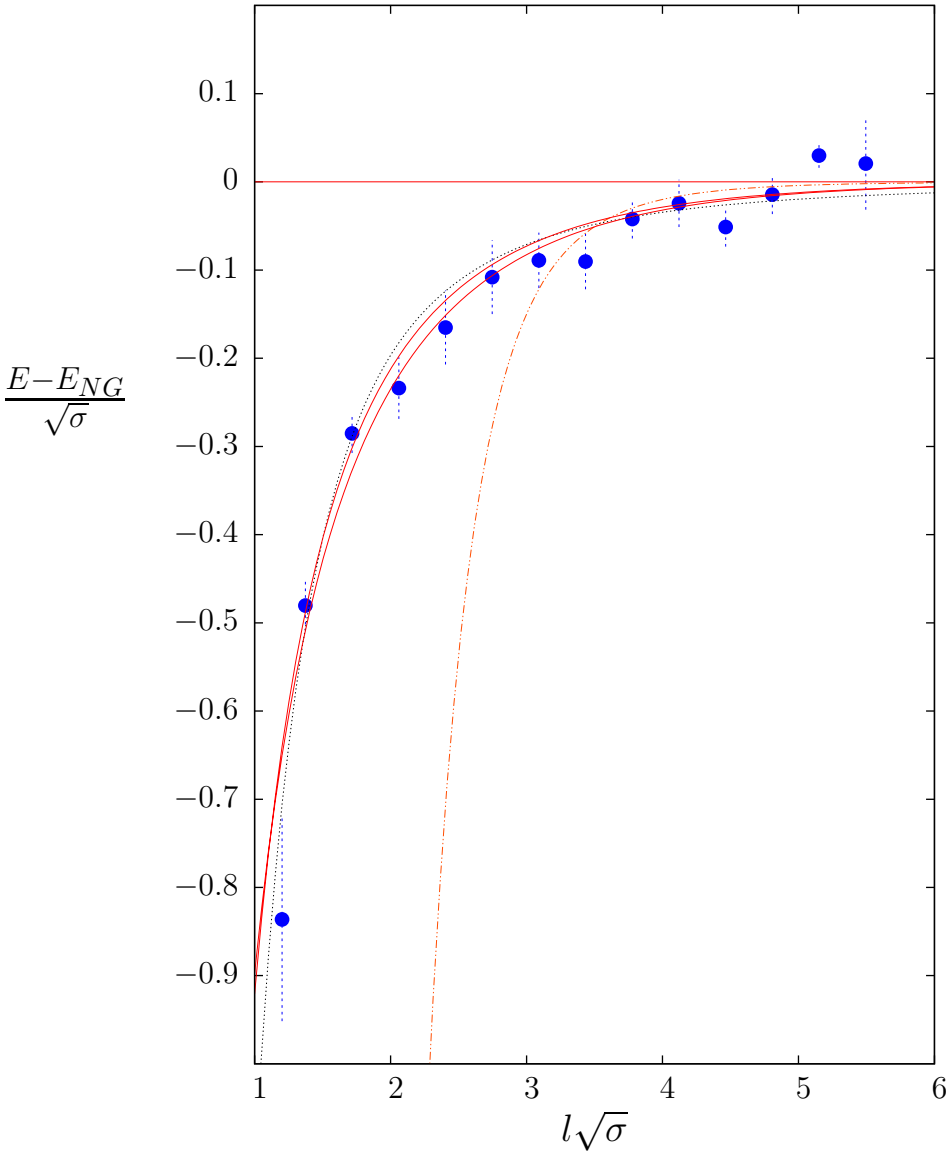

Figure 24: Energy of first excited $q = 0$, $P = +$ state minus the Nambu-Goto prediction. Fitted corrections shown are: steep dotted curve is $\frac{c}{(l\sqrt{\sigma})^7}$; solid red curves are two fits of the form $\frac{c}{(l\sqrt{\sigma})^7}\left(1+\frac{c'}{l^2\sigma}\right)^{-\gamma}$; dashed black curve is a best fit of the form $\frac{c}{(l\sqrt{\sigma})^\gamma}$. See text for parameters. For SU(6) at $\beta = 171$.

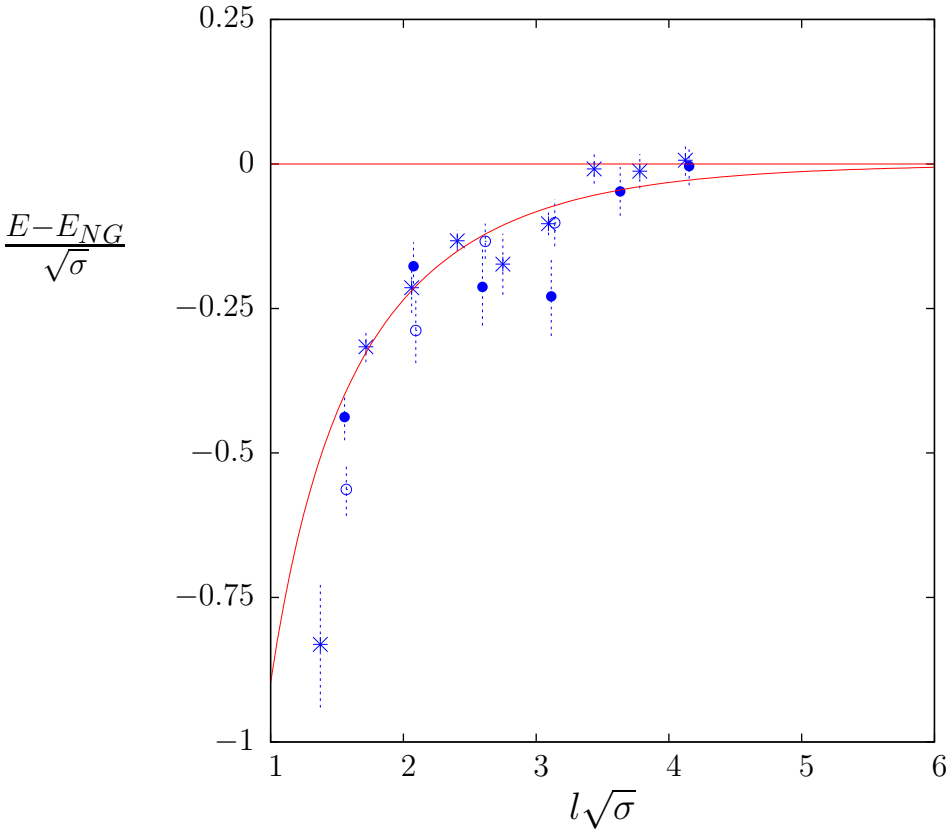

Figure 25: Energy of first excited $q = 0$, $P = +$ state minus the Nambu-Goto prediction. For SU(6) at $\beta = 90$, $\star$, SU(5) at $\beta = 80$, $\bullet$, and SU(4) at $\beta = 50$, $\circ$. Curve is $-1.0 * ((25.0 * *2.75)/(l\sqrt{\sigma})^7 \times (1.0 + 25.0/l^2\sigma)^{-2.75}$, as in Fig 24.

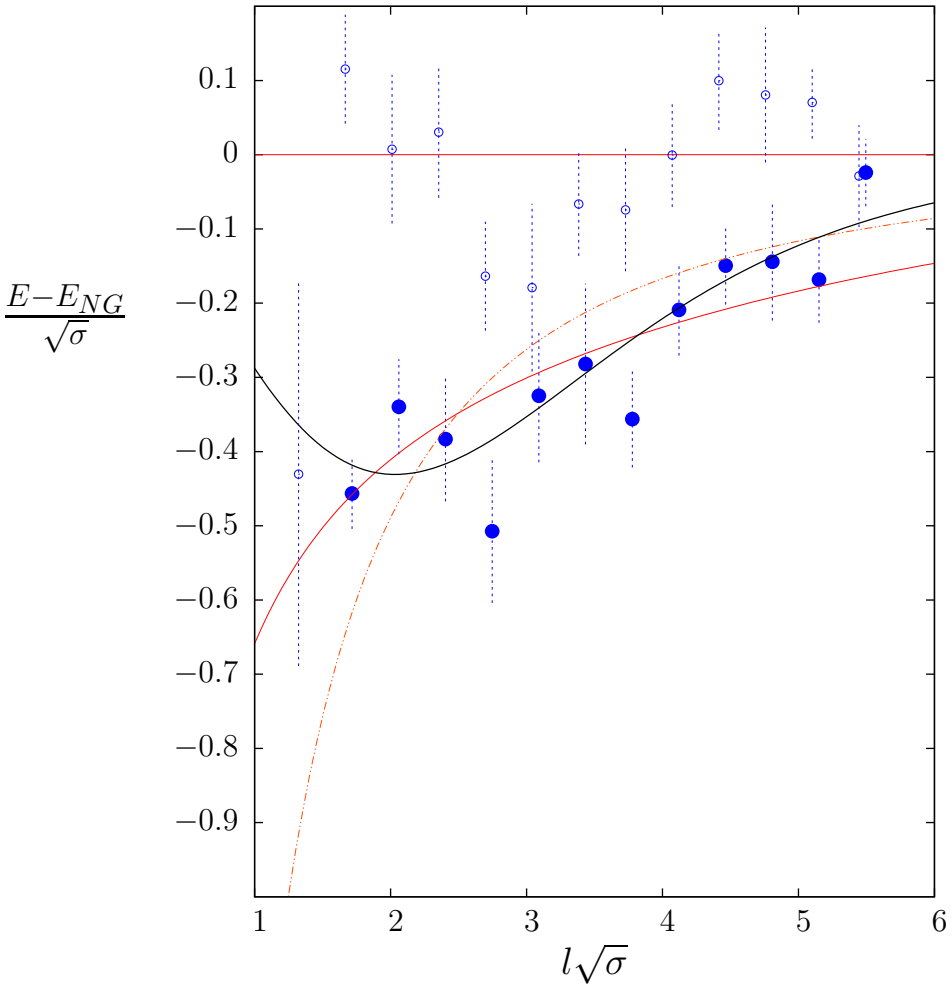

Figure 26: Energy of second (•) and third (○) excited $q = 0$, $P = +$ states minus the Nambu-Goto predictions. Fitted corrections shown are of the form $\frac{c}{(l\sqrt{\sigma})^7}\left(1+\frac{c'}{l^2\sigma}\right)^{-\gamma}$, with parameters $(\gamma,\, c') =:$ (2.75, 926.0), dashed red line; (3.18, 282.0), solid red line; (4.16, 21.9), solid black line. For SU(6) at $\beta = 171$.

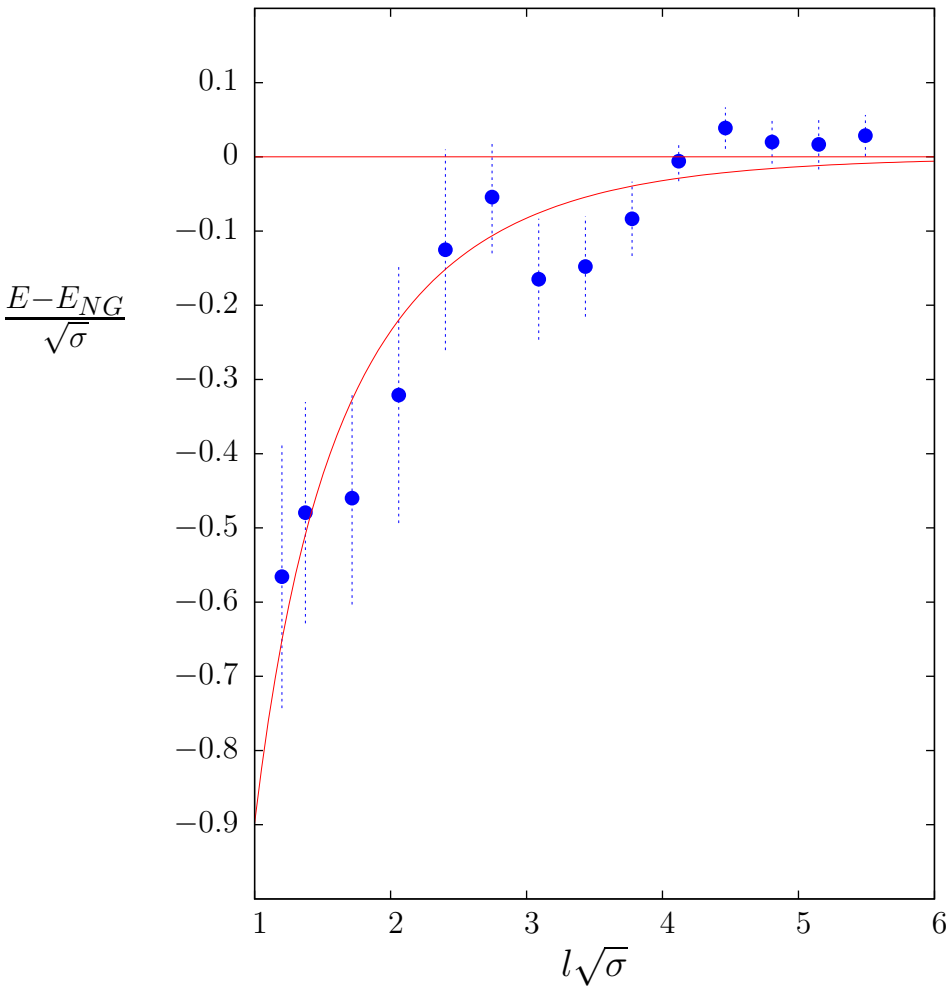

Figure 27: Energy of $q = 1, P = +$ ground state minus the Nambu-Goto value. For SU(6) at $\beta = 171$. Solid red curve is $\frac{c}{(l\sqrt{\sigma})^7}\left(1 + \frac{25}{l^2\sigma}\right)^{-2.75}$.

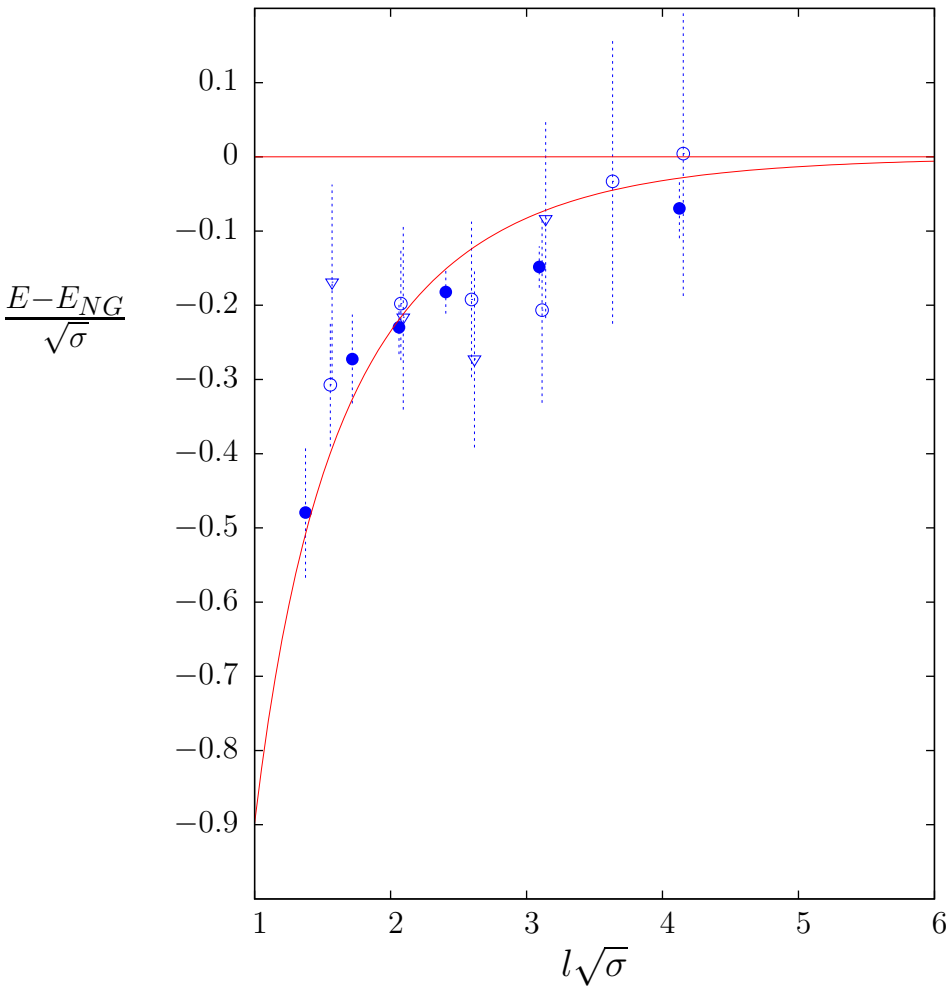

Figure 28: Energy of $q = 1, P = +$ ground state minus the Nambu-Goto value. For SU(6) at $\beta = 90$, $\bullet$, SU(5) at $\beta = 80$, $\circ$, and SU(4) at $\beta = 50$, $\triangledown$. Solid red curve is $\frac{c}{(l\sqrt{\sigma})^7}\left(1+\frac{25}{l^2\sigma}\right)^{-2.75}$.

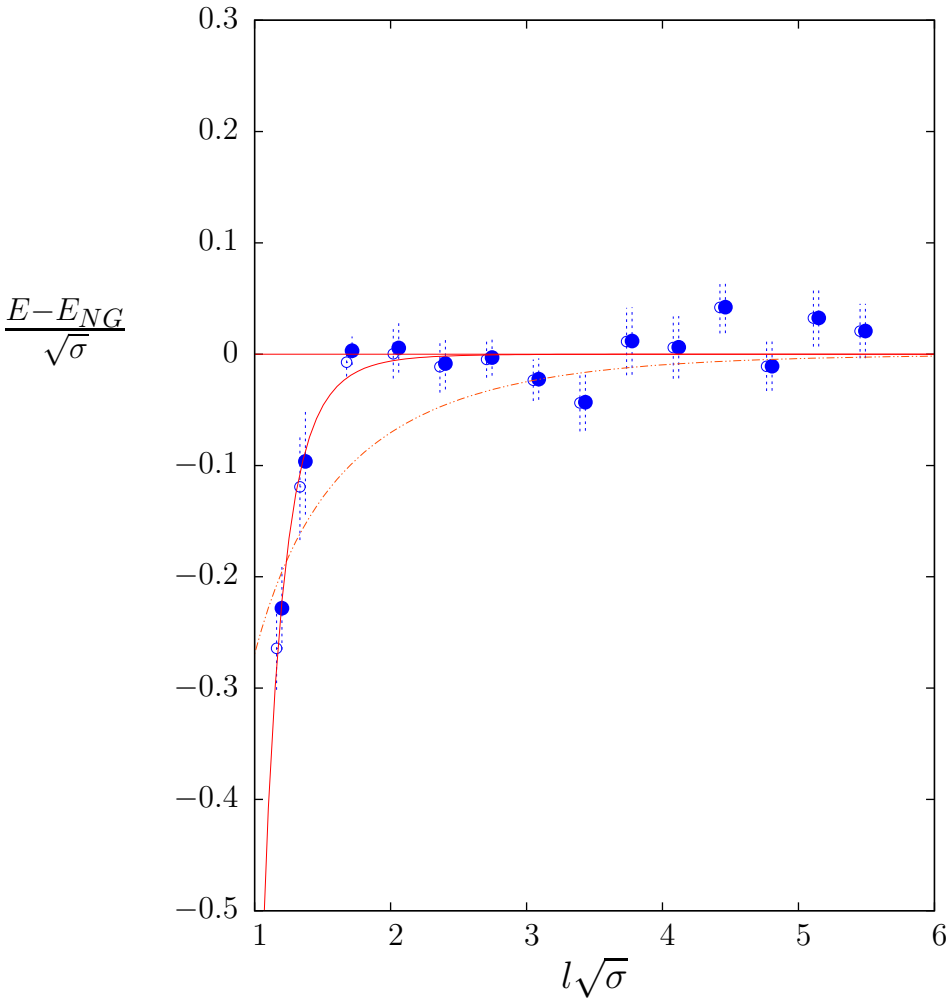

Figure 29: Energy of the $q = 1, P = -$ ground state minus the Nambu-Goto value. Using free lattice, •, and continuum, ∘, dispersion relations. (Latter slightly shifted for clarity.) For SU(6) at $\beta = 171$. Solid curve is $\propto \frac{1}{(l\sqrt{\sigma})^7}$, and dotted curve is $\propto \frac{1}{(l\sqrt{\sigma})^7}\left(1+\frac{25}{l^2\sigma}\right)^{-2.75}$.

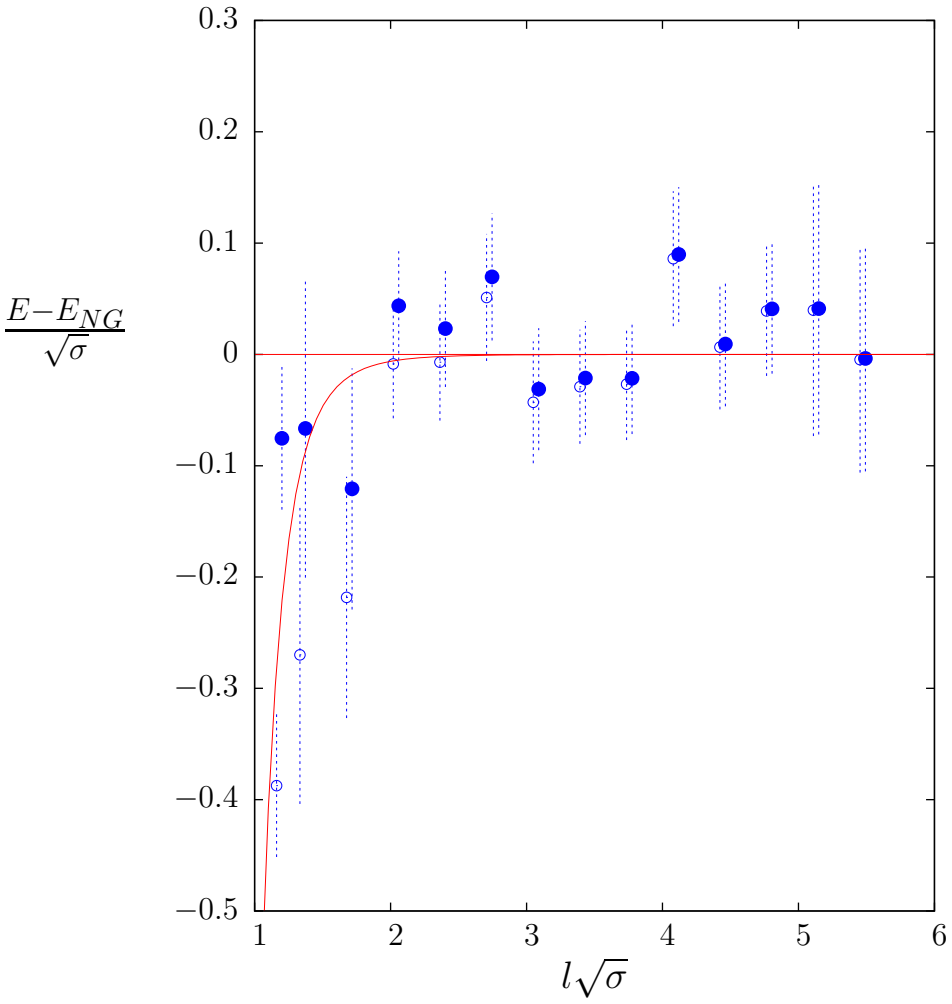

Figure 30: Energy of the $q = 2, P = -$ ground state minus the Nambu-Goto value. Using free lattice, •, and continuum, ∘, dispersion relations. (Latter slightly shifted for clarity.) For SU(6) at $\beta = 171$. Curve is $\propto \frac{1}{(l\sqrt{\sigma})^7}$.

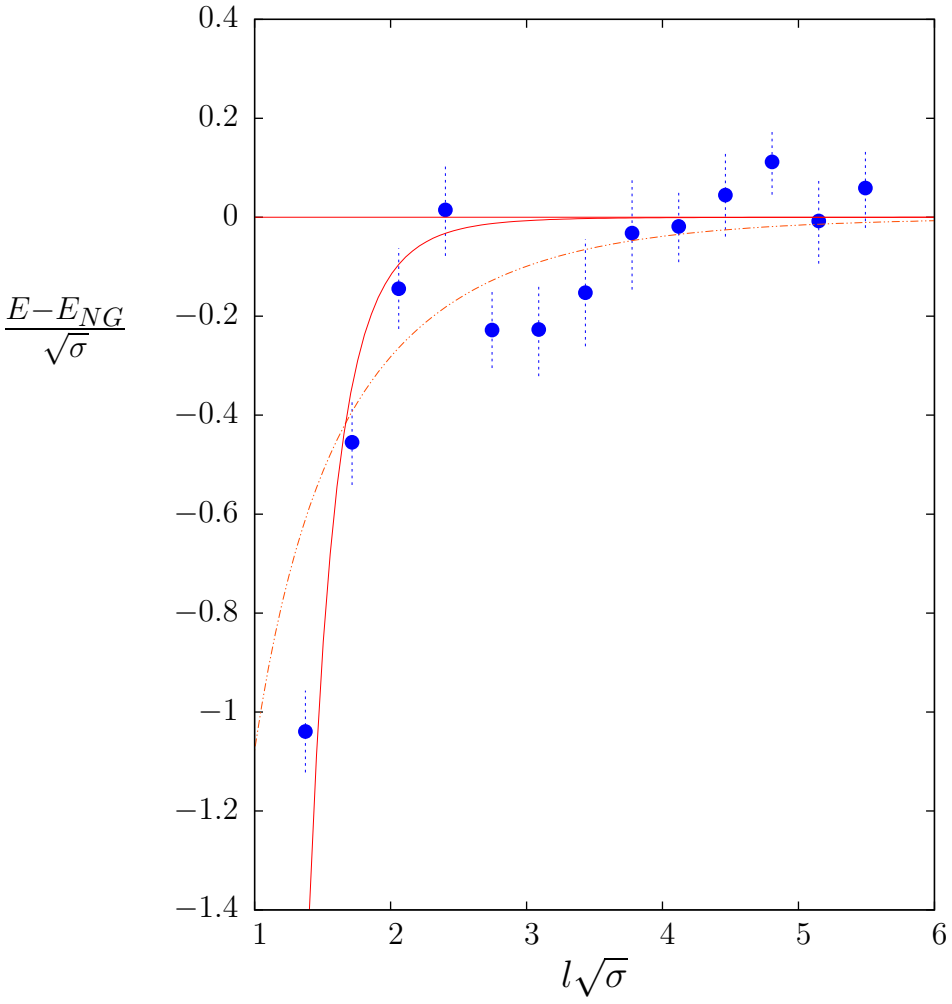

Figure 31: Energy of the $q = 0, P = -, P_r = +$ ground state minus the Nambu-Goto value, •. For SU(6) at $\beta = 171$. Solid curve is $\propto \frac{1}{(l\sqrt{\sigma})^7}$, and dotted curve is $\propto \frac{1}{(l\sqrt{\sigma})^7}\left(1 + \frac{25}{l^2\sigma}\right)^{-2.75}$.